BENEFICIATION OF PULP AND PAPER MILL SLUDGE: PRODUCTION OF CELLULOSE NANOFIBRILS (CNFs)

by

Thabisile Brightwell Jele

A dissertation submitted to the School of Engineering, College of Agriculture, Engineering and Science at the University of KwaZulu-Natal, Durban, South Africa in partial fulfilment of the academic requirements for the degree of Master of Science in Engineering in Chemical Engineering

Supervisor: Prof. Bruce Sithole

PREFACE

This dissertation is being submitted for the degree of Master of Science in Engineering at the School of Engineering of the College of Agriculture, Engineering and Science, University of KwaZulu-Natal, Howard College Campus, South Africa.

I certify, except where acknowledged in the text, that the content of this work is of the candidate alone and has not been submitted before for any degree or examination to this or any other university or institution for this or any other degree or award.

Signed _____

Prof. Bruce Sithole

14 June 2022

Date

DECLARATION 1- PLAGIARISM

I, Thabisile Brightwell Jele declare that:

1. The research reported in this thesis, except where otherwise indicated, is my original research.

2. This thesis has not been submitted for any degree or examination at any other university.

3. This thesis does not contain other persons' data, pictures, graphs or other information, unless specifically acknowledged as being sourced from other persons.

4. This thesis does not contain other persons' writing, unless specifically acknowledged as being sourced from other researchers. Where other written sources have been quoted, then:

a. Their words have been re-written but the general information attributed to them has been referenced

b. Where their exact words have been used, then their writing has been placed in italics and inside quotation marks, and referenced.

5. This thesis does not contain text, graphics or tables copied and pasted from the Internet, unless specifically acknowledged, and the source being detailed in the thesis and in the References sections.

31st January 2022

Signed _____ Date _____

Thabisile B Jele

Student Number :220111319

DECLARATION 2-PUBLICATIONS

LIST OF PUBLICATIONS

Publication 1: Jele, T.B., Lekha, P. and Sithole, B., 2021. Role of cellulose nanofibrils in improving the strength properties of paper: a review. *Cellulose*, pp.1-27.

Publication 2: Jele, T.B., Lekha, P., Sithole, B., Andrew, J.,2022. Characterisation of pulp and papermill sludge for beneficiation. *Cellulose.*

31st January 2022

Signed _____ _____

Date

Thabisile B Jele

Student Number: 220111319

ACKNOWLEDGEMENT

Firstly, I would like to thank my Lord, Jesus Christ - the giver of life. My profound gratitude goes to my supervisors, Prof B Sithole and Dr P Lekha, for the lifetime opportunity to pursue a Masters degree under their guidance. I would like to acknowledge the Council for Scientific and Industrial Research (CSIR), Biorefinery Industry Development Facility (BIDF) for financial and technical support. I would like to acknowledge the contribution and assistance of the BIDF team and fellow postgraduate colleagues in this postgraduate journey. I appreciate the technical support by Mr Seemela, Ms Londani, and Dr Jonas Johakim in the BIDF laboratory.

My most profound gratitude goes towards my parents, Mr and Mrs Jele, for being my pillars of strength throughout this postgraduate journey. For their words of encouragement and prayers, l am very grateful. I also would like to thank Mrs Naidoo for accommodating me in her home during my studies.

I am also grateful to all the institutions (UKZN Westville, CSIR Pretoria) for their technical input access to laboratories and equipment.

ABSTRACT

Depletion of landfill space, the cost of waste disposal, and environmental concerns are pushing Pulp and Paper Mills (PPMs) to make changes and improvements in the way waste is handled. Pulp and paper mill sludge (PPMS) is a solid by-product of the wastewater treatment of the PPM industry; thus, it is considered a waste. This study was conducted to investigate the feasibility of producing cellulose nanofibrils (CNFs) from waste material such as PPMS instead of using high purity cellulose products such as chemical pulps as the starting material.

Three PPMS samples collected from different South African (SA) mills were chemically and physically characterised to investigate their suitability for various beneficiation pathways. The overall objective was to analyse and allocate the most suitable beneficiation process to each PPMS sample based on the characterisation results and literature. The possible beneficiation pathways of the pulp and paper mill sludge (PPMS) samples were discussed in line with their characteristics. The characteristics of PPMS were influenced by the pulping technique employed at each mill, the raw material and the type of effluent treatment employed. Thermal analysis revealed that the calorific values of all PPMS samples studied were too low for energy harvesting (thermal processing). The high ash content of PPMS C (de-inking) and PPMS A (recycle) was suitable for biocomposites whose strength could be enhanced by fillers present in PPMS samples. The higher glucose content in PPMS B (virgin) compared to PPMS A (recycle) and PPMS C was favourable for bioethanol and bio-oil production. The high cellulose and low ash content of PPMS B were found suitable for the production of nanocellulose.

Highly fibrillated CNFs were produced from three different PPMS samples by grinding using the automated Super mass colloider (SMC) after washing and bleaching to remove impurities. Chemical composition analysis showed a considerable reduction in ash content due to screen washing, successful cellulose concentration, and lignin removal by bleaching. The crystallinity index (CrI) was calculated to be 51.1%, 58.1% and 59.4% for CNF A, CNF B and CNF C, respectively. TGA analysis showed a progressive decrease in thermal stability from untreated PPMS to CNFs.The overall yield for the production of CNFs from PPMS A, PPMS B and PPMS C was 27.2%, 32% and 42.8%, respectively.

Finally, a description of the transition from manual grinding using the SMC to an automated operation was done. The automated system was designed to pump the feedstock through the SMC via sample holding tanks for a predetermined number of passes. The automated operation alleviated challenges associated with the manual operation, which included high labour demands, loss of material due to spillages, thus affecting yield and posing a safety risk in the working environment, inconsistent product due to human error in counting the number of cycles, low productivity due to long working hours. The introduction of the automated SMC system was a worthwhile investment justifiable by improving efficiency and operator safety

Contents

LIST OF FIGURES

LIST OF TABLES

NOMENCLATURE

Abbreviation	Description
CNFs	Cellulose Nanofibrils
CNCs	Cellulose Nanocrystals
PPMS	Pulp and Paper Mill Sludge
PPM	Pulp and Paper Mill
TEMPO	Tetramethylpiperidin-1-yl-oxidanyl
TMP	Thermomechanical Pulp
CTMP	Chemo Thermomechanical Pulp
C-PAM-B	Cationic Polyacrylamide Hydrated Bentonite
C-PAM	Cationic Polyacrylamide
PAE	Polyamide Amine Epichlorohydrin
GCC	Ground Calcium Carbonate
PCC	Precipitated Calcium Carbonate
GCC-B	Ground Calcium Carbonate with bentonite
ASA	Alkenyl succinic anhydride
BKP	Bleached Kraft Pulp
DIP	Deinked Recycled Pulp
ONP	Old Newspaper Prints
NaClO	Sodium hypochlorite
$CaCO_3$	Calcium Carbonate
SiO_2	Silicon Dioxide

Al_2O_3	Aluminum Oxide
CaO	Calcium Oxide
MgO	Magnesium Oxide
TiO_2	Titanium dioxide
NH_4^+	Ammonium ion
K_2O	Potassium oxide
Fe_2O_3	Iron (III) oxide
CrI	Crystalline index
RN-PS	Recycled newsprint sludge
CR-PS	Corrugated recycled sludge
MDF	Medium-density fibreboards
TS	Thickness swell
LE	Linear expansion
IB	Internal bond
MOE	Modulus of elasticity
MOR	Modulus of rupture
DTG	Derivative Thermogravimetric
TGA	Thermogravimetric analysis
XRD	X-ray diffraction
EDX	Energy Dispersive X-Ray Analyser
FTIR	Fourier-transform infrared spectroscopy
T_{max}	Maximum thermal decomposition temperature

T_{onset}	Onset temperature
NaBr	Sodium bromide
SSA	Specific Surface Area
UBSWP	Unbleached Softwood Pulp
RBA	Relative Bonded Area
RE-CNF	Refined CNF
EN-CNF	Enzymatic CNF
CM-CNF	Carboxymethylated CNF
EKP	*Eucalyptus* Kraft Pulp
BHKP	Bleached Hardwood Kraft Pulp
SBKP	Softwood bleached Kraft Pulp
UBK	Unbleached Kraft
MPSP	Minimum Product Selling Price

1 CHAPTER ONE: INTRODUCTION

1.1 Background and motivation

Environmental consciousness is the driving force to replace fossil oil-based products with renewable, biodegradable, and non-toxic materials. For this reason, there has been a remarkable interest in the exploitation of natural resources such as cellulose, chitin/chitosan, alginate, carrageenan, natural rubber, polypeptides and proteins (Cherian et al. 2010; Chiaoprakobkij et al. 2011; Butchosa et al. 2013). Cellulose is advantageous because of its abundance, ability to form nano-sized derivatives with excellent properties such as high aspect ratio, surface area, low density, and mechanical strength. The nanosized derivatives are cellulose nanocrystals (CNCs) and cellulose nanofibrils (CNFs) (Kim et al. 2019). CNFs combine the advantageous properties of cellulose, such as biodegradability, the potential for chemical modification and renewability, to their specific nanosize attributes. The cost of production of CNFs is attributed to high energy consumption during mechanical treatment, cost of chemicals for pretreatment, low yields from feedstock and the cost of feedstock. A cheaper source of CNFs compared to the conventional source (*viz.*, pulp) reduces the overall production cost of CNFs significantly. For instance, if a zero cost source such as PPMS is used, the production process becomes cost efficient.

The biorefinery concept entails extracting the most value from raw material input, minimization, and beneficiation of waste produced. Integrating the biorefinery concept with the Pulp and Paper Mill (PPM) industry by reuse and/or valorization of PPMS is a waste management solution that offers an expansion of the range of products produced in addition to traditional wood, pulp, and paper products. This is crucial to ensure that the PPM industry remains relevant despite its contraction due to the global shift towards digital media and paperless communication, thus affecting revenue in the printing and writing department (Veitch 2018; Zambrano et al. 2020). Currently, in South Africa, PPMS is considered waste and disposed of in landfills. Landfilling causes environmental problems such as greenhouse emissions and the leaching of toxic chemicals into the surface and underground water (Marques et al. 2008). The increased awareness of environmental risks associated with PPMS landfilling, tightened legislation in waste management, landfilling costs, and limited landfill space are the major driving forces for the PPM industry to seek alternative solutions for sustainable management of the PPMS (Mahmood and Elliott 2006). The use of PPMS sustainably and profitably may offer several benefits for the environment, develop new markets for the sector, increase revenue streams and employment opportunities, and ensure the industry remains relevant despite its contraction due to the global shift towards digital media and paperless communication (Alkasrawi et al. 2016; Zambrano et al. 2020). PPMS is an attractive resource due to its composition and the fact that it is already pre-treated according to mill processes such as chemical and mechanical pulping, unlike virgin raw materials that require extensive treatments to remove or soften lignin and other impurities (Leão et al. 2012). PPMS is readily available due to its constant production in local PPMs (Crespo et al. 2012; Dwiarti et al. 2012).

CNFs have a wide range of possible applications such as automotive, construction, paper, hygiene, absorbent, aerospace, oil and gas, medical, food industry (Belbekhouche et al. 2011; Charreau et al. 2013). In the papermaking industry, CNFs are used to reinforce the strength properties of paper. CNFs improve the mechanical, functional and barrier properties of different types of paper.

1.2 Problem statement

South Africa produces pulp and paper from plantation-grown trees to meet the high paper consumption (approximately 2 million annually) in the country (PAMSA 2018). The PPMs form a very important sector that

contributes significantly to the economy and society. Inevitably, the PPMs produce approximately 0.5 million tonnes of waste per annum in the form of sludge from their operations (Robus et al. 2016). The majority of the previously proposed and studied beneficiation pathways are either environmentally unfriendly or economically unviable. For instance, heavy metals in PPMS from recycle mills deems PPMS unsuitable for use as a soil amendment (Marques et al. 2008). The high moisture content is a major drawback in thermal processing applications such as incineration and pyrolysis for energy recovery. Furthermore, the variation and fluctuation in composition of PPMS from one PPM to another due to the difference in raw materials and pulping methods pose a need to develop and optimize beneficiation methods suited for each type of PPMS. This project aimed to produce cellulose nanofibers using mechanical grinding.

1.3 Research question

Will South Africa benefit from cellulose nanofibrils (CNFs) extracted from PPMS?

Extraction of a valuable product such as CNFs alleviates the environmental hazards associated with the disposal of PPMS, reduces tonnages of PPMS disposed, and decreases costs associated with transportation and landfill disposal fee but can also generate revenue for the paper mill industry.

1.4 Aims and objectives

The overall aim of the project was to provide a waste management solution to the PPM industry by producing CNFs from PPMS.

The specific objectives addressed during this study were as follows:

1. To characterise and compare three types of PPMS samples and identify possible beneficiation pathways based on their characteristics
2. To produce and characterise CNFs from the three PPMS samples using a range of analytical and microscopy techniques

1.5 Limitations

This research is limited because the energy consumption for the production of CNFs was not measured due to the lack of a power meter attached to the automated Supermasscolloider (SMC).

1.6 Thesis organisation

This dissertation is composed of four self-contained chapters. The chapters are presented in the format of journal articles to facilitate publication.

Chapter 1: Introduction to the project, which included the motivation and overview of the research.

Chapter 2: Published review article focusing on the role of cellulose nanofibrils in improving the strength properties of paper. The paper explains the role played by CNFs as an additive to improve strength properties of papers and the factors affecting the improvement in paper quality when CNFs are added as additives.

Chapter 3: Extensive characterisation of different types of PPMS. The possible beneficiation pathways of the pulp and paper mill sludge (PPMS) samples were discussed in line with their characteristics.

Chapter 4: Production of highly fibrillated CNFs from three types of PPMS samples using an automated SMC. The CNFs were analysed using a range of analytical and microscopic techniques. The characteristics of CNFs were compared with untreated PPMS and bleached PPMS.

Chapter 5: Describes the working principle and components of the automated SMC.

Chapter 6: General conclusions of the entire research study, recommendations and proposed future works.

:

1.7 References

Alkasrawi M, Al-Hamamre Z, Al-Shannag M, Abedin MJ, Singsaas E (2016) Conversion of paper mill residuals to fermentable sugars. BioResources 11 (1)**:** 2287-2296. https://doi.org/10.15376/biores.11.1.2287-2296

Belbekhouche S, Bras J, Siqueira G, Chappey C, Lebrun L, Khelifi B, Marais S, Dufresne A (2011) Water sorption behavior and gas barrier properties of cellulose whiskers and microfibrils films. Carbohydrate Polymers 83 (4)**:** 1740-1748. https://doi.org/10.1016/j.carbpol.2010.10.036

Butchosa N, Brown C, Larsson PT, Berglund LA, Bulone V, Zhou Q (2013) Nanocomposites of bacterial cellulose nanofibers and chitin nanocrystals: fabrication, characterisation and bactericidal activity. Green chemistry 15 (12)**:** 3404-3413. https://doi.org/10.1039/c3gc41700j

Charreau H, L Foresti M, Vazquez A (2013) Nanocellulose patents trends: a comprehensive review on patents on cellulose nanocrystals, microfibrillated and bacterial cellulose. Recent patents on nanotechnology 7 (1)**:** 56-80. https://doi.org/10.2174/187221013804484854

Cherian BM, Leão AL, De Souza SF, Thomas S, Pothan LA, Kottaisamy M (2010) Isolation of nanocellulose from pineapple leaf fibres by steam explosion. Carbohydr Polym 81 (3)**:** 720-725. https://doi.org/10.1016/j.carbpol.2010.03.046

Chiaoprakobkij N, Sanchavanakit N, Subbalekha K, Pavasant P, Phisalaphong M (2011) Characterisation and biocompatibility of bacterial cellulose/alginate composite sponges with human keratinocytes and gingival fibroblasts. Carbohydr Polym 85 (3)**:** 548-553. https://doi.org/10.1016/j.carbpol.2011.03.011

Crespo CF, Badshah M, Alvarez MT, Mattiasson B (2012) Ethanol production by continuous fermentation of d-(+)-cellobiose, d-(+)-xylose and sugarcane bagasse hydrolysate using the thermoanaerobe Caloramator boliviensis. Bioresour Technol 103 (1)**:** 186-191. https://doi.org/10.1016/j.biortech.2011.10.020

Dwiarti L, Boonchird C, Harashima S, Park EY (2012) Simultaneous saccharification and fermentation of paper sludge without pretreatment using cellulase from Acremonium cellulolyticus and thermotolerant Saccharomyces cerevisiae. Biomass Bioenergy 42**:** 114-122. https://doi.org/10.1016/j.biombioe.2012.02.019

Kim KM, Lee JY, Jo HM, Kim SH (2019) Cellulose nanofibril grades' effect on the strength and drainability of security paper. BioResources 14 (4)**:** 8364-8375.

Leão AL, Cherian BM, de Souza SF, Sain M, Narine S, Caldeira MS, Toledo MAS (2012) Use of primary sludge from pulp and paper mills for nanocomposites. Mol Cryst 556 (1)**:** 254-263. https://doi.org/10.1080/15421406.2012.635974

Mahmood T, Elliott A (2006) A review of secondary sludge reduction technologies for the pulp and paper industry. Water Res 40 (11)**:** 2093-2112. https://doi.org/10.1016/j.watres.2006.04.001

Marques S, Alves L, Roseiro J, Gírio F (2008) Conversion of recycled paper sludge to ethanol by SHF and SSF using Pichia stipitis. Biomass bioenergy 32 (5)**:** 400-406. https://doi.org/10.1016/j.biombioe.2007.10.011

PAMSA (2018). South African pulp and paper production, import and export statistics for 2018. Paper Manufacturers Association of South Africa. https://www.thepaperstory.co.za/wp-content/uploads/2021/01/PAMSA-2018-Industry-Statistics-Summary-edited.pdf

Robus CL, Gottumukkala LD, Van Rensburg E, Görgens JFJRE (2016) Feasible process development and techno-economic evaluation of paper sludge to bioethanol conversion: South African paper mills scenario. Renew Energy 92**:** 333-345. https://doi.org/10.1016/j.renene.2016.02.017

Veitch C. (2018). *The manufacture of Paper and paper product* [Online]. [Accessed October 2021].https://www.whoownswhom.co.za/store/info/4615

Zambrano F, Starkey H, Wang Y, de Assis CA, Venditti R, Pal L, Jameel H, Hubbe MA, Rojas OJ, Gonzalez R (2020) Using micro-and nanofibrillated cellulose as a means to reduce weight of paper products: A review. BioResources 15 (2)**:** 4553-4590. https://doi.org/10.15376/biores.15.2.zambrano

2 CHAPTER TWO: ROLE OF CELLULOSE NANOFIBRILS IN IMPROVING THE STRENGTH PROPERTIES OF PAPER: A REVIEW (This paper was published in the Journal of Cellulose and is available online https://doi.org/10.1007/s10570-021-04294-8)

Thabisile Brightwell Jele[1], Prabashni Lekha[2], Bruce Sithole[1, 2]

[1]*University of KwaZulu-Natal (Howard Campus), Discipline of Chemical Engineering, College of Agriculture, Engineering and Sciences, Durban,* [2]*Council for Scientific and Industrial Research, Biorefinery Industry Development Facility, Durban, South Africa*

[*]Corresponding Authors: thabisilejele94@gmail.com; sitholeb1@ukzn.ac.za

2.1 Abstract

The pursuit for sustainability in the papermaking industry calls for the elimination or reduction of synthetic additives and the exploration of renewable and biodegradable alternatives. Cellulose nanofibrils (CNFs), due to their inherent morphological and biochemical properties, are an excellent alternative to synthetic additives. These properties enable CNFs to improve the mechanical, functional, and barrier properties of different types of paper. The nanosize diameter, micrometre length, semicrystalline structure, high strength, and modulus of CNFs have a direct influence on the mechanical properties of paper, such as tensile index, burst index, Scott index, breaking length, tear index, Z-strength, E-modulus, strain at break, and tensile stiffness. This review details the role played by CNFs as an additive to improve strength properties of paper and the factors affecting the improvement in paper quality when CNFs are added as additives. The paper also includes techno-economic aspects of the process and identifies areas that need further research.

Keywords: cellulose nanofibrils, paper additive, mechanical properties, strength properties

2.2 Introduction

The growing cognisance of environmental concerns has shifted attention from petroleum-based materials to natural organic materials in various applications. Nanomaterials are becoming popular because of their extraordinary properties attributed to the nanosize dimension (Alagarasi 2013; Zeng et al. 2020). In particular, cellulose nanomaterials exhibit high strength and barrier properties (Abe and Yano 2009; Lee et al. 2017). Cellulose is the main component of plant cell walls responsible for providing protection, strength, and support when the cells increase in size. The basic structure of cellulose, represented in Fig. 1, shows that cellulose is a long, linear chain polymer in which D-glucose units are joined in a 1, 4 β-linkage.

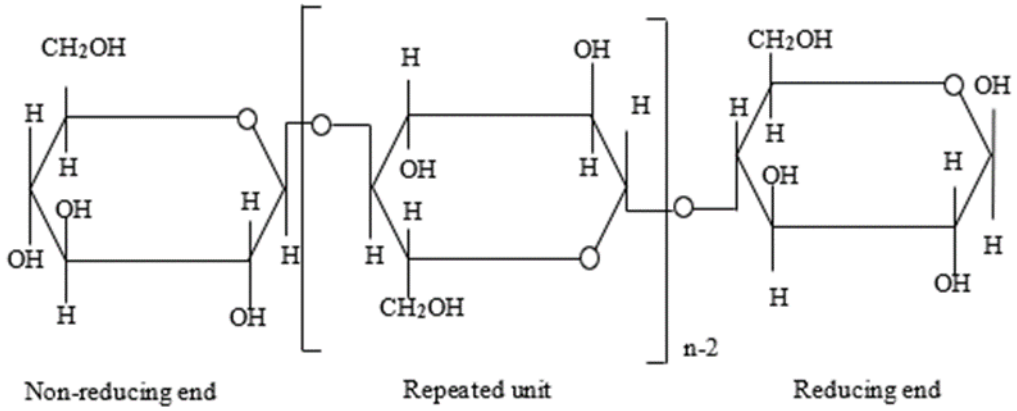

Figure 2-1 Basic structure of cellulose redrawn from French (2017)

Cellulose has two nanosize derivatives, which are cellulose nanocrystals (CNCs) and CNFs (Nechyporchuk et al. 2016). Figure 2-1 shows the production steps of CNCs and CNFs from biomass. The nanosized rod-like fibres obtained by cleavage of the amorphous regions while preserving the crystalline regions are termed CNCs (Moon et al. 2011; Khalil et al. 2014; Naz et al. 2019). The nanosized long entangled fibres obtained by mechanical shearing forces are termed CNFs (Abe et al. 2007; Nechyporchuk et al. 2016; Kumar et al. 2021).

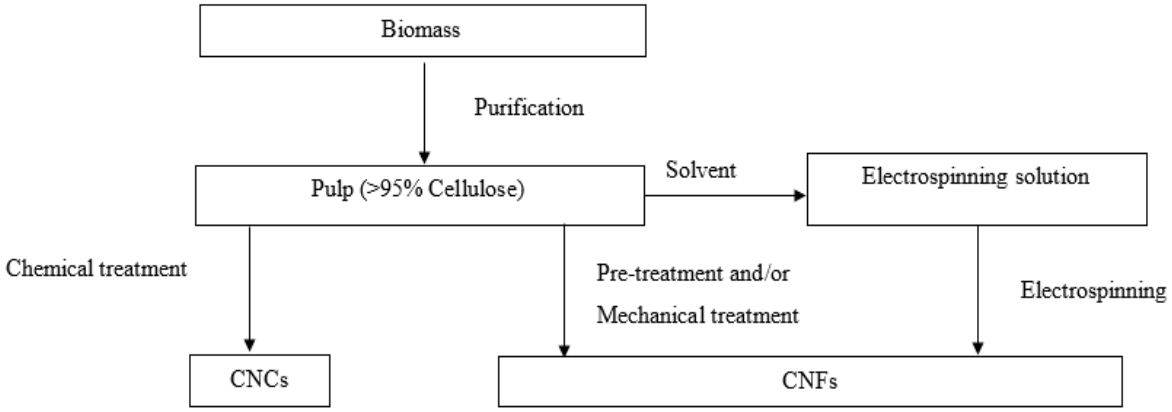

Figure 2-2 Production steps of CNFs and CNCs from biomass redrawn from de Assis et al. (2017)

CNCs by standard definition (ISO/TS 20477:2017) have an aspect ratio of less than 50 and contain crystalline and paracrystalline regions. CNFs, by standard definition, have an aspect ratio of more than 10 and contain crystalline and amorphous regions. Its dimensions are typically 3-100 nm in width and up to 100 µm in length (ISO/TS 20477:2017) (Fotie et al. 2020). CNCs and CNFs with diameters larger than e.g. 5 nm are usually aggregations of several CNFs or CNCs. The crystalline region is highly ordered and has low flexibility and is responsible for rigidity and tensile strength. The amorphous region is the less ordered region, which plays a role in extensibility and flexibility (Moon et al. 2011). These properties give CNFs a broad spectrum of applications. Each application has specific demands from the CNF properties (Johansson 2011; Adnan et al. 2018). The applications include rheology modifiers, emulsion stabilisers, nanocomposites, papermaking, films, aerogels, bio-medicals, cosmetics, pharmaceuticals, hygiene, foods and absorbent products (Cowie et al. 2014; Lindstrom et al. 2015; Zeng et al. 2020). The CNF market or application can be divided into low volume, high volume, and novel, as illustrated in Figure 2-3 (Li et al. 2013).

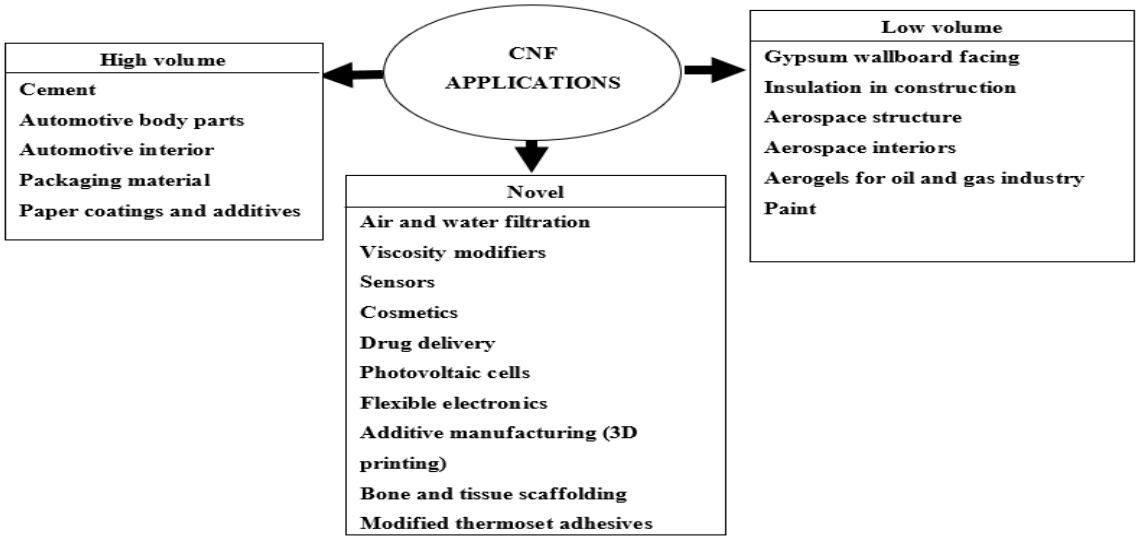

Figure 2-3 A list of applications of CNFs (Cowie et al. 2014; Cao et al. 2019)

Papermaking is an example of a high volume application where the fibrous nature of cellulose is of paramount importance (Cowie et al. 2014). Even though CNFs were identified many years back as a paper additive, the major challenge impeding its commercial use has been the high production cost, low yields from feedstocks, its negative impact on drying, pressing due to poor drainage properties, and poor retention of CNFs within pulp (Su et al. 2013; Bardet and Bras 2014; Hubbe 2014). The production cost is attributed to the high energy requirements in processing CNFs. The main raw material in papermaking is wood. The general processes in papermaking are feedstock preparation (debarking and chipping), pulping (chemical and mechanical), and sheet preparation (forming, pressing, and drying) (Gullichsen et al. 2000). In addition to pulp, additives, such as fillers, flocculants, sizing, and retention agents are used to facilitate handling and improve end-use properties such as opacity and wet or dry strength properties of paper (Ankerfors et al. 2014; Diab et al. 2015). CNFs can be added at various stages of the papermaking process. For instance, they can be added directly into pulp. This increases the pulp total surface area, which also causes water retention by hydrogen bonding, thereby causing drainage problems. Externally, CNFs can be used as a coating on the finished paper to improve barrier, printing and functional properties (viz., antimicrobial, conductive, luminescent, etc.) (Bardet and Bras 2014). It is well known that CNFs improve the physical and mechanical properties of paper, diminish drainability, and create runnability problems (Ahola et al. 2008; Johnson et al. 2016). For instance, a 130% increase in tensile index was reported for paper produced using bleached softwood pulp, polyamide amine epichlorohydrin (PAE) and 10 wt% carboxymethylated CNFs. Alcalá et al. (2013) reported a 169% increase in tensile index for paper produced using unbleached hardwood kraft pulp combined with cationic starch and 12 wt% 2,2,6,6-tetramethylpiperidin-1-yl-oxidanyl (TEMPO)-oxidised CNFs. Low dosages of CNFs in the presence or absence of retention aids and additives led to little improvement in the mechanical strength of CNF reinforced paper. As an example, 4 wt% of mechanically produced CNFs resulted in only a 21% increase in the tensile index for thermomechanical pulp (TMP) paper (Eriksen et al. 2008). Mashkour et al. (2015) produced paper using 10 wt% of mechanically produced and acetylated CNFs combined with softwood pulp in the presence of cationic polyacrylamide (C-PAM) as a retention aid. A 17% increase in the tensile index was reported. However, some authors have reported a negative effect of CNFs on the tensile strength of paper (Ämmälä et al. 2013; Diab et al. 2015). Therefore, it is important to understand the mechanisms of paper strengthening, effects of dosage, source, production method, and grade of CNFs. The main mechanisms involved in the reinforcement of paper with CNFs are (i) CNFs act as a bridge between fibres promoting fibre to fibre contact and an increase in bonded area, (ii) CNFs create an entangled nanoscale network embedded in the microfibre network, thus improving the strength of the paper, (iii) CNFs increase the contact area as many hydrogen bonds form between CNFs and pulp fibres, (iv) The nanosized dimension of CNFs result in increased surface area and in the number of available hydroxyl groups for interaction, thus promoting the formation of fibre to fibre contact and bonding, which in turn solidifies the structure of the paper (Boufi et al. 2017; Latifah et al. 2020). Reviews have been compiled which detail the strategies in which CNFs can be incorporated in papermaking, the interaction of CNFs with other additives, the impact of CNFs on paper properties, the best CNF grades, and the optimum amounts of CNFs employed (Bardet and Bras 2014; Brodin et al. 2014; Osong et al. 2016; Boufi et al. 2017; Jawaid et al. 2017; Lengowski et al. 2019; Balea et al. 2020; Das et al. 2020; Zambrano et al. 2020). A summary of reported studies is presented in Table 2-1, which includes the source of CNFs, production method, type of pulp for papermaking, additive or retention aid, filler, CNF dosage, mechanical properties, and references arranged in ascending order of the publication year. This review addresses the role

played by CNFs as an additive to improve the strength properties of paper and the factors affecting the improvement in paper quality when CNFs are added as additives.

Table 2-1 A review of studies published on the impact of CNFs on paper properties

CNF Source	**CNF production method**	**Type of pulp for papermaking**	**Additive or retention aid**	**Filler**	**CNFs (wt%)**	**Mechanical properties of sheets**	**Reference**
Bleached sulphite pulp	Carboxymethylation Microfluidisation	Bleached pine kraft pulp	Additive: PAE	None	10	Dry tensile index ~ 65 N ·m·g^{-1} Wet tensile index ~ 8.5 N ·m·g^{-1}	(Ahola et al. 2008)
Bleached sulphate kraft pulp	Grinding	TMP	None	None	4	Tensile index ~ 48 kN·m·kg^{-1}	(Eriksen et al. 2008)
Unrefined bleached softwood kraft fibres	Grinding	TMP	None	Clay	2.9	Tensile index ~ 60 N·m·g^{-1} Z-strength ~ 425 kPa	(Mörseburg and Chinga-Carrasco 2009)
Bleached hardwood kraft pulp	Refining Carboxymethylation Microfluidisation	Bleached softwood kraft pulp	Additives: High and medium molar mass cationic polyelectrolytes	None	10	Tensile index ~ 110 N·m·g^{-1}	(Taipale et al. 2010)

(-) information not provided in the cited reference

Table 2-1 A review of studies published on the impact of CNFs on paper properties (continued)

CNF Source	**CNF production method**	**Type of pulp for papermaking**	**Additive or retention aid**	**Filler**	**CNFs (wt%)**	**Mechanical properties of sheets**	**Reference**
Bleached chemical birch pulp.	Grinding	Bleached chemical softwood pulp (pine)	Additive: Cationic starch	None	5	Tensile index ~ 90 $N \cdot m \cdot g^{-1}$	(Manninen et al. 2011)
Bleached sulphite softwood pulp fibres from spruce	Mechanical beating Enzymatic treatment Homogenisation Microfluidisation	Sulphite softwood pulp fibres from spruce	None	Precipitated calcium carbonate (PCC)	10	Tensile strength = 160 ± 9 MPa Specific strength = 165 MPa $g^{-1} \cdot cm^{-3}$ Strain to Failure = 4.2 ± 0.5% Young's Modulus = 10.1 ± 0.3GPa Specific modulus =10.4 ± 0.8 $GPa \cdot g^{-1} \cdot cm^{-3}$	(Sehaqui et al. 2011)
Commercial dried, bleached *Eucalyptus* pulp	TEMPO-mediated oxidation High pressure homogenisation	Commercial dried, bleached E*ucalyptus* pulp	Retention agents: Cationic starch Colloidal silica	None	9	Tensile index = 51.3 $N \cdot m \cdot g^{-1}$ Burst index = 3.4 $KPa \cdot m^2 \cdot g^{-1}$ Scott Bond = 469 $J \cdot m^{-2}$	(González et al. 2012)

(-) information not provided in the cited reference

Table 2-1 A review of studies published on the impact of CNFs on paper properties (continued)

CNF Source	**CNF production method**	**Type of pulp for papermaking**	**Additive or retention aid**	**Filler**	**CNFs (wt%)**	**Mechanical properties of sheets**	**Reference**
Never-dried Pinus radiata kraft pulp	Homogenisation	Unbeaten newsprint grade TMP	Retention aid: Cationic polymer	Ground calcium carbonate (GCC)	5	Tensile index ~ 31 kN m kg^{-1} Strain at break ~ 1.7%	(Hii et al. 2012)
Pulp	Pre-refining Fibrillation	Chemical hardwood and softwood machine pulp mixture	Additive: cationic Starch		2	Tensile strength ~ 4.1 $kN \cdot m^{-1}$	(Kajanto and Kosonen 2012)
Softwood	Grinding	Softwood pulp	None	None	20	Tensile strength = 5621 ± 336 $N \cdot m^{-1}$ Tear Strength ~ 500 mN	(Afra et al. 2013)
		Bagasse pulp	None	None	20	Tensile strength ~ 4500 $N \cdot m^{-1}$ Tear Strength ~ 500 mN	
Bleached birch chemical wood pulp	TEMPO-mediated oxidation Periodate-chlorite oxidation Homogenisation	Kraft pulp	-	GCC	4	Tensile index ~ 60 $kN \cdot m \cdot kg^{-1}$ Tear index ~ 10 $N \cdot m^2 \cdot kg^{-1}$	(Ämmälä et al. 2013)

(-) information not provided in the cited reference

Table 2-1 A review of studies published on the impact of CNFs on paper properties (continued)

CNF Source	**CNF production method**	**Type of pulp for papermaking**	**Additive or retention aid**	**Filler**	**CNFs (wt%)**	**Mechanical properties of sheets**	**Reference**
Unbleached kraft pulp of Kenaf and Scotch Pine	PFI mill refining Enzymatic pre-treatment Homogenisation	Unbleached softwood kraft pulp	Retention aid: C-PAM	None	10	Tensile index increase = 32% Strain at break = 3.9% Tensile strength index = 61.5 ± 0.8 $N \cdot m \cdot g^{-1}$ Tensile energy absorption index = 1.5 ± 0.3 $kJ \cdot g^{-1}$ Tensile strength = 43.1 ± 0.5 MPa elasticity modulus = 4.6 ± 0.1 GPa Tensile stiffness = 6.5 ± 0.1 $N \cdot m \cdot g^{-1}$ Burst index = 6.9 ± 0.2 $kPa \cdot m^2 \cdot g^{-1}$	(Charani et al. 2013)
Bleached *Eucalyptus* pulp	TEMPO-mediated oxidation High pressure homogenisation	Enzyme-treated Pulp	Retention agents: Cationic starch Colloidal Silica	-	4.5	Tensile index = 50 $N \cdot m \cdot g^{-1}$Breaking length = 5102 ± 296 mBurst Index = 2.6 ± 0.26 $kPa \cdot m^2 \cdot g^{-1}$	(González et al. 2013)

Table 2-1 A review of studies published on the impact of CNFs on paper properties (continued)

CNF Source	**CNF production method**	**Type of pulp for papermaking**	**Additive or retention aid**	**Filler**	**CNFs (wt%)**	**Mechanical properties of sheets**	**Reference**
Bleached softwood sulphite pulp	Mechanical beating Enzymatic treatment Homogenisation	Bleached softwood pulp	Additive: Xyloglucan	-	10	Tensile index = 84.2 ± 1.6 $N \cdot m \cdot g^{-1}$ Tensile energy absorption (TEA) =123 ± 10.7 $J \cdot m^{-2}$ Wet tensile index = 0.75 ± 0.1 $N \cdot m \cdot g^{-1}$	(Sehaqui et al. 2013)
Bleached softwood sulphite pulp	Enzymatic pre-treatment PFI beating High pressure homogenisation	Beaten bleached hardwood and softwood kraft mixture	C-PAM Colloidal silica Cationic starch	PCC	5	Tensile strength index ~ 24 $kN \cdot m \cdot kg^{-1}$ Tensile stiffness index ~ 3.8 $mN \cdot m \cdot kg^{-1}$ Tear index ~ 5.3 $mN \cdot m^2 \cdot g^{-1}$ Fracture toughness ~ 5.5 $J \cdot m \cdot kg^{-1}$ Z-strength ~ 490 kPa Bending resistance ~ 60 mN	(Ankerfors et al. 2014)

(-) information not provided in the cited reference

Table 2-1 A review of studies published on the impact of CNFs on paper properties (continued)

CNF Source	CNF production method	Type of pulp for papermaking	Additive or retention aid	Filler	CNFs (wt%)	Mechanical properties of sheets	Reference
Softwood bleached kraft pulp	Ball milling	Eucalyptus kraft hardwood pulp	PAE	-	10	Dry tensile index ~ 35 $N \cdot m \cdot g^{-1}$ Wet Tensile index ~ 9 $N \cdot m \cdot g^{-1}$	(Su et al. 2014)
	Ball milling	Eucalyptus kraft hardwood pulp	-	-	10	Dry tensile index ~ 27 $N \cdot m \cdot g^{-1}$ Wet Tensile index ~ 2 $N \cdot m \cdot g^{-1}$	
Commercial bleached Eucalyptus pulp	TEMPO-mediated oxidation High-pressure homogenisation.	Deinked recycled pulp (DIP) suspension and old newspapers and old magazines	Retention aid: Cationic starch	-	4.5	Breaking length = 6054 ± 126 m Tensile Index = 59.4 ± 1.2 $N \cdot m \cdot g^{-1}$ Tensile Strength = 43.1 ± 0.9 MPa Young's Modulus = 4863 ± 203 MPa Elongation = 1.41 ± 0.3% Tear index = 6.1 ± 0.6 $mN \cdot m^2 \cdot g^{-1}$ Scott bond = 471.9 ± 36.9 $J \cdot m^{-2}$	(Delgado-Aguilar et al. 2015)
Bleached soda bagasse pulp	Enzymatic Refining Homogenisation	Bleached soda bagasse pulp	C-PAM	-	5	Tensile index ~ 60 $N \cdot m \cdot g^{-1}$	(Petroudy et al. 2014)

(-) information not provided in the cited reference

Table 2-1 A review of studies published on the impact of CNFs on paper properties (continued)

CNF Source	CNF production method	Type of pulp for papermaking	Additive or retention aid	Filler	CNFs (wt%)	Mechanical properties of sheets	Reference
Bleached kraft hardwood pulp	PFI mill beating Enzyme hydrolysis Homogenisation	Kraft hardwood pulp	Retention aid: Cationic starch and colloidal silica	-	3	Breaking length = 3891 ± 126 m Tensile index = 38 ± 1.2 $N \cdot m \cdot g^{-1}$	(Delgado Aguilar et al. 2015)
	PFI mill beating Homogenisation	Kraft hardwood pulp	Retention aid: Cationic starch and colloidal silica	-	3	Breaking length = 3512 ± 118 m Tensile index = 34.3 ± 1.2 $N \cdot m \cdot g^{-1}$	
	TEMPO-oxidation pH = 10 Homogenisation	Bleached kraft hardwood pulp	Retention aid: Cationic starch and colloidal silica	-	3	Breaking length = 4128 ± 112 m Tensile index = 40.3 ± 1.1 $N \cdot m \cdot g^{-1}$	
	Acid treatment Homogenisation	Bleached kraft hardwood pulp	Retention aid: Cationic starch and colloidal silica	-	3	Breaking length = 3595 ± 105 m Tensile index = 35.3 ± 1 $N \cdot m \cdot g^{-1}$	
	TEMPO-oxidation pH = 7, Homogenisation	Bleached kraft hardwood pulp	Retention aid: Cationic starch, Colloidal silica	-	3	Breaking length = 3874 ± 120 m Tensile index = 37.8 ± 1.2 $N \cdot m \cdot g^{-1}$	

Table 2-1 A review of studies published on the impact of CNFs on paper properties (continued)

CNF Source	**CNF production method**	**Type of pulp for papermaking**	**Additive or retention aid**	**Filler**	**CNFs (wt%)**	**Mechanical properties of sheets**	**Reference**
Bleached kraft bagasse pulp	Grinding	Beaten softwood and bagasse pulps	Retention aid: cationic polymer	Ground calcium carbonate With bentonite (GCC-B)	0.1	Tensile energy index = 1.3 ± 0.1 $J \cdot g^{-1}$ Burst index = 5 ± 0.4 $kPa \cdot m^2 \cdot g^{-1}$ Tear index = 13 ± 0.7 $mN \cdot m^2 \cdot g^{-1}$ Breaking length = 5.4 ± 0.1 km Elongation = 3.5 ± 0.4 mm Young's modulus = 3.5 ± 0.2 GPa	(Diab et al. 2015)
Softwood fibres	Grinding Acetylation of CNF	Unbeaten softwood acetylated pulp	Retention aid: C-PAM	-	10	Tensile index ~ 75 $N \cdot m \cdot g^{-1}$ Burst index ~ 6 $kpa \cdot m^2 \cdot g^{-1}$	(Mashkour et al. 2015)
Rice straw	Grinding	Beaten bleached rice straw and bagasse pulp	None	-	30	Breaking length = 8.9 km Burst factor = 4.9 gm^{-2} Tear factor = 2.1 mN g^{-1} m^{-2}	(Adel et al. 2016)
Cornstalk	Grinding	Beaten bleached rice straw and bagasse pulp	None	-	30	Breaking length = 8.8 km Burst factor = 4.7 $g \cdot m^{-2}$ Tear factor = 2.6 mN $g^{-1} \cdot m^{-2}$	

(-) information not provided in the cited reference

Table 2-1 A review of studies published on the impact of CNFs on paper properties (continued)

CNF Source	**CNF production method**	**Type of pulp for papermaking**	**Additive or retention aid**	**Filler**	**CNFs (wt%)**	**Mechanical properties of sheets**	**Reference**
Wheat straw	Mechanical beating High pressure homogenisation	Semi chemical wheat pulp slurry	Retention Agents: Cationic Starch Colloidal Silica	-	4	Breaking length = 6674 ± 77 m Burst index = 3.7 ± 0.1 $kPa \cdot m^2 \cdot g^{-1}$ Tear index = 4.3 ± 0.04 $mN \cdot m^2 \cdot g^{-1}$	(Espinosa et al. 2016)
Bleached bagasse pulp	PFI mill refining	Bleached bagasse fibres	None	-	20	Tensile index = 64.7 ± 1.2 $N \cdot m \cdot g^{-1}$ Burst index = 5.3 ± 0.2 $kPa \cdot m^2 \cdot g^{-1}$ Tear index = 9.1 ± 0.3 $mN \cdot m^2 \cdot g^{-1}$	(Kumar et al. 2016)
Bleached hardwood pulp	PFI mill refining	Bleached hardwood pulp	None	-	20	Tensile index = 61.7 ± 1 $N \cdot m \cdot g^{-1}$ Burst index = 5.1 ± 0.4 $kPa \cdot m^2 \cdot g^{-1}$ Tear index = 10.1 ± 0.5 $mN \cdot m^2 \cdot g^{-1}$	

(-) information not provided in the cited reference

Table 2-1 A review of studies published on the impact of CNFs on paper properties (continued)

CNF Source	CNF production method	Type of pulp for papermaking	Additive or retention aid	Filler	CNFs (wt%)	Mechanical properties of sheets	Reference
Bleached softwood pulp	PFI mill refining	Bleached softwood pulp	None	-	20	Tensile index = 70.3 ± 1.2 $N \cdot m \cdot g^{-1}$ Burst index = 7.2 ± 0.3 $kPa \cdot m^2 \cdot g^{-1}$ Tear index = 13.5 ± 1.5 $mN \cdot m^2 \cdot g^{-1}$	(Kumar et al. 2016)
Eucalyptus sawdust	TEMPO-mediated oxidation High-pressure homogenisation.	Unbleached eucalyptus pulp	Cationic starch Colloidal silica	-	9	Tensile index = 53.3 ± 1.1 $N \cdot m \cdot g^{-1}$ Young's Modulus = 6 ± 0.1 GPa Burst Index = 6.1 ± 0.1 $kPa \cdot m^2 \cdot g^{-1}$	(Vallejos et al. 2016)
Cornstalk pulp and rape stalk pulp	PFI mill refining TEMPO mediated oxidation Homogenisation	Old-newspaper and old magazines	Retention aid: chitosan	-	0.5	Tensile index ~ 52 $N \cdot m \cdot g^{-1}$	(Balea et al. 2017)
			Retention aid: CPAM and poly quaternary ammonium chloride	-	0.5	Tensile index ~ 41 $N \cdot m \cdot g^{-1}$	
Bleached hardwood Kraft Pulp	Valley beater Grinding	Mixture of Hardwood and Softwood bleached Kraft Pulp	Cationic starch CPAM	PCC	2	Tensile index = 21.9 ± 1.1 $N \cdot m \cdot g^{-1}$	(He et al. 2017)

Table 2-1 A review of studies published on the impact of CNFs on paper properties (continued)

CNF Source	**CNF production method**	**Type of pulp for papermaking**	**Additive or retention aid**	**Filler**	**CNFs (wt%)**	**Mechanical properties of sheets**	**Reference**
Eucalyptus globulus bleached kraft pulp	TEMPO-mediated oxidation, sodium bromide (NaBr), sodium hypochlorite (NaClO), Homogenisation	-	Internal strength agent: cationic starch, sizing agent: Alkenyl succinic anhydride (ASA). Retention aid: CPAM	PCC	3	Tensile index = 23.6 ± 0.1 $N \cdot m \cdot g^{-1}$ Tensile index w/o PCC = 54.9 ± 2.8 $N \cdot m \cdot g^{-1}$	(Lourenço et al. 2017)
Masson pine chemical pulp	Enzymatic Microfluidisation Rhodamine B isothiocyanate (RBITC)	Eucalyptus mechanical pulp	Polyquaternium-11 Poly (N-isopropyl acrylamide) (PAM)	-	10	Tensile index ~ 16 $N \cdot m \cdot g^{-1}$ Tensile energy absorption index ~ 100 $mJ \cdot g^{-1}$ Young's Modulus ~ 0.6 GPa	(Ding et al. 2018)
			Cationic starch	-	10	Tensile index ~ 20 $N \cdot m \cdot g^{-1}$ Tensile energy absorption index ~ 140 $mJ \cdot g^{-1}$ Young's Modulus ~ 0.7 GPa	
Softwood kraft pulp	Grinding Refining	Cotton linters mixed pulp	-	-	10	Tensile index ~ 35 $N \cdot m \cdot g^{-1}$ Folding endurance ~1500	(Park et al. 2018)

(-) information not provided in the cited reference

Table 2-1 A review of studies published on the impact of CNFs on paper properties (continued)

CNF Source	**CNF production method**	**Type of pulp for papermaking**	**Additive or retention aid**	**Filler**	**CNFs (wt%)**	**Mechanical properties of sheets**	**Reference**
-	Mechanical	Unbeaten semi-bleached soda bagasse pulp	Cationic starch	-	2	Tensile index = 41.3 $N \cdot m \cdot g^{-1}$ Burst index = 2.3 $kPa \cdot m^2 \cdot g^{-1}$ Tear = 7.6 $mN \cdot m^2 \cdot g^{-1}$	(Tajik et al. 2018)
Recycled old newsprint	TEMPO-mediated oxidation Homogenisation	Recycled old newsprint	Retention aid: Cationic Polyacrylamide Hydrated Bentonite clay (C-PAM-B)	-	3	Tensile index increase = 35%	(Balea et al. 2019)
Old corrugated containers	TEMPO-mediated oxidation Homogenisation	Old corrugated containers pulp	Retention aid: C-PAM-B	-	3	Tensile index increase ~ 60% Burst index increase ~ 20%	(Balea et al. 2019)

(-) information not provided in the cited reference

Table 2-1 A review of studies published on the impact of CNFs on paper properties (continued)

CNF Source	**CNF production method**	**Type of pulp for papermaking**	**Additive or retention aid**	**Filler**	**CNFs (wt%)**	**Mechanical properties of sheets**	**Reference**
Bleached Eucalyptus pulp	PFI mill beating Carboxymethylation Homogenisation	Bleached Eucalyptus pulp	None	PCC	3	Tensile index = 37.6 ± 1.8 N· m· g^{-1} Burst index = 2.2 ± 0.2 kPa $m^2 \cdot g^{-1}$ Tear index = 5.2 ± 0.3 mN· $m^2 \cdot g^{-1}$	(Lourenço et al. 2019b)
	PFI mill beating Carboxymethylation Homogenization	Bleached Eucalyptus pulp	Cationic starch, ASA and CPAM	PCC	3	Tensile index = 23.1 ± 0.7 N· m· g^{-1} Burst index =1.2 ± 0.1 kPa $m^2 \cdot g^{-1}$ Tear index = 4.9 ± 0.4 mN· $m^2 \cdot g^{-1}$	
	TEMPO-mediated oxidation Homogenisation	Bleached Eucalyptus pulp	-	PCC	3	Tensile index = 32.5 ± 1 N· m·g^{-1} Burst index =1.9 ± 0.1 kPa $m^2 \cdot g^{-1}$ Tear index = 4.7 ± 0.4 mN· $m^2 \cdot g^{-1}$	
	TEMPO-mediated oxidation Homogenisation	Bleached Eucalyptus pulp	Cationic starch, ASA and C-PAM	PCC	3	Tensile index = 25.2 ± 1.5 N· m·g^{-1} Burst index =1.4 ± 0.1 kPa $m^2 \cdot g^{-1}$ Tear index = 4.5 ± 0.3 mN· $m^2 \cdot g^{-1}$	

(-) information not provided in the cited reference

Table 2-1 A review of studies published on the impact of CNFs on paper properties (continued)

CNF Source	**CNF production method**	**Type of pulp for papermaking**	**Additive or retention aid**	**Filler**	**CNFs (wt%)**	**Mechanical properties of sheets**	**Reference**
Bleached Eucalyptus pulp	PFI mill beating Enzymatic Homogenisation	Bleached Eucalyptus pulp	Internal strength agent: cationic starch, sizing agent: ASA, Retention aid: CPAM	PCC	3	Tensile index ~ 36 N· m·g^{-1}	(Lourenço et al. 2019a)
	PFI mill refining Homogenisation	Bleached *Eucalyptus* pulp	-	PCC	3	Tensile index ~ 42 N· m·g^{-1}	
Recycled bleached de-inked pulp	PFI mill refining Homogenisation	*Eucalyptus* pulp	-	-	20	Tensile index = 55 N·m·g^{-1}	(Ang et al. 2020)
Bleached mixed hardwood pulp	Chemo-refining (Potassium hydroxide, sodium periodate ($NaIO_4$), sodium chlorite ($NaClO_2$), valley beating)	Bleached mixed hardwood pulp	Alcofix (poly diallyl dimethyl ammonium chloride-cationic polyDADMAC), Cationic starch Alkyl ketene dimer (AKD)	None	5	Breaking length ~ 5182 ± 167 m Burst factor ~ 39.4 ± 0.7 g·m^{-2} Tear factor ~ 86.2 ± 1.5 g·m^{-2}	(Kumar et al. 2020)

Table 2-1 A review of studies published on the impact of CNFs on paper properties (continued)

CNF Source	**CNF production method**	**Type of pulp for papermaking**	**Additive or retention aid**	**Filler**	**CNFs (wt%)**	**Mechanical properties of sheets**	**Reference**
Bleached kraft pulp	TEMPO-mediated oxidation PFI mill refining Homogenisation	Bleached kraft pulp	-	-	10	Burst index = 4 kPa·m^2·g^{-1} Tear index = 11 mN·m^2 ·g^{-1} Tensile index = 62 N·m·g^{-1}	(Latifah et al. 2020)
Eucalyptus	Grinding	*Eucalyptus*	-	-	9	Tensile index = 38.2 N·m·g^{-1} Burst index = 2.9 Kpa·m^2·g^{-1} Tear index =10.6 mN·m^2·g^{-1}	(Potulski et al. 2020)
Bleached softwood kraft pulp	Refining	Old corrugated container (OCC) pulp	Retention aid: Cationic starch		6	Tensile index ~ 42.5 kN·m·kg^{-1} Bursting index ~ 2.5 Kpa·m^2·g^{-1}	(Sanchez-Salvador et al. 2020)
Bleached softwood kraft pulp	TEMPO-mediated oxidation Homogenisation	Old corrugated container (OCC) pulp	Retention aid: Cationic starch	-	6	Tensile index ~ 37.5 kN·m·kg^{-1} Bursting index ~ 2.3 Kpa·m^2·g^{-1}	

(-) information not provided in the cited reference

Table 2-1 A review of studies published on the impact of CNFs on paper properties (continued)

CNF Source	CNF production method	Type of pulp for papermaking	Additive or retention aid	Filler	CNFs (wt%)	Mechanical properties of sheets	Reference
Bleached softwood kraft pulp	Enzymatic Grinding	Recycled pulp Hardwood pulp	-	-	10	Tensile index = 27.3 $N \cdot m \cdot g^{-1}$ Burst index = 1.4 $Kpa \cdot m^2 \cdot g^{-1}$	(Zeng et al. 2021)
	Grinding Microfluidisation	Recycled pulp Hardwood pulp	-	-	8	Tensile index = 29.9 $N \cdot m \cdot g^{-1}$ Burst index = 1.5 $Kpa \cdot m^2 \cdot g^{-1}$	
SBKP	PFI mill refining Microfluidisation	Recycled pulp	-	-	5	Tensile index ~ 34.7 $N \cdot m \cdot g^{-1}$ Burst index ~ 2.5 $Kpa \cdot m^2 \cdot g^{-1}$	(Hu et al. 2021)
	Ball milling Ultrasonication	Recycled pulp	-	-	5	Tensile index ~ 34 $N \cdot m \cdot g^{-1}$ Burst index ~ 2.4 $Kpa \cdot m^2 \cdot g^{-1}$	
	Grinding Microfluidisation	Recycled pulp	-	-	5	Tensile index ~ 32 $N \cdot m \cdot g^{-1}$ Burst index ~ 2.2 $Kpa \cdot m^2 \cdot g^{-1}$	
	PFI mill refining	Recycled pulp	-	-	5	Tensile index ~ 30.8 $N \cdot m \cdot g^{-1}$ Burst index ~ 2.2 $Kpa \cdot m^2 \cdot g^{-1}$	
	Grinding	Recycled pulp	-	-	5	Tensile index ~ 31 $N \cdot m \cdot g^{-1}$ Burst index ~ 2.2 $Kpa \cdot m^2 \cdot g^{-1}$	
	Ball milling	Recycled pulp	-	-	5	Burst index ~ 2.4 $Kpa \cdot m^2 \cdot g^{-1}$	

(-) information not provided in the cited reference

2.2 The role played by CNFs in paper

The unique dimensions and characteristics of CNFs that play a role in improving the strength properties of paper are described in the following sections. Figure 2-4 shows the characteristics of CNFs, such as the nanometre diameter, micrometre length, crystalline region, and amorphous region.

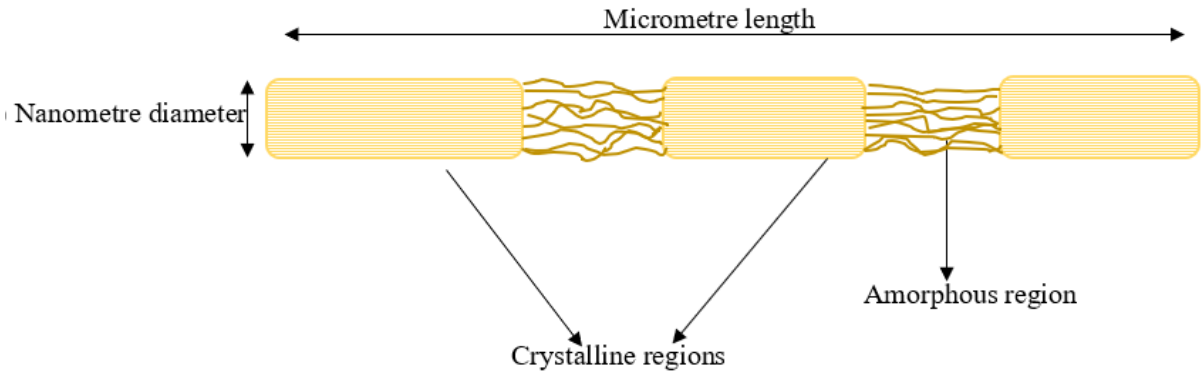

Figure 2-4 CNF structure and characteristics redrawn from Nagarajan et al. (2021)

2.2.1 Nanometre lateral dimension

In general, CNFs have a large surface to volume ratio and specific surface area (SSA) because of their nanosized lateral dimensions (Ottesen 2018). When CNFs are combined with microfibres present in pulp suspensions, the SSA of the fibrous network increases, resulting in an increased available surface for bonding (Adel et al. 2016). In this situation, two phases are formed, namely the microscale and the nanoscale. Spence et al. (2010) reported that the SSA of unbleached softwood pulp fibres (UBSWP) was in the range of 3 ± 2 $m^2 \cdot g^{-1}$ whereas CNFs obtained from bleached hardwood pulp ranged from 30 $m^2 \cdot g^{-1}$ to 70 $m^2 \cdot g^{-1}$. As an example, the addition of 6 wt% of CNFs with a SSA of 55 $m^2 \cdot g^{-1}$ to 100 g of UBSWP fibres with SSA of 1 $m^2 \cdot g^{-1}$ will subsequently result in the microscale phase generated having a SSA of 100 m^2 per 100 g of pulp and a nanoscale phase of 330 m^2 (Spence et al. 2010; Alcalá et al. 2013). As a consequence of the large SSA, dispersed CNFs enhance the bonding between pulp fibres and evenly distribute stress in the paper under loading. Colloidal interaction and mechanical interlocking are also promoted by the large surface area of CNFs (Taipale et al. 2010). An increase in surface area results in an increase of available hydroxyl groups for interaction, thus promoting the formation of fibre to fibre contact and bonding, which in turn solidifies the structure of the paper. The strength of paper increases with an increase in the number of fibre bonds. Therefore, the presence of CNFs naturally improves the overall tensile strength of paper by increasing the fraction of fibres that are bonded relative to the total area available for bonding (*viz*., relative bonded area) (Mörseburg and Chinga-Carrasco 2009).

Furthermore, the nanosized dimension is also advantageous in reducing the porosity of paper from microsize to nanosize (Mörseburg and Chinga-Carrasco 2009; Mashkour et al. 2015; Moodley 2018). It was reported that CNFs offer better packing in the network of pulp fibres and fillers, thus reducing porosity (Mashkour et al. 2015; Balea et al. 2016a). CNFs fill microvoids and pores around fibre joints, extending the contact domain and improving the contact between fibres at the molecular level during paper drying (Afra et al. 2013; González et al. 2013). Espinosa et al. (2016) reported that an increase in CNF dosage (0 to 4%) decreased paper porosity (56 ± 0.3 to 52.6 ± 0.3%). Syverud et al. (2009) reported an increase in air resistance from 41 s per 100 ml to approximately 200 s per 100

ml for paper treated with CNFs, indicating that the pores between fibres were closed or reduced in size by the addition of CNFs. The decrease in air permeability was also justified by the densification of CNF reinforced paper, which reflected a high number of fibre to fibre interactions influenced by the presence of CNFs (Taipale et al. 2010; Charani et al. 2013; Bossu et al. 2019). Su et al. (2014) examined the microscopic structure of hardwood pulp and hardwood pulp reinforced with CNFs. The latter showed a smoother and compact surface. The former sample had a more porous and rougher surface. Moodley (2018) used the surface and cross-sectional micrographs (Figure 2-5) to illustrate the difference in porosity of unbleached kraft paper (UBK) and CNF reinforced UBK paper. Figure 2-5 shows a directly proportional relationship between the quantity of CNFs added to paper and the increase in paper compactness. Alcalá et al. (2013) confirmed that fibres reinforced with CNFs showed a more compact fibre network resulting in a more solid structure. Even though the nanosized lateral dimensions are highly beneficial in enhancing the mechanical strength properties of paper, the drainage rates are always negatively affected (Mashkour et al. 2015).

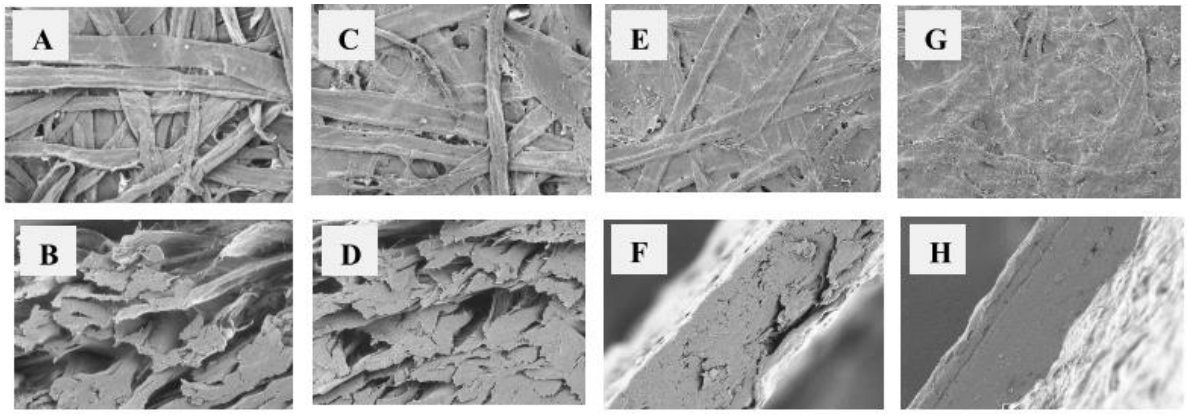

Figure 2-5 Micrographs of (A) surface of UBK paper, (B) cross-section of UBK paper, (C) surface of 20% CNF reinforced UBK paper, (D) cross-section of 20% CNF reinforced UBK paper, (E) surface of 50% CNF reinforced UBK paper, (F) cross-section of 50% CNF reinforced UBK paper, (G) surface of 100% CNF reinforced UBK paper, (H) cross section of 100% CNF reinforced UBK paper. Adapted with permission from Moodley (2018)

2.2.2 Micrometre length

Fibre length is one of the significant factors which influences the fracture toughness and tear index quality of paper (Subramanian et al. 2011). The length of the fibres enables a continuous network to be formed even at low concentrations of fibres (Karlsson 2007). The length of CNFs contributes to the formation of fibre joints, thus creating stronger networks (Johansson 2011). The length of CNFs differs depending on the production pretreatment, mechanical treatment, and characterisation technique employed. Ishii et al. (2011) reported an average length of 2.2 µm by use of both Transmission Electron Microscopy (TEM) and dynamic viscoelasticity measurements for CNFs produced by TEMPO-mediated oxidation and mechanical disintegration. Su et al. (2014) suggested two roles played by the length of CNFs, illustrated in Figure 2-6. Firstly, CNFs act as a bridge between fibres, which increases connectivity, adhesion, and the bonded area. Secondly, shorter CNFs bond together, thus improving the strength of the paper. Fibre to fibre bonds are mostly hydrogen bonds. Hydrogen bonding is only possible for fibres in close proximity (less 0.35 nm apart). CNFs bridge adjacent fibres, provide more hydroxyl groups, increase the chances of bonding and form entangled networks. Furthermore, CNFs can act as a binder to

strengthen fibre-filler interactions by bridging the void created by fillers (Hii et al. 2012; Ämmälä et al. 2013). Phipps et al. (2017) reported that CNFs produced by co-grinding with a calcium carbonate filler acts to fill in the voids created between filler and pulp fibres in paper by wrapping around filler particles promoting bonding by bridging. The presence of CNFs curbs the disruption of the bonded area caused by the filler. The length of CNFs allows for its entanglement around fibres, consequently filling empty spaces in the paper (Adel et al. 2016). Zeng et al. (2021) reported that CNFs with lengths in the range 2 and 4 μm did not increase the strength of recycled paper. It was concluded that short CNFs were unable to bridge adjacent fibres and were poorly retained within the fibre matrix. Longer fibres increase the tear strength because they are able to distribute the stress over more fibres and more bonds, whereas short fibres concentrate the stress in a smaller region. Therefore, the decrease in tear resistance is due to the short CNFs and the decrease in the number of bonds which causes fibres to break and pull out of the fibre network (Karlsson 2007; Afra et al. 2013). The Z-strength of paper is mainly affected by the fibre to fibre bond strength, while the tensile strength correlates with fibre length (Ankerfors et al. 2014). Fractionating CNFs according to length and only using the fraction with longer fibres has been reported to increase the tensile strength by an additional 10% at the same optimal dosage of 10 wt% obtained for non-fractioned fibres (Manninen et al. 2011). The dependence of tensile strength on fibre length is represented by Equation1 below:

$$\frac{1}{T} = \frac{9}{8Z} + \frac{3w_f}{\tau_f \, l_f \, RBA} \qquad (1)$$

Where T is the tensile strength, Z is the zero-span tensile strength of paper, w_f is fibre width, τ_f is the breaking stress of bonds, l_f is the fibre length, and RBA is the relative bonded area (Page 1969; Karlsson 2007).

Hierarchical structures in the form of different lateral and length scales of fibres are formed in CNF and pulp mixtures (Sehaqui et al. 2011). The presence of two length scales (micro and nano) has been reported to be the reason for the increased strength of paper bio-composites. The nanoscale network of nanofibres transfers the load between wood fibres, thus delaying the material's damage and failure when exposed to stress and strain (Sehaqui et al. 2011). This mechanism is believed to occur at fibre to fibre joints in the paper (Sehaqui et al. 2011).

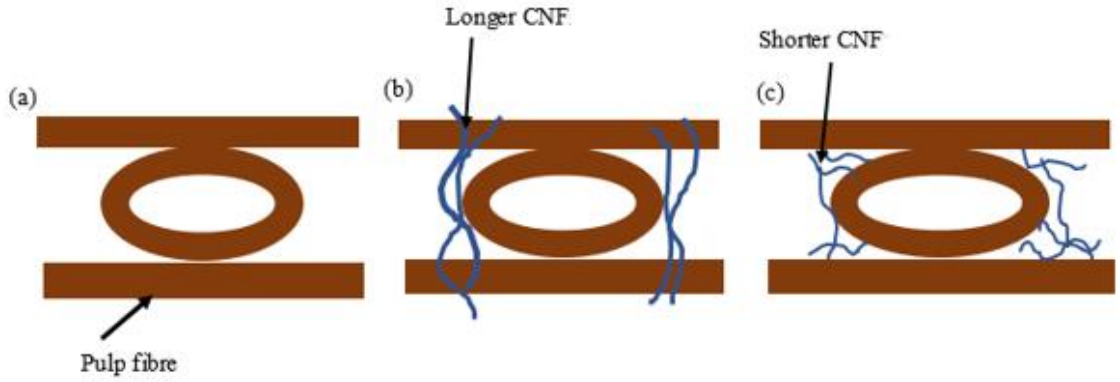

Figure 2-6 Role played by longer CNFs vs shorter CNFs in a pulp fibre matrix redrawn from Su et al. (2014)

2.2.3 Semi-crystalline structure

The crystalline structure is responsible for rigidity, the resistance of flow, and the strength of CNFs (Hubbe 2014). The strength of CNFs contributes to the overall strength of paper and increases its load-bearing capacity. On the other hand, the amorphous region contributes to the flexibility of CNFs. High fibre flexibility increases the fibre

conformability around each other, affecting the chances of fibre-fibre contact, the number of bonds, and the bonded area in a paper sheet (Karlsson 2007). The flexibility of CNF increases the degree of bonding, hence the increased tensile strength of paper and also decreases its susceptibility to brittle failure (Johansson 2011; Hubbe 2014). Due to their slenderness and flexibility, CNFs are prone to entanglements, which are responsible for the increase in the wet strength of paper (de Oliveira et al. 2008; Sehaqui et al. 2013).

Moreover, an additional nanoscale network is formed due to the web of flexible CNFs. The nanoscale network may also form in between pulp fibres resulting in a non-porous, smooth surface (Petroudy et al. 2014). This web implanted among the pulp fibres contributes to the mechanical properties of paper (Bardet and Bras 2014). De Oliveira et al. (2008) compared the effect of flexible CNFs and rigid glass fibres. An increase in the solid content of CNFs resulted in entanglement friction between CNFs and pulp fibres. The friction became more pronounced upon drying, thus increasing the cohesion between fibres and the web strength of paper (de Oliveira et al. 2008). In contrast, the rigid glass fibres reduced the wet web strength of paper due to the lack of entanglements. The amorphous region is important because it offers more hydrogen bonding groups (Kajanto and Kosonen 2012). However, the amorphous region retains a lot of water which negatively impacts the drainage rate of paper (Balea et al. 2020).

2.2.4 High strength and modulus

The strength of paper depends on the strength of fibres and the bonds that connect them (Sehaqui et al. 2013; Vallejos et al. 2016). Mashkour et al. (2015) reported that the strength properties of paper, such as burst strength, were mainly affected by the relative bonding area (RBA), bonding strength, and single fibre strength. Individual CNFs have a strength comparable to that of engineering materials. This strength, combined with the inherent tendency of CNFs to form entangled networks, contributes to the overall strength of paper. Different fibres have different shear bond strengths. Reports have shown that the inherent strength of a single CNF was in the range 0.8 to 10 GPa and 30 to 250 GPa for tensile strength and Young's Modulus, respectively, depending on the measuring technique, source, production and fabrication method of the CNF (Zimmermann et al. 2004; Alcalá et al. 2013). Saito et al. (2013) reported that CNFs obtained from wood had a tensile strength of 1.6 to 3 GPa by using sonication induced fragmentation for measurement. Given the high values of strength for CNFs, its incorporation in pulp creates a favourable interface for improving the physical and mechanical properties of paper (Alcalá et al. 2013). The dependence of tensile strength on fibre strength is shown in Equation 2 below:

$$\frac{1}{T} = \frac{1}{F} + \frac{1}{B} \qquad (2)$$

Where T is the tensile strength, F is the fibre strength index, and B is the bonding strength index (Page 1969).

2.2.5 Aspect ratio

The high length to diameter ratio allows CNFs to be entangled around fibres, thereby filling up empty spaces in a paper (González et al. 2012). Also, the aspect ratio of CNFs is directly proportional to the viscosity of CNF suspension. High aspect ratio fibres result in high intrinsic viscosity because of the large rotational volume to fibre volume ratio (Jowkarderis and van de Ven 2014). The high aspect ratio combined with high SSA increases fibre to fibre interactions of CNFs, resulting in gel formation at low concentrations. The viscosity of CNFs is not favourable because of the difficulty to disperse CNFs in the paper furnish (Bajpai 2016). Hu et al. (2021) compared the reinforcing effects of CNFs 1 (diameter = 39 nm, aspect ratio = 155) and CNFs 2 (diameter = 35 nm, aspect ratio = 125) on recycled paper. The tensile index with CNFs 1 and CNFs 2 was 34 and 31 $N \cdot m \cdot g^{-1}$, respectively.

CNFs 1 and CNFs 2 were produced by a combination of PFI mill refining and microfluidisation. It was concluded that CNFs with higher aspect ratio resulted in superior reinforcement effects than CNFs with low aspect ratio regardless of the CNF diameters. However, short CNFs with a high aspect ratio were poorly retained within pulp fibres.

2.2.6 Lightweight

In general, CNFs are lightweight due to their nanosized dimensions. However, they increase the density of the paper structure (Afra et al. 2013; Alcalá et al. 2013; Espinosa et al. 2016; Hai and Seo 2018; Zeng et al. 2021). Sehaqui et al. (2013) demonstrated a direct proportional relationship between the tensile index and paper hand sheets density. Mashkour et al. (2015) reported a 16% and 8% increase in paper density by adding unmodified and acetylated CNFs, respectively.

2.2.7 Chemical modification and surface charge

The potential for chemical modification of CNFs is due to hydroxyl groups. Reactions occur mainly by the hydroxyl groups. For instance, CNFs form complexes with cationic starch. Pulp fibres adsorbed a maximum of 1 wt% cationic starch, whereas CNFs allowed for adsorption of higher dosages of cationic starch and improvement of mechanical properties of paper (Ankerfors et al. 2014; Ru et al. 2019).

Chemical pretreatments such as TEMPO-mediated oxidation, sulphonation, carboxymethylation, and quaternisation cause substitution of hydroxyl groups in CNF with carboxylate (aldehyde), sulphonate, carboxymethyl, and quaternary ammonium (Lee et al. 2017). Ahola et al. (2008) reported that the carboxyl group content in carboxymethylated CNFs influence the adsorption properties and covalent bond formation with PAE, which is a wet strength agent of paper. The addition of PAE mixed with CNF increased the wet and dry strength of paper.

Acetylated CNFs were used to produce hydrophobic paper (Mashkour et al. 2015). Mashkour et al. (2015) reported a decrease in water absorption of 23.1% for paper reinforced by partially acetylated CNFs. However, acetylation of CNFs decreased the number of hydroxyl groups, negatively affecting the mechanical strength of the paper. Lourenço et al. (2017) studied the effect of carboxyl charged CNFs in papermaking. Paper (without filler) reinforced by CNFs with 0.6 $mmol \cdot g^{-1}$ carboxyl content had a higher tensile index (54.9 ± 2.8 $N \cdot m \cdot g^{-1}$) than the tensile index (45.7 ± 2.7 $N \cdot m \cdot g^{-1}$) for paper possessing CNFs with 1.6 $mmol \cdot g^{-1}$ carboxyl content. It was concluded that highly charged CNFs had more affinity for CPAM than pulp fibres, repelling the negatively charged pulp fibres, thus increasing inter fibre distance. In the presence of filler, the less charged carboxyl CNFs resulted in better filler retention of 93.4 ± 0.7% than highly charged carboxyl CNFs with filler retention of 66.7 ± 0.3%.

2.3 Factors affecting the improvement in paper quality

The factors affecting the quality of CNFs reinforced paper are the strategy of CNF addition, CNF grade, CNF dosage, and CNF source, described in the following sections.

2.3.1 Effect of the strategy of CNF addition

In general, there are four strategies in which CNFs can be incorporated as an additive in papermaking (Bardet and Bras 2014; Bajpai 2016; Ding et al. 2018). The first strategy is the direct addition of CNFs in the pulp suspension. The second strategy involves premixing CNFs with another furnish component such as filler before addition into pulp. The third strategy involves adding CNFs in layers on pulp (bi-layer system) (Ahola et al. 2008). The fourth strategy is the pre-flocculation of CNFs with a retention polymer before the addition to pulp (Bajpai 2016). In a

comparative study, the bilayer strategy resulted in a better strength-enhancing effect (dry tensile index of ~ 62.5 $N \cdot m \cdot g^{-1}$) than the addition of nano-aggregates of CNFs and PAE to the pulp (dry tensile index of ~ 52 $N \cdot m \cdot g^{-1}$). This was because the former strategy allowed uniform distribution of substances on the pulp fibre surfaces in the paper matrix. The latter resulted in an inhomogeneous distribution of the fibres, and, hence, the strength properties were not improved (Ahola et al. 2008; Brodin et al. 2014). Also, the PAE-CNF aggregates were very anionic at high CNF dosages resulting in the poor attraction between CNFs and fibres (Ahola et al. 2008). Another approach compared the effect of interchanging layers of clay, CNFs, and fractionated thermomechanical pulp (TMP) in paper sheets. The arrangement that produced the best quality paper was where the top layer comprised clay, followed by the TMP accept fraction of pulp, then CNFs as the next layer and the bottom layer made up of the TMP reject fraction. This type of arrangement promoted the maximum interaction of the hydroxyl groups between CNFs and pulp. It increased the dry tensile index by approximately 5 $N \cdot m \cdot g^{-1}$ greater than when CNFs were either in the bottom or top layers of the sheet structure of the paper (Mörseburg and Chinga-Carrasco 2009). He et al. (2017) compared the effects of adding CNFs as a composite filler (PCC-CNFs) to adding CNFs as a wet-end additive. In the case where CNFs were used as a wet-end additive, materials were added in the following sequence: pulp-filler-CNFs-cationic starch-CPAM. In the case where CNFs were used as a composite filler, materials were added in the following sequence: pulp-composite filler-CPAM. The composite filler was prepared in the following sequence: CNFs-PCC-cationic starch. At a CNF dosage of 2%, the tensile index of paper reinforced with CNFs as a wet-end additive and composite filler was 21.9 ± 1.1 $N \cdot m \cdot g^{-1}$ and 22.4 ± 0.8 $N \cdot m \cdot g^{-1}$ respectively. The tensile index was slightly higher for paper with the CNF composite filler due to better retention of PCC-CNF aggregates within the paper sheet. The PCC-CNF aggregates were larger than the individual PCC particles. Ding et al. (2018) studied the retention of fluorescent CNFs (FCNFs) in papermaking in the presence of either polyquaternium-11 and PAM or cationic starch. The retention efficiency decreased with an increase in FCNF dosage. At a FCNF dosage of 10%, the mechanical strength properties (tensile index, burst index, Young's modulus and tensile energy absorption index and elongation) of paper with cationic starch were higher than for paper with polyquaternium-11 and PAM. It was concluded that FCNFs combined with cationic starch formed strong bonds with pulp fibres due to free hydroxyl groups in cationic starch (Merayo et al. 2017a; Ding et al. 2018). Tajik et al. (2018) studied the mechanical properties of CNF reinforced soda bagasse paper in the presence of cationic starch. The highest tensile index of 41.3 $N \cdot m \cdot g^{-1}$ was achieved at 2% and 0.6% CNF dosage and cationic starch dosage, respectively.

2.3.2 Effect of CNF grade

Several authors have reported that CNF produced by different mechanical methods influence the mechanical properties in distinct ways (Eriksen et al. 2008; Syverud et al. 2009). For instance, CNFs produced by homogenisation had a greater effect on the tensile index than CNFs produced by grinding, even though grinding produced on average smaller fibrils than those yielded by homogenisation (Eriksen et al. 2008). The highest tensile strength achieved by adding 4 wt% CNFs obtained by homogenisation was approximately 50 $kN \cdot m \cdot kg^{-1}$. With the addition of 4 wt% CNFs produced by grinding, the tensile index was 48.5 $kN \cdot m \cdot kg^{-1}$ (Eriksen et al. 2008). It was concluded that these different grades of CNFs had different mechanisms to improve the strength of paper.

(Delgado Aguilar et al. 2015) carried out a comparative study between CNFs produced by three different pretreatment methods (chemical (*viz.*, TEMPO mediated oxidation and acid hydrolysis), enzymatic treatment and mechanical beating) before high-pressure homogenisation. The highest index was found in CNFs produced from

TEMPO mediated oxidation due to its high fibrillation degree. The acid-hydrolysed CNFs also resulted in high tensile index values owing to a high fibrillation degree of 95% facilitated by sulphate ester groups. The lowest tensile index was in CNFs produced by mechanical means because mechanical methods produced nonhomogeneous fibres, which formed entangled and disordered networks in the paper. However, to compensate for low fibrillation, poorly fibrillated CNFs were added in higher dosages to achieve the same effect as that of highly fibrillated CNFs.

Kim et al. (2019) classified CNFs according to production methods, i.e., refined CNFs (RE-CNFs), enzymatic CNFs (EN-CNFs), and carboxymethylated CNFs (CM-CNFs). The CM-CNFs were more efficient in tensile strength, folding endurance, and sheet density improvement than RE-CNFs and EN-CNFs. The EN-CNFs were the least effective compared to RE-CNFs and CM-CNFs. However, in all the cases, the deterioration of the drainage rate as the CNF dosage increased was observed. The CM-CNFs were preferred, where strength improvement was a priority, but drainage could be afforded.

Su et al. (2014) reported that CNFs produced by homogenisation had better retention in the pulp fibre web due to their inhomogeneous size distribution. On the other hand, CNFs produced by ball milling were poorly retained in pulp fibres due to their small fibre size. However, the small fibres from ball milling produced a more compact and dense paper structure in the presence of a retention aid. Balea et al. (2017) confirmed that the retention system, morphology and composition of CNFs directly impacted the improvement of mechanical properties of paper.

Lourenço et al. (2019a) compared mechanically produced CNFs to enzymatically produced CNFs in improving the strength properties of paper with filler in the presence and absence of cationic starch, ASA and cationic polyacrylamide. For mechanically produced CNFs, the highest tensile strength was reported as 47 $N \cdot m \cdot g^{-1}$ and 34 $N \cdot m \cdot g^{-1}$ in the absence and presence of additives, respectively. For enzymatically produced CNFs, the highest tensile strength was reported as 42 $N \cdot m \cdot g^{-1}$ and 36 $N \cdot m \cdot g^{-1}$ in the absence and presence of additives, respectively. Better tensile strength was obtained for mechanical CNFs in the absence of additives because the filler retention was significantly lower (around 45% versus 80% with the enzymatic CNF). In the presence of additives, the results improved for the enzymatic CNFs, where filler retentions were higher than 90%.

Lourenço et al. (2019b) conducted a comparative study between CM-CNFs and TEMPO-CNFs. The TEMPO-CNFs resulted in a filler-containing paper with higher strength than paper with carboxymethylated CNFs. The conclusion indicated that the source of CNFs, method of CNF production, charge and size of CNFs had an influence on the behaviour of CNFs in papermaking.

Lourenço et al. (2020) studied the interactions between additives (cationic starch, ASA, PCC and CPAM) and CNFs in improving the strength properties of paper. Mechanically produced cellulose microfibrils (CMFs) in the presence of all additives resulted in high retention of PCC and increased strength properties of paper. EM-CNFs improved the dry and wet tensile index of paper due to their length, which promoted better retention of fillers. Paper reinforced with TEMPO-CNFs or CM-CNFs in the presence of all additives resulted in the lowest improvement in strength properties. The high negative charge of TEMPO-CNFs and CM-CNFs was detrimental to the bonding ability of CNFs with cationic additives.

Campano et al. (2018) compared the dispersion of CNFs within pulp fibres in the presence of two different dispersing agents viz., (i) mixture of a moisturising and a detergent surfactant (ii) moisturising agent. Two retention agents (CPAM and cationic starch) were used in the study. The mixture of a moisturising and detergent surfactant was poor in dispersing nanocellulose material. At a CNF dosage of 1.5% and 0.003 wt% moisturising

agent, the tensile index values of paper with cationic starch and CPAM was approximately 49 $N \cdot m \cdot g^{-1}$ and 39 $N \cdot m \cdot g^{-1}$, respectively.

Kumar et al. (2020) produced CNFs using an eco-friendly and energy-efficient method (*viz*., $NaIO_4$, $NaClO_2$ and valley beater). The CNF reinforced paper resulted in a 27%, 32%, and 87% increase in breaking length, burst factor and double-fold, respectively.

Tozluoglu and Poyraz (2016) conducted a comparative study on the effectiveness of CNFs produced by four different chemical pretreatment methods (viz., enzymatic, TEMPO, phthalimide-N-oxy (PINO) and periodate oxidation) in improving the strength properties of paper. At a CNF dosage of 3%, the tensile index values were approximately 58.9, 58, 55, and 53 $N \cdot m \cdot g^{-1}$ for paper reinforced with periodate oxidation-CNFs, enzymatic-CNFs, PINO oxidation-CNFs and TEMPO-CNFs, respectively. Periodate-CNFs reinforced paper had the highest tensile index due to the low viscosity of periodate-CNFs. The low viscosity of periodate-CNFs ensured homogenous distribution within pulp fibres. Tarrés et al. (2016) studied the influence of enzyme dosage and treatment time on the reinforcing ability of enzymatic CNFs in paper. The specific surface area increased but the diameter of the enzymatic-CNFs decreased as the enzyme dosage and the treatment time increased. Consequently, the breaking length of the enzymatic-CNFs reinforced paper improved with increased enzyme treatment time (2-4 h) and dosage (80-320 $g \cdot ton^{-1}$).

2.3.3 Effect of CNF dosage

González et al. (2012) reported an increase in all mechanical properties (tensile index, burst index, Scott bond, and tear index) of paper as the dosage of CNFs increased from 0 to 9 wt%. However, with the progressive addition of CNFs, the drainage rate was severely affected. Syverud et al. (2009) explained that the increase in tensile index with respect to CNF dosage was exponential. The maximum tensile index was achieved at 10% CNF dosage; however, the most significant change was observed from 5% CNF dosage. Eriksen et al. (2008) confirmed a similar trend between CNF dosage and an increase in tensile strength. After using a dosage range between 0 and 8 wt%, the most significant increase in the tensile index was observed at 4 wt% CNFs. In some studies, small dosages of CNFs were enough to produce a significant improvement in mechanical properties. For instance, Adel et al. (2016) reported that 5 wt% of CNFs resulted in a better enhancement in mechanical properties than 20 wt% of softwood applied as a paper additive on rice straw and bagasse pulp. Alcalá et al. (2013) reported a linear increase in tensile strength and Young's modulus as the dosage of CNFs added was increased from 3 wt% to 9 wt%. The maximum values for tensile strength and Young's modulus were 50.1 ± 6.8 MPa and 6.1 ± 0.5 GPa, respectively, at 9 wt% CNF dosage. Further increase in dosage to 12 wt% did not yield a significant improvement in mechanical properties due to the decrease in the area available for bonding to the fibre surface as more CNFs were added to the pulp (Alcalá et al. 2013; Jawaid et al. 2017). Taipale et al. (2010) also reported a linear increase of tensile strength with respect to CNF dosage. This confirms that high amounts of CNFs in paper webs create more fibre entanglements and increase the inner friction area between fibres, leading to improved wet strength (Su et al. 2013). However, high dosages of CNF are detrimental to the drainage rates of paper sheets (Ahola et al. 2008; Taipale et al. 2010; Hii et al. 2012). Petroudy et al. (2014) studied the addition of different dosages of CNF on bagasse pulp in the presence of a retention aid. The conclusion made was that a small dosage of CNFs (e.g., 1%) added to pulp required 0.1% of C-PAM (retention aid) to achieve a high tensile index of approximately 60 $N \cdot m \cdot g^{-1}$ while maintaining an acceptable drainage rate. Potulski et al. (2020) reported a direct proportion relationship between the CNF dosage and mechanical properties of CNF reinforced paper. This relationship was

true in all the properties of paper, such as tensile index, burst index, and tear index. Hu et al. (2021) studied the effects of CNFs produced by mechanical methods in improving the mechanical properties of recycled paper. The combinations of mechanical methods used were (i) PFI mill refining and microfluidisation (RM-CNFs), (ii) ball milling and ultrasonication (BU-CNFs), (iii) grinding and microfluidisation (GM-CNFs), (iv) PFI mill refining (R-CNFs) (v) grinding (G-CNFs). The tensile index of recycled paper reinforced with CNFs produced from all the aforementioned mechanical methods increased with an increase in CNF dosage (0-5%). At a CNF dosage of 5%, the tensile index was approximately 34.7, 34, 32, 30.8, and 31 $N \cdot m \cdot g^{-1}$ for recycled paper reinforced with RM-CNFs, BU-CNFs, GM-CNFs, R-CNFs, and G-CNFs, respectively. The tensile index of recycled paper without CNFs was 25.6 $N \cdot m \cdot g^{-1}$. Vallejos et al. (2016) confirmed that an increase in CNF dosage (0-9%) resulted in an increase in the tensile index, Young's modulus, and burst index of paper. At a CNF dosage of 9%, the tensile index increased from 27.3 ± 1 to 53.3 ± 1.1 $N \cdot m \cdot g^{-1}$. The burst index increased from 1.4 ± 0.1 to 6.1 ± 0.1 $kPa \cdot m^2 \cdot g^{-1}$. The Young's Modulus increased from 3.9 ± 0.1 to 6 ± 0.1 GPa. Laitinen et al. (2020) produced boxboard reinforced using CNFs from recycled boxboard pulp. The dosages of CNFs used were in the range 2-6 wt%. A linear increase in mechanical properties (tensile strength index and tensile stiffness index) of the manufactured boxboard with CNF dosage was observed. However, from an economic point of view, the best way to improve the strength properties of the boxboard was to add 4 wt% CNFs obtained by moderate grinding energy (3–4 $kW \cdot h \cdot kg^{-1}$). At a CNF dosage of 4 wt%, the price of the boxboard sheet was increased by 15-20%. High dosages of CNFs were detrimental to the drainage time and the overall boxboard production process.

2.3.4 Effect of the source of CNF

Balea et al. (2016b) compared the effectiveness of cornstalk-CNFs with *Eucalyptus* kraft pulp CNFs (EKP-CNFs) to improve the properties of recycled paper. Only 0.5 wt% cornstalk-CNFs achieved a 20% increase in tensile strength, whereas 1.5 wt% of EKP-CNFs was needed to achieve the same improvement. The low dose of cornstalk-CNFs required for effective paper improvement compensated for their low production yield. Merayo et al. (2017b) obtained the highest tensile indices of approximately 60 $N \cdot m \cdot g^{-1}$ and 55 $N \cdot m \cdot g^{-1}$ for recycled paper reinforced with EKP-CNFs and cornstalk-CNFs, respectively. Hai et al. (2018) conducted a comparative study in which CNFs from various sources (hardwood, softwood, cotton linters, and cattail) were used as additives when producing paper from hardwood pulp. The softwood-CNFs, hardwood-CNFs, cattail-CNFs, and cotton-CNFs had average diameters of 46, 40, 30, and 70 nm, respectively. The highest tensile strength was recorded for paper reinforced with softwood-CNFs (45 $N \cdot m \cdot g^{-1}$) followed by hardwood-CNFs (42.5 $N \cdot m \cdot g^{-1}$), cattail-CNFs (40 $N \cdot m \cdot g^{-1}$) and lastly, cotton linter-CNFs (~38 $N \cdot m \cdot g^{-1}$). The non-wood sources showed the lowest tensile strength and bonding properties due to their low hemicellulose content compared to the woody sources (Bajpai 2016; Hai and Seo 2018). Ang et al. (2020) demonstrated that the addition of 20 wt% CNFs produced from recycled de-inked pulp to bleached *Eucalyptus* pulp resulted in paper with a tensile strength of approximately 55 $N \cdot m \cdot g^{-1}$. The tensile strength of paper made from bleached Eucalyptus pulp without CNFs was 30 $N \cdot m \cdot g^{-1}$. Therefore, recycled pulp was proved to be a viable source for CNF production that can be used as a paper additive. González et al. (2013) produced paper with a tensile strength of 60.2 $N \cdot m \cdot g^{-1}$ using bleached *Eucalyptus* pulp-CNFs and bleached *Eucalyptus* pulp. The tensile strength was 68% higher than that of the reference paper made from pure bleached *Eucalyptus* pulp.

Balea et al. (2017) compared the effectiveness of two agricultural residues *viz*., corn stalk and rape stalk produced by different pretreatments methods, which were refining, TEMPO mediated oxidation, and bleaching before

mechanical treatment to reinforce recycled paper. TEMPO mediated oxidation resulted in the highest yield and quality of CNFs, followed by bleaching and, lastly, refining. It was concluded that bleaching was the most inexpensive method of pretreating agricultural residues. The corn stalk CNFs produced by bleaching resulted in 20% improvement in tensile index. The rape stalk CNFs obtained from bleaching resulted in 50% improvement in the tensile index.

Balea et al. (2019) studied the effectiveness of CNFs produced from recycled fibres in improving the tensile strength of old newspaper prints (ONP) and old corrugated container (OCC) pulps in the presence of a three-component retention system (*viz*., coagulant, C-PAM, and hydrated bentonite clay). Different amounts of CNFs were added (*viz*., 1, 2, 3 wt%) to paper. It was reported that 3 wt% of CNFs improved the tensile index of ONP by 30%. On the other hand, 3 wt% of CNFs improved the tensile index of OCC by 60%. The optimisation of the retention system used counteracted the negative effect on the drainage rate caused by the CNFs.

Park et al. (2018) compared the extent to which CNFs produced from softwood bleached kraft pulp (SBKP) and bleached hardwood kraft pulp (BHKP) improved the mechanical properties of paper made from cotton linters mixed pulp. CNFs produced from SBKP resulted in the greatest improvement in mechanical properties (*viz.*, folding endurance > 1200, tensile index > 30 $N \cdot m \cdot g^{-1}$) of the paper. The CNFs produced from SBKP had high viscosity, lower fibre diameter and higher zeta-potential compared to CNFs produced from BHKP.

2.4 Techno-economic considerations

The emergence of CNFs can be summed up in stages: basic manufacturing research, proof of concept, production in laboratory, capacity to produce a prototype, capability in production, and demonstration of production rates. Despite the investment gap that has slowed down its commercialisation, the increasing number of CNF producers at demonstration scale worldwide is evidence of the great efforts in developing a CNF industry. The market of CNFs is growing slowly, with an annual growth rate of 30% due to technical and commercial challenges. In the year 2025, it is anticipated that the market will grow up to 25100 metric tonnes/year (Miller 2019).

The most sustainable way of production and application of CNFs in papermaking is by in situ production. In situ production provides an opportunity for paper producers to expand the range of products and apply expert knowledge in the optimisation and development of functional properties for speciality grade paper. The ultimate goal is to replace the existing petroleum-based materials in the papermaking process. This is only achievable if the cost of CNFs is comparable to or lower than traditional additives. Currently, the high production cost of CNFs is attributed to the high energy demands of mechanical treatment and the high cost of chemicals for the pretreatment of CNF sources. For instance, in situ production of CNFs by TEMPO oxidation would increase the cost of paper from 60 to 300 € per tonne of paper (Balea et al. 2020). de Assis et al. (2018) conducted a financial and risk assessment on the minimum product selling price (MPSP) of CNFs. Three scenarios were considered. The first scenario was a stand-alone company that produced CNFs from pulp. The cost of pulp, electricity and depreciation accounted for 60%, 15% and 12 to 14% of the production cost, respectively. The second scenario was the coproduction of CNFs in a mill that produced pulp. The minimum product selling price for scenario 2 (USD 1893 t^{-1} dry CNFs) was lower than that of scenario 1 (USD 2 440 t^{-1} dry CNFs) due to reduced capital investment, labour, pulp, transport, and handling costs. The third scenario was called the on-demand co-location, where the CNFs produced were incorporated in the papermaking process within the same facility. Scenario 3 resulted in additional cost savings on labour. Besides co-location, the cost of CNF source (pulp) was studied. Choosing a cheaper source of CNFs greatly reduced the minimum selling price of CNFs, which was beneficial in

competing with the cost of traditional paper additives. Also, if zero cost sources such as agricultural waste and recycled fibres are used, considering that studies have proven that CNFs from waste is as effective as CNFs from bleached pulp, the production process becomes cost-efficient (Balea et al. 2017).

2.5 Conclusions

Most of the studies in this review suggested that the main role played by CNFs is that of a binder for fibres in paper. The mechanisms involved in papermaking were influenced by the inherent properties of CNFs, such as the high aspect ratio and high strength and modulus. The high aspect ratio enabled CNFs to entangle around fibres, filling voids and bridging adjacent pulp fibres. The compact and strong network of fibres formed resulted in improved mechanical properties of paper such as tensile index, burst index, Scott index, breaking length, tear index, Z-strength, E-modulus, strain at break, and tensile stiffness. CNFs provided a sustainable route to papermaking while enhancing the mechanical, functional, and barrier properties of paper.

However, the drainage properties were always negatively affected, especially in the pressing and drying sections of the papermaking process. In addition to the properties of CNFs: dosage, the strategy of addition and source of CNFs influenced the extent of paper improvement. Despite the wide range of sources of CNFs, high energy requirements were still a major setback in the production of CNFs. However, investigation of the use of CNFs from zero cost agricultural waste and recycled paper pulp as paper additives have proven to improve paper properties. The negative or zero-cost of the waste compensated for the high production costs of CNFs. Furthermore, by taking advantage of similar raw materials in papermaking and CNF production, in situ production of CNFs eliminated transport and handling costs and ensured optimisation of the product to meet the required properties for speciality grade paper products. Finally, although CNFs improved mechanical, optical and air barrier properties, the hydrophilicity of paper increased. This further limited the applications of paper. The main challenges associated with CNFs are poor compatibility with hydrophobic polymers, high polarity (presence of many hydroxyl groups), which causes re-bonding between individual CNFs when dried, and, when mixed in non-polar solvents or at low pH, results in the loss of the nanoscale dimension (Jawaid et al. 2017). Therefore, CNFs should be stored as suspensions with low solid content, which is a major limiting factor in large scale applications such as papermaking. Future research should investigate the effect of morphological and biochemical properties of the sources of CNFs on their performance as paper additives. There is limited research on the recyclability of paper reinforced with CNFs.

2.6 Declarations

Funding This review was supported by the Council for Scientific and Industrial Research, Biorefinery Industry Development Facility, Durban, South Africa.

Conflicts of interest Not applicable.

Availability of data and material Not applicable

Code availability Not applicable

Authors Contributions Thabisile Brightwell Jele had the idea for the article, Thabisile Brightwell Jele performed the literature search and drafted, the manuscript whereas Prabashni Lekha and Bruce Sithole critically revised the drafts and approved the review for publication.

Ethics approval Not applicable

Consent to participate Not applicable

Consent for publication All authors consent to the publication of this review.

2.7 Acknowledgments

The authors acknowledge the Council for Scientific and Industrial Research, Biorefinery Industry Development Facility for supporting this work as part of the literature review of a MSc project. The authors would like to thank the Department of Science and Innovation for financial support via the General Budget Support (GBS) programme.

2.8 References

Abe K, Iwamoto S, Yano H (2007) Obtaining cellulose nanofibers with a uniform width of 15 nm from wood. Biomacromol 8 (10)**:** 3276-3278. https://doi.org/10.1021/bm700624p

Abe K, Yano H (2009) Comparison of the characteristics of cellulose microfibril aggregates of wood, rice straw and potato tuber. Cellulose 16 (6)**:** 1017-1023. https://doi.org/10.1007/s10570-009-9334-9

Adel AM, El-Gendy AA, Diab MA, Abou-Zeid RE, El-Zawawy WK, Dufresne A (2016) Microfibrillated cellulose from agricultural residues. Part I: Papermaking application. Ind Crops Prod 93**:** 161-174. https://doi.org/10.1016/j.indcrop.2016.04.043

Adnan S, Azhar A, Jasmani L, Samsudin M (2018) Properties of paper incorporated with nanocellulose extracted using microbial hydrolysis assisted shear process. IOP conference series: materials science and engineering. IOP Publishing, 012022.

Afra E, Yousefi H, Hadilam MM, Nishino T (2013) Comparative effect of mechanical beating and nanofibrillation of cellulose on paper properties made from bagasse and softwood pulps. Carbohydr Polym 97 (2)**:** 725-730. https://doi.org/10.1016/j.carbpol.2013.05.032

Ahola S, Österberg M, Laine J (2008) Cellulose nanofibrils—adsorption with poly (amideamine) epichlorohydrin studied by QCM-D and application as a paper strength additive. Cellulose 15 (2)**:** 303-314. https://doi.org/10.1007/s10570-007-9167-3

Alagarasi A (2013) Introduction to Nanomaterials. John Wiley & Sons, National Center for Environmental Research

Alcalá M, González I, Boufi S, Vilaseca F, Mutjé P (2013) All-cellulose composites from unbleached hardwood kraft pulp reinforced with nanofibrillated cellulose. Cellulose 20 (6)**:** 2909-2921. https://doi.org/10.1007/s10570-013-0085-2

Ämmälä A, Liimatainen H, Burmeister C, Niinimäki J (2013) Effect of tempo and periodate-chlorite oxidized nanofibrils on ground calcium carbonate flocculation and retention in sheet forming and on the physical properties of sheets. Cellulose 20 (5)**:** 2451-2460. https://doi.org/10.1007/s10570-013-0012-6

Ang S, Haritos V, Batchelor W (2020) Cellulose nanofibers from recycled and virgin wood pulp: A comparative study of fiber development. Carbohydr Polym 234**:** 115900. https://doi.org/10.1016/j.carbpol.2020.115900

Ankerfors M, Lindström T, Söderberg D (2014) The use of microfibrillated cellulose in fine paper manufacturing–Results from a pilot scale papermaking trial. Nordic Pulp Paper Res J 29 (3)**:** 476-483. https://doi.org/10.3183/npprj-2014-29-03-p476-483

Bajpai P (2016) Pulp and Paper Industry: Nanotechnology in Forest Industry. Elsevier, India

Balea A, Blanco Á, Monte MC, Merayo N, Negro C (2016a) Effect of bleached eucalyptus and pine cellulose nanofibers on the physico-mechanical properties of cartonboard. BioResources 11 (4)**:** 8123-8138. https://doi.org/10.15376/biores.11.4.8123-8138

Balea A, Merayo N, De La Fuente E, Negro C, Blanco Á (2017) Assessing the influence of refining, bleaching and TEMPO-mediated oxidation on the production of more sustainable cellulose nanofibers and their

application as paper additives. Ind Crops Prod 97: 374-387. https://doi.org/10.1016/j.indcrop.2016.12.050

Balea A, Merayo N, Fuente E, Delgado-Aguilar M, Mutje P, Blanco A, Negro C (2016b) Valorization of corn stalk by the production of cellulose nanofibers to improve recycled paper properties. BioResources 11 (2): 3416-3431. https://doi.org/10.15376/biores.11.2.3416-3431

Balea A, Monte MC, Merayo N, Campano C, Negro C, Blanco A (2020) Industrial Application of nanocelluloses in papermaking: a review of challenges, technical solutions, and market perspectives. Molecules 25 (3): 526. https://doi.org/10.3390/molecules25030526

Balea A, Sanchez-Salvador JL, Monte MC, Merayo N, Negro C, Blanco A (2019) In situ production and application of cellulose nanofibers to improve recycled paper production. Molecules 24 (9): 1800. https://doi.org/10.3390/molecules24091800

Bardet R, Bras J (2014) Cellulose nanofibers and their use in paper industry. In: Sain M (ed) Handbook of Green materials: Bionanomaterials: separation processes, characterisation and properties. World Scientific, pp 207-232

Bossu J, Czibula CV, Winter A, Gindl-Altmutter W, Eckhart R, Zankel A, Bauer W (2019) Combined effect of the morphology and rate of addition of fine cellulosic materials produced from chemical pulp on paper properties. International paper physics conference. 247-259.

Boufi S, González I, Delgado-Aguilar M, Tarrès Q, Mutjé P (2017) Nanofibrillated cellulose as an additive in papermaking process. Carbohydr Polym 154: 153-173. https://doi.org/10.1016/j.carbpol.2016.07.117

Brodin FW, Gregersen ØW, Syverud K (2014) Cellulose nanofibrils: Challenges and possibilities as a paper additive or coating material–A review. Nord Pulp Paper Res J 29 (1): 156-166. https://doi.org/10.3183/npprj-2014-29-01-p156-166

Campano C, Merayo N, Balea A, Tarrés Q, Delgado-Aguilar M, Mutjé P, Negro C, Blanco Á (2018) Mechanical and chemical dispersion of nanocelluloses to improve their reinforcing effect on recycled paper. Cellulose 25 (1): 269-280.

Cao D, Xing Y, Tantratian K, Wang X, Ma Y, Mukhopadhyay A, Cheng Z, Zhang Q, Jiao Y, Chen L (2019) 3D printed high-performance lithium metal microbatteries enabled by nanocellulose. J Adv Mater 31 (14): 1807313. https://doi.org/10.1002/adma.201807313

Charani PR, Dehghani-Firouzabadi M, Afra E, Blademo Å, Naderi A, Lindström T (2013) Production of microfibrillated cellulose from unbleached kraft pulp of Kenaf and Scotch Pine and its effect on the properties of hardwood kraft: microfibrillated cellulose paper. Cellulose 20 (5): 2559-2567. https://doi.org/10.1007/s10570-013-9998-z

Cowie J, Bilek ET, Wegner TH, Shatkin JA (2014) Market projections of cellulose nanomaterial-enabled products-Part 2: Volume estimates. Tappi J 13 (6): 57-69. https://doi.org/10.32964/tj13.6.57

Das AK, Islam MN, Ashaduzzaman M, Nazhad MM (2020) Nanocellulose: its applications, consequences and challenges in papermaking. Package Technol Res: 1-8.

de Assis CA, Houtman C, Phillips R, Bilek E, Rojas OJ, Pal L, Peresin MS, Jameel H, Gonzalez R (2017) Conversion economics of forest biomaterials: Risk and financial analysis of CNC manufacturing. Biofuel Bioprod Biorefin 11 (4): 682-700. https://doi.org/10.1002/bbb.1782

de Assis CA, Iglesias MC, Bilodeau M, Johnson D, Phillips R, Peresin MS, Bilek E, Rojas OJ, Venditti R, Gonzalez R (2018) Cellulose micro-and nanofibrils (CMNF) manufacturing-financial and risk assessment. Biofuel Bioprod Biorefin 12 (2)**:** 251-264. https://doi.org/10.1002/bbb.1835

de Oliveira MH, Maric M, van de Ven TG (2008) The role of fiber entanglement in the strength of wet papers. Nord Pulp Paper Res J 23 (4)**:** 426-431. https://doi.org/10.3183/npprj-2008-23-04-p426-431

Delgado-Aguilar M, González I, Pèlach M, De La Fuente E, Negro C, Mutjé P (2015) Improvement of deinked old newspaper/old magazine pulp suspensions by means of nanofibrillated cellulose addition. Cellulose 22 (1)**:** 789-802. https://doi.org/10.1007/s10570-014-0473-2

Delgado Aguilar M, González Tovar I, Tarrés Farrés Q, Alcalà Vilavella M, Pèlach Serra MÀ, Mutjé Pujol P (2015) Approaching a low-cost production of cellulose nanofibers for papermaking applications. BioResources. https://doi.org/10.15376/biores.10.3.5345-5355

Diab M, Curtil D, El-shinnawy N, Hassan ML, Zeid IF, Mauret E (2015) Biobased polymers and cationic microfibrillated cellulose as retention and drainage aids in papermaking: Comparison between softwood and bagasse pulps. Ind Crops Prod 72**:** 34-45. https://doi.org/10.1016/j.indcrop.2015.01.072

Ding Q, Zeng J, Wang B, Gao W, Chen K, Yuan Z, Xu J, Tang D (2018) Effect of retention rate of fluorescent cellulose nanofibrils on paper properties and structure. Carbohydr Polym 186**:** 73-81. https://doi.org/10.1016/j.carbpol.2018.01.040

Eriksen Ø, Syverud K, Gregersen Ø (2008) The use of microfibrillated cellulose produced from kraft pulp as strength enhancer in TMP paper. Nord Pulp Paper Res J 23 (3)**:** 299-304. https://doi.org/10.3183/npprj-2008-23-03-p299-304

Espinosa E, Tarrés Q, Delgado-Aguilar M, González I, Mutjé P, Rodríguez A (2016) Suitability of wheat straw semichemical pulp for the fabrication of lignocellulosic nanofibres and their application to papermaking slurries. Cellulose 23 (1)**:** 837-852. https://doi.org/10.1007/s10570-015-0807-8

Fotie G, Limbo S, Piergiovanni L (2020) Manufacturing of Food Packaging Based On Nanocellulose: Current Advances and Challenges. Nanomaterials 10 (9)**:** 1726. https://doi.org/10.3390/nano10091726

French AD (2017) Glucose, not cellobiose, is the repeating unit of cellulose and why that is important. Cellulose 24 (11)**:** 4605-4609. https://doi.org/10.1007/s10570-017-1450-3

González I, Boufi S, Pèlach MA, Alcalà M, Vilaseca F, Mutjé P (2012) Nanofibrillated cellulose as paper additive in eucalyptus pulps. BioResources 7 (4)**:** 5167-5180. https://doi.org/10.15376/biores.7.4.5167-5180

González I, Vilaseca F, Alcalá M, Pèlach M, Boufi S, Mutjé P (2013) Effect of the combination of biobeating and NFC on the physico-mechanical properties of paper. Cellulose 20 (3)**:** 1425-1435. https://doi.org/10.1007/s10570-013-9927-1

Gullichsen J, Fogelholm C-J, Fapet O (2000) Chemical Pulping-Papermaking Science and Technology. Fapet Oy, Jyväskylä

Hai LV, Seo YB (2018) Properties of nanofibrillated cellulose prepared by mechanical means. Cellul Chem Technol 52 (9-10)**:** 741-747.

He M, Yang G, Cho B-U, Lee YK, Won JM (2017) Effects of addition method and fibrillation degree of cellulose nanofibrils on furnish drainability and paper properties. Cellulose 24 (12)**:** 5657-5669. https://doi.org/10.1007/s10570-017-1495-3

Hii C, Gregersen ØW, Chinga-Carrasco G, Eriksen Ø (2012) The effect of MFC on the pressability and paper properties of TMP and GCC based sheets. Nord Pulp Paper Res J 27 (2): 388. https://doi.org/10.3183/npprj-2012-27-02-p388-396

Hu F, Zeng J, Cheng Z, Wang X, Wang B, Zeng Z, Chen K (2021) Cellulose nanofibrils (CNFs) produced by different mechanical methods to improve mechanical properties of recycled paper. Carbohydr Polym 254: 117474. https://doi.org/10.1016/j.carbpol.2020.117474

Hubbe MA (2014) Prospects for maintaining strength of paper and paperboard products while using less forest resources: A review. BioResources 9 (1): 1634-1763. https://doi.org/10.15376/biores.9.1.1634-1763

Ishii D, Saito T, Isogai A (2011) Viscoelastic Evaluation of Average Length of Cellulose Nanofibers Prepared by TEMPO-Mediated Oxidation. Biomacromolecules 12: 548-50. https://doi.org/10.1021/bm1013876

Jawaid M, Boufi S, Khalil A (2017) Cellulose-Reinforced nanofibre composites: Production, properties and applications. Woodhead Publishing, Cambridge

Johansson A (2011) Correlations between fibre properties and paper properties. Dissertation, KTH Royal Institute of Technology.

Johnson DA, Paradis MA, Bilodeau M, Crossley B, Foulger M, Gelinas P (2016) Effects of cellulosic nanofibrils on papermaking properties of fine papers. Tappi J 15 (6): 395-402. http://dx.doi.org/10.32964/TJ15.6.395

Jowkarderis L, van de Ven TG (2014) Intrinsic viscosity of aqueous suspensions of cellulose nanofibrils. Cellulose 21 (4): 2511-2517. https://doi.org/10.1007/s10570-014-0292-5

Kajanto I, Kosonen M (2012) The potential use of micro-and nanofibrillated cellulose as a reinforcing element in paper. Forest Sci Technol 2 (6): 42-48.

Karlsson H (2007) Some aspects on strength properties in paper composed of different pulps. Dissertation, Karlstad University

Khalil HA, Davoudpour Y, Islam MN, Mustapha A, Sudesh K, Dungani R, Jawaid M (2014) Production and modification of nanofibrillated cellulose using various mechanical processes: a review. Carbohydr Polym 99: 649-665. https://doi.org/10.1016/j.carbpol.2013.08.069

Kim KM, Lee JY, Jo HM, Kim SH (2019) Cellulose Nanofibril Grades' Effect on the Strength and Drainability of Security Paper. BioResources 14 (4): 8364-8375.

Kumar A, Singh S, Singh A (2016) Comparative study of cellulose nanofiber blending effect on properties of paper made from bleached bagasse, hardwood and softwood pulps. Cellulose 23 (4): 2663-2675. https://doi.org/10.1007/s10570-016-0954-6

Kumar V, Pathak P, Bhardwaj NK (2020) Facile chemo-refining approach for production of micro-nanofibrillated cellulose from bleached mixed hardwood pulp to improve paper quality. Carbohydr Polym 238: 116186. https://doi.org/10.1016/j.carbpol.2020.116186

Kumar V, Pathak P, Bhardwaj NK (2021) Micro-nanofibrillated cellulose preparation from bleached softwood pulp using chemo-refining approach and its evaluation as strength enhancer for paper properties. Appl Nanosci 11 (1): 101-115. https://doi.org/10.1007/s13204-020-01575-9

Laitinen O, Suopajärvi T, Liimatainen H (2020) Enhancing packaging board properties using micro-and nanofibers prepared from recycled board. Cellulose 27: 7215-7225. https://doi.org/10.1007/s10570-020-03264-w

Latifah J, Nurrul-Atika M, Sharmiza A, Rushdan I (2020) Extraction of nanofibrillated cellulose from Kelempayan (Neolamarckia cadamba) and its use as strength additive in papermaking. J of Trop For Sci 32 (2)**:** 170-178. https://doi.org/10.26525/jtfs32.2.170

Lee H, Sundaram J, Mani S (2017) Production of cellulose nanofibrils and their application to food: a review. J Nanotechnol**:** 1-33. https://doi.org/10.1007/978-981-10-4678-0_1

Lengowski EC, Júnior EAB, Kumode MMN, Carneiro ME, Satyanarayana KG (2019) Nanocellulose in the paper making. Sustainable polymer composites and nanocomposites. Springer, 1027-1066

Li Q, McGinnis S, Sydnor C, Wong A, Renneckar S (2013) Nanocellulose life cycle assessment. ACS Sustain Chem Eng 1 (8)**:** 919-928. https://doi.org/10.1021/sc4000225

Lindstrom T, Naderi A, Wiberg A (2015) Large scale applications of nanocellulosic materials-A comprehensive review. J. of Korea TAPPI 47 (6)**:** 5-21. https://doi.org/10.7584/KTAPPI.2015.47.6.005

Lourenço AF, Gamelas JA, Nunes T, Amaral J, Mutjé P, Ferreira P (2017) Influence of TEMPO-oxidised cellulose nanofibrils on the properties of filler-containing papers. Cellulose 24 (1)**:** 349-362. https://doi.org/10.1007/s10570-016-1121-9

Lourenço AF, Gamelas JA, Sarmento P, Ferreira PJ (2019a) Enzymatic nanocellulose in papermaking–The key role as filler flocculant and strengthening agent. Carbohydr Polym 224**:** 115200. DOI: https://doi.org/10.1016/j.carbpol.2019.115200

Lourenço AF, Gamelas JA, Sarmento P, Ferreira PJ (2020) A comprehensive study on nanocelluloses in papermaking: the influence of common additives on filler retention and paper strength. Cellulose 27 (9)**:** 5297-5309. https://doi.org/10.1007/s10570-020-03105-w

Lourenço AF, Godinho D, Gamelas JA, Sarmento P, Ferreira PJ (2019b) Carboxymethylated cellulose nanofibrils in papermaking: influence on filler retention and paper properties. Cellulose 26 (5)**:** 3489-3502. https://doi.org/10.1007/s10570-019-02303-5

Manninen M, Kajanto I, Happonen J, Paltakari J (2011) The effect of microfibrillated cellulose addition on drying shrinkage and dimensional stability of wood-free paper. Nord Pulp Paper Res J 26 (3)**:** 297-305. https://doi.org/10.3183/npprj-2011-26-03-p297-305

Mashkour M, Afra E, Resalati H, Mashkour M (2015) Moderate surface acetylation of nanofibrillated cellulose for the improvement of paper strength and barrier properties. RSC Adv 5 (74)**:** 60179-60187. https://doi.org/10.1039/C5RA08161K

Merayo N, Balea A, de la Fuente E, Blanco Á, Negro C (2017a) Interactions between cellulose nanofibers and retention systems in flocculation of recycled fibers. Cellulose 24 (2)**:** 677-692. https://doi.org/10.1007/s10570-016-1138-0

Merayo N, Balea A, de la Fuente E, Blanco Á, Negro C (2017b) Synergies between cellulose nanofibers and retention additives to improve recycled paper properties and the drainage process. Cellulose 24 (7)**:** 2987-3000. https://doi.org/10.1007/s10570-017-1302-1

Miller J (2019) Nanocellulose: Market perspectives. Tappi J 18 (5)**:** 313-316.

Moodley RS (2018) Evaluation of paper substrates for microfluidic application in medical diagnostic kits. Dissertation, University of KwaZulu-Natal.

Moon RJ, Martini A, Nairn J, Simonsen J, Youngblood J (2011) Cellulose nanomaterials review: structure, properties and nanocomposites. Chem Soc Rev 40 (7)**:** 3941-3994. https://doi.org/10.1039/C0CS00108B

Mörseburg K, Chinga-Carrasco G (2009) Assessing the combined benefits of clay and nanofibrillated cellulose in layered TMP-based sheets. Cellulose 16 (5)**:** 795-806. https://doi.org/10.1007/s10570-009-9290-4

Nagarajan K, Ramanujam N, Sanjay M, Siengchin S, Surya Rajan B, Sathick Basha K, Madhu P, Raghav G (2021) A comprehensive review on cellulose nanocrystals and cellulose nanofibers: Pretreatment, preparation, and characterisation. Polym Compos 42 (4)**:** 1588-1630. https://doi.org/10.1002/pc.25929

Naz S, Ali JS, Zia M, Manufacturing (2019) Nanocellulose isolation characterisation and applications: a journey from non-remedial to biomedical claims. Bio-Des Manuf 2 (3)**:** 187-212. https://doi.org/10.1007/s42242-019-00049-4

Nechyporchuk O, Belgacem MN, Bras J (2016) Production of cellulose nanofibrils: A review of recent advances. Ind Crops Prod 93**:** 2-25. https://doi.org/10.1016/j.indcrop.2016.02.016

Osong SH, Norgren S, Engstrand P (2014) Paper strength improvement by inclusion of nano-ligno-cellulose to chemi-thermomechanical pulp. Nord Pulp Paper Res J 29 (2)**:** 309-316. https://doi.org/10.3183/npprj-2014-29-02-p309-316

Osong SH, Norgren S, Engstrand P (2016) Processing of wood-based microfibrillated cellulose and nanofibrillated cellulose, and applications relating to papermaking: a review. Cellulose 23 (1)**:** 93-123. https://doi.org/10.1007/s10570-015-0798-5

Ottesen V (2018) Cellulose Nanofibrils as Paper Additive and Coating Material: Properties, Distribution and Interaction Effects. Dissertation, Norwegian University of Science and Technology.

Page D (1969) A theory for the tensile strength of paper. Tappi J 52**:** 674-681.

Park TU, Lee JY, Jo HM, Kim KM (2018) Utilization of cellulose micro/nanofibrils as paper additive for the manufacturing of security paper. BioResources 13 (4)**:** 7780-7791. https://doi.org/10.15376/biores.13.4.7780-7791

Petroudy SRD, Syverud K, Chinga-Carrasco G, Ghasemain A, Resalati H (2014) Effects of bagasse microfibrillated cellulose and cationic polyacrylamide on key properties of bagasse paper. Carbohydr Polym 99**:** 311-318. https://doi.org/10.1016/j.carbpol.2013.07.073

Phipps J, Larson T, Ingle D, Eaton H (2017). The Effect of Microfibrillated Cellulose on the Strength and Light Scattering of Highly Filled Papers. *Advances in Pulp and Paper Research*. Trans of the XVIth Fund Res Symp Oxford.

Potulski DC, Viana LC, da Fonte AN, Carneiro ME, de Muniz GIB, Klock U (2020) Nanofibrillated cellulose applied as reinforcement for short-fiber paper. Floresta 50 (3)**:** 1411-1420. https://doi.org/10.5380/rf.v50i3.59251

Ru J, Tong C, Chen N, Shan P, Zhao X, Liu X, Chen J, Li Q, Liu X, Liu H (2019) Morphological and property characteristics of surface-quaternized nanofibrillated cellulose derived from bamboo pulp. Cellulose 26 (3)**:** 1683-1701. https://doi.org/10.1007/s10570-018-2146-z

Saito T, Kuramae R, Wohlert J, Berglund LA, Isogai A (2013) An ultrastrong nanofibrillar biomaterial: the strength of single cellulose nanofibrils revealed via sonication-induced fragmentation. Biomacromolecules 14 (1)**:** 248-253. https://doi.org/10.1021/bm301674e

Sanchez-Salvador JL, Balea A, Monte MC, Negro C, Miller M, Olson J, Blanco A (2020) Comparison of mechanical and chemical nanocellulose as additives to reinforce recycled cardboard. Sci Rep 10 (1)**:** 1-14. https://www.nature.com/articles/s41598-020-60507-3

Sehaqui H, Allais M, Zhou Q, Berglund L (2011) Wood cellulose biocomposites with fibrous structures at micro- and nanoscale. Compos Sci Technol 71 (3)**:** 382-387. https://doi.org/10.1016/j.compscitech.2010.12.007

Sehaqui H, Zhou Q, Berglund LA (2013) Nanofibrillated cellulose for enhancement of strength in high-density paper structures. Nord Pulp Paper Res J 28 (2)**:** 182-189. https://doi.org/10.3183/npprj-2013-28-02-p182-189

Spence KL, Venditti RA, Rojas OJ, Habibi Y, Pawlak J (2010) The effect of chemical composition on microfibrillar cellulose films from wood pulps: water interactions and physical properties for packaging applications. Cellulose 17 (4)**:** 835-848. https://doi.org/10.1007/s10570-010-9424-8

Su J, Mosse WK, Sharman S, Batchelor WJ, Garnier G (2013) Effect of tethered and free microfibrillated cellulose (MFC) on the properties of paper composites. Cellulose 20 (4)**:** 1925-1935. https://doi.org/10.1007/s10570-013-9955-x

Su J, Zhang L, Batchelor W, Garnier G (2014) Paper engineered with cellulosic additives: effect of length scale. Cellulose 21 (4)**:** 2901-2911. https://doi.org/10.1007/s10570-014-0298-z

Subramanian R, Hiltunen E, Gane PA (2011) Potential use of micro-and nanofibrillated cellulose composites exemplified by paper. In: Kalia S (ed) Cellulose Fibers: Bio-and Nano-Polymer Composites. Springer, Berlin pp 121-152

Syverud K, Gregersen Ø, Chinga-Carrasco G, Eriksen Ø (2009) The influence of microfibrillated cellulose, MFC, on paper strength and surface properties. Nord Pulp Paper Res J**:** 899-930. https://doi.org/10.15376/frc.2009.2.899

Taipale T, Österberg M, Nykänen A, Ruokolainen J, Laine J (2010) Effect of microfibrillated cellulose and fines on the drainage of kraft pulp suspension and paper strength. Cellulose 17 (5)**:** 1005-1020. https://doi.org/10.1007/s10570-010-9431-9

Tajik M, Torshizi HJ, Resalati H, Hamzeh Y (2018) Effects of cationic starch in the presence of cellulose nanofibrils on structural, optical and strength properties of paper from soda bagasse pulp. Carbohydr Polym 194**:** 1-8. https://doi.org/10.1016/j.carbpol.2018.04.026

Tarrés Q, Saguer E, Pèlach M, Alcalà M, Delgado-Aguilar M, Mutjé P (2016) The feasibility of incorporating cellulose micro/nanofibers in papermaking processes: the relevance of enzymatic hydrolysis. Cellulose 23 (2)**:** 1433-1445. https://doi.org/10.1007/s10570-016-0889-y

Tozluoglu A, Poyraz B (2016) Effects of cellulose micro/nanofibers as paper additives in kraft and kraft-$NaBH_4$ pulps. Nord Pulp Paper Res J 31 (4)**:** 561-572. https://doi.org/10.3183/npprj-2016-31-04-p561-572

Vallejos ME, Felissia FE, Area MC, Ehman NV, Tarrés Q, Mutjé P (2016) Nanofibrillated cellulose (CNF) from eucalyptus sawdust as a dry strength agent of unrefined eucalyptus handsheets. Carbohydr Polym 139**:** 99-105. https://doi.org/10.1016/j.carbpol.2015.12.004

Zambrano F, Starkey H, Wang Y, de Assis CA, Venditti R, Pal L, Jameel H, Hubbe MA, Rojas OJ, Gonzalez R (2020) Using micro-and nanofibrillated cellulose as a means to reduce weight of paper products: A review. BioResources 15 (2)**:** 4553-4590. https://doi.org/10.15376/BIORES.15.2.4553-4590

Zeng J, Liu L, Li J, Dong J, Cheng Z (2020) Properties of cellulose nanofibril produced from wet ball milling after enzymatic treatment vs. mechanical grinding of bleached softwood kraft fibers. BioResources 15 (2)**:** 3809-3820. https://doi.org/10.15376/biores.15.2.3809-3820

Zeng J, Zeng Z, Cheng Z, Wang Y, Wang X, Wang B, Gao W (2021) Cellulose nanofibrils manufactured by various methods with application as paper strength additives. Sci Rep 11 (1)**:** 1-16. https://doi.org/10.1038/s41598-021-91420-y

Zimmermann T, Pöhler E, Geiger T (2004) Cellulose fibrils for polymer reinforcement. Adv Eng Mater 6 (9)**:** 754-761. https://doi.org/10.1002/adem.200400097

3 CHAPTER THREE: CHARACTERISATION OF PULP AND PAPER MILL SLUDGE FOR BENEFICIATION (This paper was published in the Journal of Cellulose and is available online https://doi.org/10.1007/s10570-022-04578-7)

Thabisile Brightwell Jele[1], Prabashni Lekha[2], Bruce Sithole[1, 2]

[1]*University of KwaZulu-Natal (Howard Campus), Discipline of Chemical Engineering, College of Agriculture, Engineering and Sciences, Durban,* [2]*Council for Scientific and Industrial Research, Biorefinery Industry Development Facility, Durban, South Africa*

[*]Corresponding Author: thabisilejele94@gmail.com; sitholeb1@ukzn.ac.za

3.1 Abstract

In this study, three different pulp and paper mill sludge (PPMS) samples collected from different South African mills were chemically and physically characterised to investigate their suitability for various beneficiation pathways. The overall objective was to identify the most suitable beneficiation opportunities for each PPMS sample based on characteristics. The potential beneficiation pathways (identified) were biofuels, building materials (cement and brick), biopolymer/composites, cellulose nanomaterials, composting, land application, animal feed, and thermal processing (energy). Each beneficiation pathway was more suitable for one type of PPMS due to varying characteristics. The characteristics of PPMS were influenced by the pulping technique employed at each mill, the raw materials and the type of effluent treatment employed. Thermal analysis revealed that the calorific values of all PPMS samples studied were too low for energy harvesting (thermal processing). The high ash content of PPMS C and PPMS A was suitable for biocomposites whose strength could be enhanced by fillers present in PPMS samples. The higher glucose content in PPMS B compared to PPMS A and PPMS C was favourable for bioethanol and bio-oil production. The high cellulose and low ash content of PPMS B were found suitable for the production of nanocellulose.

Keywords: pulp, paper, sludge, characterisation, beneficiation

3.2 Introduction

Beneficiation of waste is a waste management technique that may reduce landfilling costs, increase employment opportunities, extra revenue, and efficient use of resources in many industries. The initial stage of any beneficiation process is characterisation. It entails determining the physical, chemical, biological and radiological properties of waste. Pulp and paper mills (PPM) are one of the largest industries globally that could benefit from the beneficiation of waste to compensate for its low resource utilization rate, around 65% (Cherian and Siddiqua 2019). South Africa generates approximately 500 000 tonnes of waste pulp and paper mill sludge (PPMS) per annum (Boshoff et al. 2016; Gibril et al. 2018). The rate of PPMS production is around 40-50 kg of dry PPMS per tonne of paper produced (Goel and Kalamdhad 2017; Kaur et al. 2020; Haile et al. 2021). The variation in PPMS characteristics is directly linked to the technology used to pulp the wood (e.g. chemical or mechanical), the raw material used in the mill (e.g. wood or recovered paper) and the type of effluent treatment employed. Consequently, PPMS can be classified into various categories, *viz.* virgin, printed recycle, deinking, and corrugated recycle (Boshoff et al. 2016). Traditionally, in South Africa, PPMS is disposed of by landfilling. However, landfilling leads to greenhouse gas emissions, ground and surface water pollution caused by leachate generation at the landfill site. The increased awareness of environmental risks associated with PPMS landfilling,

tightened legislation in waste management, landfilling costs, and limited landfill space are the major driving forces for the PPMs to seek alternative solutions for sustainable management of PPMS (Mahmood and Elliott 2006). Applications of PPMS include agriculture (composting and land application), cement production, brick manufacturing, road construction, agriculture, anaerobic digestion (biogas production), biohydrogen production, incineration (energy harvesting), production of ethanol, pyrolysis (production of bio-oil or char), manufacture of composites and recovery of minerals, nanocellulose production, isolation of enzymes, paper and board industry, production of carbon adsorbents, production of lactic acid and production of animal feed (Lee et al. 2004; Gea et al. 2005; Marques et al. 2008; Budhavaram and Fan 2009; Ince et al. 2011; Alriksson et al. 2014; Ghribi et al. 2016; Goel and Kalamdhad 2017; Jaria et al. 2017; Lekha et al. 2017; Haile et al. 2021; Tawalbeh et al. 2021). However, some of these applications have several limitations because of the associated environmental hazards. For instance, in land application and composting, metals such as cadmium present in sludge bioaccumulated in plants tissues (Scott et al. 1995; Ince et al. 2011). PPMS from recycle mills was unsuitable for use as a soil amender due to groundwater contamination by leaching of salts, nitrates, and heavy metals (Marques et al. 2008). Incineration resulted in GHG, SOx and NOx emissions which were an environmental and health hazard (Assis and Chirwa 2021). The presence of high ash content in PPMS decreased its gross calorific value, led to equipment corrosion and created a residue that needed to be disposed (Lieskovský et al. 2017). Despite the high organic content of PPMS, its low feeding value and ash content were limiting factors for use as an animal feed. Therefore, the addition of a supplementary nitrogen component to increase the digestibility of proteins was required (Scott et al. 1995). In brick manufacturing, sludge improved porosity, density, and thermal conductivity. However, the mechanical properties of bricks reinforced with sludge were negatively affected (Goel and Kalamdhad 2017). Moreover, each of these beneficiation pathways is more suitable for one type of PPMS than another due to the deferring characteristics of PPMS. However, most of these applications have several limitations because of the associated environmental hazards. Moreover, each of these beneficiation pathways is more suitable for one type of PPMS than another due to the deferring characteristics of PPMS. Boshoff (2015) studied the composition (glucose, xylose, lignin, extractives, ash) and physio-chemical properties (water holding capacity and viscosity) of PPMS for the production of bioethanol. Significant differences were reported for viscosity and water holding capacity for the different PPMS samples. Viscosity and water holding capacity influenced the solids loading and ultimately the enzymatic hydrolysis of sugars due to the limited accessibility of enzymes to the fibres. Corrugated PPMS with the lowest viscosity and solids loading was found to be more suited for ethanol production than virgin PPMS, which had higher viscosity (18% (w/w)) and solids loading (Boshoff 2015). Duncan et al. (2020) characterised five types of PPMS (both washed and unwashed) for ethanol and isoprene production. They found that the unwashed Kraft PPMS with 23% ash, 18% $CaCO_3$ and 34% glucan content had a 99% enzyme hydrolysis efficiency in bioethanol production. The $CaCO_3$ content was the main limiting factor for all the PPMS types studied. Enzyme hydrolysis of PPMS was negatively affected by $CaCO_3$ due to the large surface area of the fibres. The highest production of isoprene was from a washed recycle PPMS with 13% ash, 13% $CaCO_3$ and 56% glucan content. Goel and Kalamdhad (2017) reported that PPMS contains fluxing agents such as K_2O, Fe_2O_3, CaO, MgO and TiO_2, which aid in the reduction of energy requirements in brick production. Simão et al. (2019) characterised PPMS for the production of waste-based cement. The PPMS was classified as non-hazardous from the toxicological analysis of the PPMS, and chemical characterisation of the PPMS showed the presence of CaO, SiO_2, Al_2O_3, and organic matter content, which qualified it for use in cement production (Goel and Kalamdhad

2017; Simão et al. 2019). Geng et al. (2007) compared deinking and primary PPMS for suitability in the manufacture of fibre boards. Primary PPMS was proved to be more suitable than deinking PPMS due to its long fibres, low ash content, low pH and high acid buffering capability (Geng et al. 2007). Migneault et al. (2010) studied the feasibility of using PPMS for medium-density fibreboards (MDF). The ash content and inorganic matter (>8%) were proven not to be detrimental to the premature wear of cutting and sanding tools of the MDF. The important properties of MDF such as thickness swell (TS), linear expansion (LE), internal bond (IB), modulus of elasticity (MOE), and modulus of rupture (MOR) all decreased with an increase in PPMS content for all types of PPMS (i.e. Thermo-Mechanical Pulping, Chemi-Thermomechanical Pulp and Kraft). On the other hand, high PPMS content resulted in smooth and uniform textured MDF. This was attributed to the small dimensions of the PPMS fibres compared to conventional fibres used in MDFs (Migneault et al. 2010). Ridout et al. (2015) characterised low and high ash PPMS for bio-oil production via fast pyrolysis. High ash PPMS produced bio-oil with a higher heating value and lower oxygen to carbon molar ratio than low ash PPMS. The $CaCO_3$ present in high ash PPMS was responsible for promoting de-oxygenation of the bio-oil leading to its high heating value. Beauchamp et al. (2002) found that deinking PPMS was environmentally safe for use as compost. The fact that PPMS characteristics vary significantly, generalisation in terms of beneficiation pathways was not recommended (Jaria et al. 2017). In this study, PPMS samples were characterised, and beneficiation pathways were identified based on these characteristics.

3.3 Materials and Methods

3.3.1 Materials

Three types of PPMS were collected from PPMs in South Africa. Each of the PPMS samples was a mix of primary and secondary sludge. Table 3-1 presents the category and equivalent ID of PPMS samples. The PPMS samples were collected in plastic bags, sealed and stored in a cold room at 4°C to minimize bacterial activity (Manesh 2012).

Table 3-1 The category and equivalent ID of PPMS samples

Sludge ID	**PPMS A**	**PPMS B**	**PPMS C**
Category	Recycle	Virgin	Deinking

3.3.2 Methods

The PPMS samples were analysed as received from the PPMs.

3.3.2.1 Moisture content

The moisture content was determined according to TAPPI Standard (T 264 cm-07). 2 g of sludge (as received) was dried to a constant weight at a temperature of 105°C in an oven (Fisher Scientific, USA). The moisture content was calculated according to Equation 3 below.

$$Moisture\ (\%) = \frac{wet\ pulp\ weight - oven\ dry\ weight\ of\ pulp}{wet\ pulp\ weight} \quad (3)$$

3.3.2.2 Bulk Density

The bulk density was determined by calculating the mass to volume ratio of oven-dried PPMS samples that filled a 25 ml measuring cylinder (Chimphango et al. 2021). The bulk density was calculated according to Equation 4 below.

$$Bulk\ density = \frac{M\ (g)}{V\ (cm^{-3})} \quad (4)$$

Where M is the mass of PPMS, V is the volume of the measuring cylinder.

3.3.2.3 Appearance

Visual inspection was used to determine the appearance of the sludge samples.

3.3.2.4 Electrical Conductivity and pH

An Orion Star A3290 multiparameter meter (Orion, USA) was used to measure pH and electrical conductivity. The pH of PPMS samples was measured using the multiparameter meter in a 1:10 (v/v) PPMS to water suspension. Three conductivity readings of air-dried PPMS samples were determined according to the method described by Wildauer (2006). 15 g of PPMS was transferred to a 250 ml Erlenmeyer flask containing 75 ml of deionized water. The stoppered flasks were put on a platform shaker (Labcon SFP 55, SA), and the mixtures were shaken for 1 h. The filtrates obtained after vacuum filtration (0.45µm filter paper) were centrifuged for 5 minutes at 10 000 rpm using a centrifuge (Hettich Universal 320R, Germany).

3.3.2.5 Fourier-transform infrared spectroscopy (FTIR)

Fourier-transform infrared spectroscopy was carried out using a Spectrum 100 FTIR spectrophotometer (PerkinElmer, USA) to investigate the chemical functional groups present in PPMS. The scanning conditions were in the spectral range of 4000-500 cm^{-1} and with a resolution of 4 cm^{-1}

3.3.2.6 The X-ray diffraction (XRD) analysis

The XRD analysis (BRUKER AXS, Germany) was used to study the crystallinity of the PPMS samples. The XRD patterns were produced with scattering radiation at 2θ = 5-90° at a rate of 1 second per step. The crystalline index (CrI) was calculated according to Equation 5 (Segal et al. 1959).

$$CrI\ (\%) = \frac{I_{200} - I_{am}}{I_{200}} \quad (5)$$

Where CrI is the crystallinity index (%), I_{200} is the maximum intensity of the most intense peak of the crystalline contribution located at around $2\theta = 22^{o}$, and I_{am} is the minimum intensity of diffraction that represents the amorphous component at around $2\theta = 18^{o}$ (Bettaieb et al. 2015).

3.3.2.7 Carbohydrate and lignin content

The polysaccharide content of PPMS samples was measured by High Performance Liquid Chromatography (HPLC) (Thermo Scientific Dionex ICS-5000^{+}, USA) according to TAPPI T249 cm-85. The lignin content was simultaneously determined by drying and weighing the insoluble material remaining after acid hydrolysis and filtration. The obtained lignin content was defined as the Klason lignin, whilst the soluble lignin fraction was determined by analysis of the hydrolysate by UV/ VIS spectroscopy (Varian Cary® 50, USA) at 205 nm.

3.3.2.8 Ash content

The ash content of the PPMS was measured by combustion in a muffle furnace at 525^{o}C for 4 h in accordance with Tappi T211 om-02.

3.3.2.9 Extractives

The total solvent extractives were determined according to the TAPPI 204 cm-97.

3.3.2.10 Morfi Analyser

The morphology of PPMS samples was carried out using a Morfi analyser (MorFi Compact TechPap, France). 0.2g (oven dry) of each of the three PPMS samples was suspended in 500 ml of H_2O, disintegrated for 5 mins and analysed while being vigorously mixed to obtain a uniform distribution of fibres. The results were analysed with TechPap MorFi software.

3.3.2.11 Scanning Electron Microscope (SEM)

The SEM (Phenom Pharos Desktop) was used to study the morphology of PPMS samples at a voltage of 10 kV. The dried samples were placed on an aluminium stub using carbon tape. Thereafter, samples were coated with gold using a sputter coater to increase conductivity. An Energy Dispersive X-Ray Analyser (EDX) was used to provide elemental identification and quantitative compositional information of the PPMS samples.

3.3.2.12 Ultimate Analysis

The ultimate analysis was conducted using a 2400 Series II CHNS/O Elemental Analyzer (PerkinElmer, USA). Approximately, 2 mg of each PPMS sample was introduced into a silver-tin capsule and placed in a furnace maintained at 975^{o}C. The results were obtained as weight percentage of carbon, hydrogen, nitrogen and sulfur.

3.3.2.13 Thermal Analysis

The Perkin Elmer Simultaneous Thermal Analyser STA 600 was used for thermal analysis of PPMS samples. The samples were heated at a rate of 10^{o}C min^{-1}and a temperature range of 30 ^{o}C to 600^{o}C under a nitrogen atmosphere which was set at a flow rate of 20 ml min^{-1} for 60 min. The thermogravimetric (TG) curve and the Derivative Thermogravimetric (DTG) curve were obtained using Origin software. A Semi-Automatic Calorimeter (AC600, USA) was used to determine the calorific values of the PPMS samples.

3.4 Results and Discussions

3.4.1 Physical Characteristics

The physical characteristics of PPMS samples such as moisture (%), density (g cm^{-3}), pH, conductivity (µs cm^{-1}), appearance are shown in Table 3-2.

Table 3-2 Physical characteristics of the PPMS samples

Characteristic	**PPMS A**	**PPMS B**	**PPMS C**
Moisture (%)	78.77 ± 0.79	81.10 ± 2.95	74.23 ± 1.08
Density (g cm^{-3})	0.73 ± 0.02	0.76 ± 0.01	0.84 ± 0.05
pH	8.10 ± 0.09	8.64 ± 0.01	8.29 ± 0.02
Conductivity (µs cm^{-1})	1105 ± 0.70	350.6 ± 0.04	1431
Appearance	Black	Brown	Grey

3.4.1.1 Visual characteristics

Figure 3-1 shows the difference in the appearance of the PPMS samples. Visual inspection of the samples showed that PPMS A, PPMS B, and PPM C was black, brown, and grey, respectively. PPMS A and PPMS B appeared as

lumps of fibres combined with tiny plastic material. PPMS C appeared to contain finer and homogenous fibres. This was reflected by the higher bulk density of PPMS C compared to PPMS A and PPMS B, as discussed in section 3.4.1.4

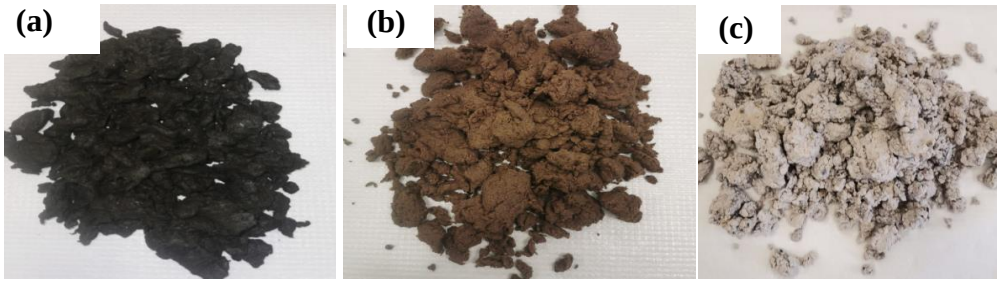

Figure 3-1 Photographs of (a) PPMS A (b) PPMS B (c) PPMS C

3.4.1.2 pH

There was little difference in the pH of all the sludge samples, which ranged from pH 8.1 to 8.6. All the PPMS types were alkaline due to the presence of $CaCO_3$ (Méndez et al. 2009). These pH values were comparable to deinking PPMS with pH values between 7.6 and 7.8 (Beauchamp et al. 2002; Elloumi et al. 2016). Bekhta et al. (2019) reported that PPMS with a pH greater than 8 was not acceptable for use as adhesive fillers in plywood manufacturing (Bekhta et al. 2019). Zhu et al. (2012) studied the conversion of PPMS from deinking mills and chemical pulping mills to ethanol using yeast. The optimum pH of PPMS for saccharification was obtained at 5 for all PPMS types studied (Zhu et al. 2012).

3.4.1.3 Moisture content

The moisture content (as received) for PPMS A, PPMS B and PPMS C was 79%, 81% and 74%, respectively. These values were comparable to the moisture content of previously studied PPMS samples (45-80%) (Strezov and Evans 2009; Abdullah et al. 2015; Bester 2018). High moisture content in PPMS resulted from water absorption due to the hygroscopic nature of cellulose fibres. In most biochemical beneficiation processes such as ethanol production, the high moisture content resulted in viscous suspensions requiring intensive mixing (Williams 2017). Boshoff et al. (2016) reported that in biofuel production, PPMS is a poor raw material because of the high moisture content. Dewatering PPMS was energy demanding (Hagelqvist 2013). In order to avoid dewatering, wet anaerobic digestion of PPMS combined with nitrogen-rich material such as municipal sludge was efficient in producing biogas (Hagelqvist 2013).

3.4.1.4 Bulk density

PPMS C had the highest bulk density (0.84 g cm^{-3}) compared to PPMS B (0.76 g cm^{-3}) and PPMS A (0.73 g cm^{-3}). As expected, the density of PPMS C was influenced by the higher ash content. The difference in the densities was attributed to the mill pulping process employed, the physical properties and the source of PPMS samples (Clark 1985). PPMS C had a finer texture than PPMS A and B, hence the higher density. A higher bulk density indicated a high proportion of short fibres (Xing et al. 2006; Migneault et al. 2010). This was confirmed by the Morfi results in Table 3-4, where PPMS B had the highest arithmetic length of 452 µm, hence its lower bulk density. Chimphango et al. (2021) compared three types of PPMS from South African mills for their suitability in making composite boards. Virgin pulp-PS was found suitable for producing low-density particleboards due to its

density of 0.58 g cm^{-3}. Corrugated recycled sludge (CR-PS) with a density of 0.97 g cm^{-3} and recycled newsprint sludge (RN-PS) with a density of 1.07 g cm^{-3} qualified for the production of average density boards (Chimphango et al. 2021).

3.4.1.5 Electrical Conductivity

The electrical conductivity was an indication of the salinity of the PPMS samples. Electrical conductivity ascertained the presence of ions in PPMS since salts transmit electricity in solution. The conductivity of PPMS samples is shown in Table 3-2. PPMS C had the highest conductivity of 1431 µS cm^{-1}. This was comparable to the electrical conductivity of PPMS from a bleached chemo-thermomechanical pulp (CTMP) mill (1466 µS cm^{-1}) (Wildauer 2006). Abdullah et al. (2015) reported the average electrical conductivity of 1300 µS cm^{-1} for six different PPMS samples (Abdullah et al. 2015).

3.4.2 Chemical Composition

3.4.2.1 Ash content

The ash content for PPMS A, PPMS B and PPMS C was 24%, 8.1%, and 38 %, respectively. PPMS A and PPMS B were classified as low ash (<30%), while PPMS C was classified as high ash (>30%) (de Alda 2008). PPMS C had the highest ash content because of the high quantities of chemicals and recycled fibres used in the mill pulping processes (Zhang et al. 2017). PPMS B had the lowest ash content because it was collected from a non-recycle mill. The ash content reported for PPMS B was similar to that of virgin wood PPMS (8.1%) reported by Chimphango et al. (2021). The high ash content in PPMS C was attributed to the recycling of recovered paper, which had high amounts of fillers in the paper (Zhang et al. 2017; Kaur et al. 2020).

Chimphango et al. (2021) reported ash contents of 8.1% for virgin, corrugated of 29.9% and recycle PPMS of 64.4%. High ash PPMS was reported to positively and negatively impact particleboard manufacturing (Chimphango et al. 2021). The inverse proportional relationship between ash content and fibrous content negatively impacted the strength properties of particleboard. In contrast, the ash content in the form of fillers (e.g. calcium carbonate) acted as a flexural strength enhancer by filling in the voids within the cement structure in boards and increasing the density of fibres. This was also confirmed in the manufacture of high-density polyethene (HDPE) composites, where cellulose and ash led to improved composite strength and stiffness (Soucy et al. 2016). Williams et al. (2017) reported that high ash content was detrimental to the hydrolysis efficiency for biofuels production processes. The ash reduced the hydrolysis efficiency, which in turn decreased the yield of the biofuels. (Robus et al. 2016; Williams 2017). Ash in the form of $CaCO_3$ had a higher affinity for cellulose enzymes than fibres. Also, ash in the form of clay was inactively bound to cellulose and reduced the availability of fibres for enzyme hydrolysis and fermentation in ethanol production (Nikolov et al. 2000; Kang et al. 2011). The best way to improve ethanol yields up to 40% was to fractionate the sludge in order to reduce the ash content by 82 to 98% (Chen et al. 2014). While high ash content in the form of $CaCO_3$ was detrimental for ethanol production, it was desirable for soil amendment for acidic soils (Ince et al. 2011). Chen et al. (2014) suggested that fractionating PPMS into two streams (an ash-rich stream and a fibre rich stream) was an efficient way of ensuring a high production yield of ethanol while providing a soil amender. Also, the high ash stream was composted and utilized in improving nitrogen mineralization rates and reducing the need for supplementary nitrogen in soils (Chen et al. 2014). Chen et al. (2014) studied the suitability of high ash fractioned sludge as a soil amendment. The ash-rich fractioned PPMS had a low C:N ratio with macronutrient preservation, hence its desirability as a soil amendment

as opposed to unfractionated sludge. Ash from PPMS was also successfully used as a replacement for sand in mortars (Wang et al. 2014).

Xing et al. (2012) reported 12% and 41.3% ash content for TMP and Kraft PPMS, respectively. The addition of the two types of PPMS to particleboard manufacture had a positive impact on properties such as IB, MOE and MOR and a negative impact on TS (Xing et al. 2012). However, high dosages of PPMS caused a decrease in MOR due to the inadequate bonding between PPMS and wood in the presence of ash (kaolin clay and calcium carbonate). The downside of ash content in the range of 20-40% was that it caused equipment erosion (Bekhta et al. 2019).

3.4.2.2 Carbohydrates, lignin and extractives

The carbohydrate, lignin and extractives content of PPMS are presented in Table 3-3. Compared with PPMS B and PPMS C, PPMS A had higher lignin and extractive content. PPMS A, PPMS B and PPMS C had lignin contents of 33.5%, 19.71% and 7.91% respectively. These lignin values corresponded with the colour of the PPMS. For instance, PPMS A had the highest lignin and the highest colour intensity (black). PPMS B had a lower lignin value than PPMS B, hence a low colour intensity (brown). PPMS C had the lowest lignin and appeared grey in colour. The grey colour may be from the ash content (37.81%). The extractive contents of all PPMS samples were lower (0.78-1.61%) than that reported in the literature (3.5-10.5%), and this may be related to the wood species used (Wang et al. 2014; Ridout et al. 2015; Schroeder et al. 2017).

The cellulose and lignin composition of PPMS directly affected beneficiation processes such as bioethanol production, nanocellulose production and composites manufacture. PPMS B, with high glucose and low lignin and ash content, qualifies for bioethanol or nanocellulose production (Leão et al. 2012; Adu et al. 2018; Bester 2018; Du et al. 2020; Duncan et al. 2020).

Table 3-3 Chemical composition of PPMS samples

Parameter (%)	PPMS A	PPMS B	PPMS C
Arabinose	0.17 ± 0.04	0.43 ± 0.06	0.05 ± 0.01
Galactose	0.61 ± 0.05	0.99 ± 0.08	0.12 ± 0.01
Glucose	36.26 ± 1.01	62.83 ± 0.20	52.37 ± 0.09
Xylose	3.11 ± 0.18	3.21 ± 0.37	10.52 ± 0.09
Mannose	0.05 ± 0.05	3.46 ± 0.02	ND
Ash	24.69 ± 0.07	8.06 ± 0.05	37.81 ± 0.07
Lignin	33.5 ± 0.45	19.71 ± 4.64	7.91 ± 3.77
Solvent extractives	1.61 ± 0.1	1.31 ± 0.05	0.78 ± 0.09

3.4.2.3 FTIR Analysis

Figure 3-2 shows the FTIR spectra of PPMS A, PPMS B and PPMS C. All the samples showed analogous spectra with characteristics of cellulose: 3332 cm^{-1} (O-H stretching), 2921 - 2922 cm^{-1} (aliphatic C-H stretching vibration),

1410 -1425 cm^{-1} (HCH and HOC bending), 1635 - 1650 cm^{-1} (O-H bending), 1030 - 1054 cm^{-1} (C-O valence vibration) (Oh et al. 2005; Široký et al. 2010; Schwanninger et al. 2004; Abdul Rahman et al. 2017; Bester 2018; Khenblouche et al. 2019). Peaks in the range 1315 – 1327 cm^{-1} relate to C-C and C-O skeletal vibration. The peaks relating to C-O-C stretching at the β-(1-4) glycosidic linkages were observed at 1144 - 1159 cm^{-1}. Peaks at 1505 - 1595 cm^{-1} were present in PPMS A and PPMS B, corresponding to aromatic skeletal vibrations (Zhuang et al. 2020). The peaks around 1745 cm^{-1} represented C═O stretching in cellulose and hemicellulose (Zhuang et al. 2020). This confirmed the presence of lignin and hemicellulose. Peaks around 1260 are typical of lignin (Abdullah et al. 2015). The broad peak at 1410cm^{-1} and peak at 871cm^{-1} for PPMS C confirmed the presence of calcium in the form of calcium carbonate (Ridout et al. 2015; Jaria et al. 2017; Bekhta et al. 2019).

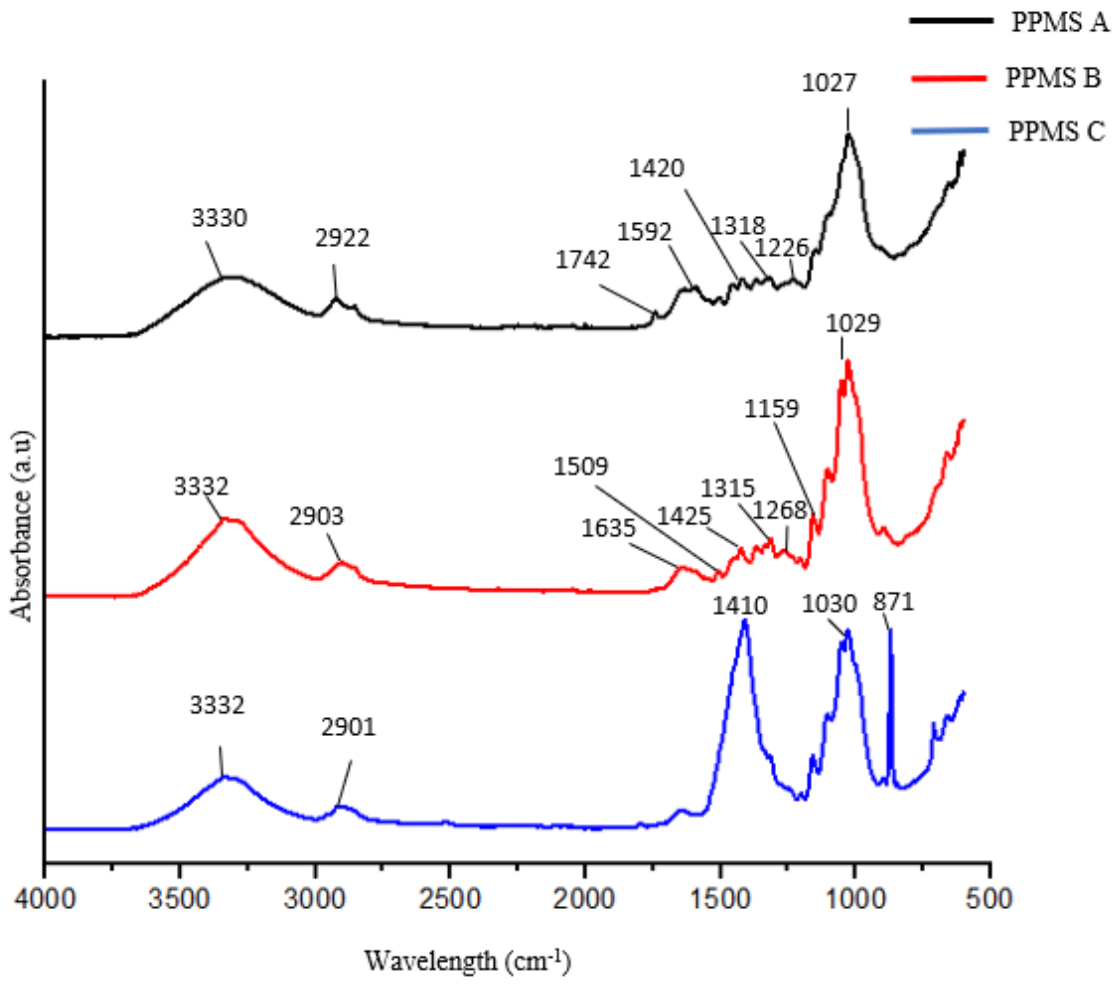

Figure 3-2 Infrared spectra of PPMS A, PPMS B and PPMS C

3.4.2.3 XRD

The XRD patterns of PPMS A, PPMS B and PPMS C are shown in Figure 3-3. The three strongest peaks were located at coordinates 2θ = 16.6, 2θ =22.6 and 2θ = 26.9 for PPMS A. The strongest peaks were located at the coordinates 2θ =15.6, θ = 22.7 and 2θ = 29.9 for PPMS B. The strongest peaks for PPMS C were observed at 2θ = 16.9, 2θ = 23.5 and 2θ = 29.9. The CrI was calculated to be 33.9%, 53.8% and 39.8% for PPMS A, PPMS B and PPMS C, respectively. The magnitude of the crystallinity peaks in Figure 3-3 confirmed the low crystallinity

of PPMS A and PPMS C, which was attributed to the low cellulose content and the presence of degraded fibres from the paper recycling process (Méndez et al. 2009).

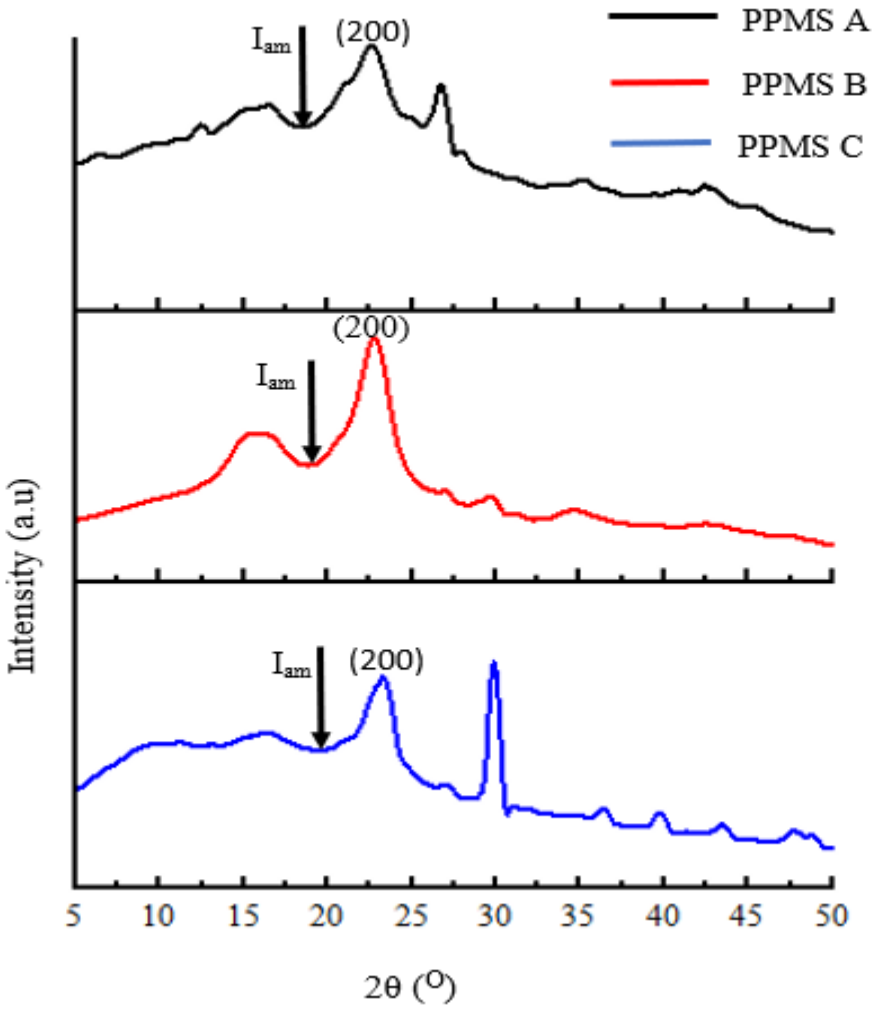

Figure 3-3 XRD patterns of PPMS A, PPMS B, PPMS C

3.4.3 Morphological analysis

3.4.3.1 Fibre Morphology

The morphological analysis of PPMS A, PPMS B and PPMS C is shown in Table 3-4. PPMS B contained the longest fibres (452 µm) followed by PPMS C (418 µm) and PPMS A (410 µm). Virgin PPMS had longer fibres than recycled PPMS fibres (Chen et al. 2014). PPMS A, PPMS B, and PPMS C had a width of 25.3 µm, 24.3 µm and 18 µm, respectively. PPMS A and PPMS C had the highest number of fines, and this was related to the recycled fibre used at both these mills. The short fibres present in PPMS were reported to be suitable for filling the gaps between hardboard fibres, thus increasing the bending strength of hardboards (Eroğlu and Saatci 1993; Davis et al. 2003)

Table 3-4 Fibre morphology of PPMS samples

Parameter	PPMS A	PPMS B	PPMS C
Fibres number/ g	4625 ± 5.44	5015 ± 2.82	5029 ± 7.07
Arithmetic Length (µm)	410 ± 0.60	452 ± 4.24	418 ± 0.70
Average length weighted in length (µm)	622 ± 1.23	713 ± 2.82	720 ± 3.53
Average Width (µm)	25.3 ± 0.11	24.3 ± 0.14	18 ± 0.28
Fines number	279131 ± 2699	65987± 3589	124383 ± 2377
Fines Length Average (µm)	27	28	25

3.4.3.2 Scanning Electron Microscopy analysis

The scanning electron micrographs of the different PPMS samples are shown in Figure 3-4. The morphologies were similar in that they were fibrous. This agreed with findings from other authors about the fibrous nature of PPMS (Singh et al. 2018; Bekhta et al. 2019). However, for PPMS C, inorganic/mineral particulates were shown attached to the fibres. This may be due to the $CaCO_3$, as confirmed by FTIR and the EDX results. Schroeder et al. (2017) studied the morphology of PPMS and confirmed the presence of mineral aggregated particles on the surface of PPMS fibres.

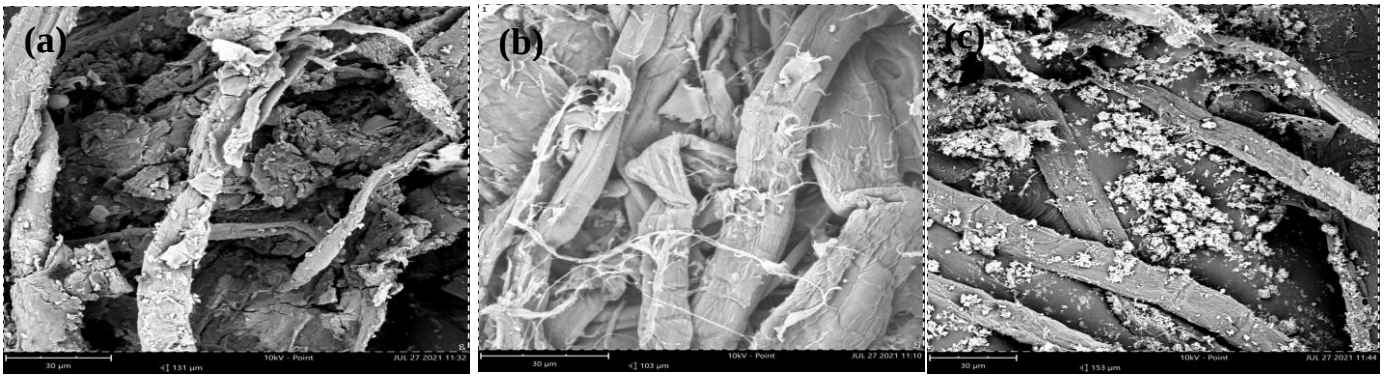

Figure 3-4 SEM images of the top surface of (a) PPMS A (b) PPMS C (c) PPMS C

3.4.4 Elemental analysis

3.4.4.1 Energy-dispersive X-ray Spectroscopy (EDX)

The common elements found in both PPMS A, PPMS B, and PPMS C were carbon, oxygen and calcium. The presence of carbon and oxygen represented the skeleton of carbohydrates and the organic nature of PPMS. As expected, the highest calcium content was in PPMS C since it had the highest ash content. The lowest ash content was shown in PPMS B, which has the lowest ash content. The calcium content for all PPMS types was in the range 0.4-21% reported for deinked PPMS (Davis et al. 2003; Rivera et al. 2016). The source of Ca was coating materials such as paper brighteners/opacifiers and fillers from recycled paper (Davis et al. 2003; Ridout et al.

2015; Rivera et al. 2016). Silicon, sodium and magnesium were only prevalent in PPMS A and PPMS B and could have originated from the talc filler ($3MgO\ 4SiO\ 2H_2O$) and kaolin ($Al_2\ Si_2\ O_5\ (OH)_4$) (Schroeder et al. 2017). Sodium was associated with the use of sodium hydroxide in the pulping process (Abdullah et al. 2015). Silicon was reported to be a component of ash. (Ahmad et al. 2013). Sulphur, niobium, and bromine were present in PPMS A only. The sulphur was assumed to be from the neutral sulphite semi-chemical pulping process. The gold present in all PPMS types could be due to the sputter coating during sample preparation for SEM. The content of elements detected in EDX was not the same as the ultimate analysis results because EDX is semi-quantitative and represents only a section of the PPMS sample (Wildauer 2006). Zhu et al. (2012) reported that metal ions present in deinking PPMS affects the performance of cellulose in the conversion of PPMS to bioethanol (Zhu et al. 2012). Abdullah et al. (2015) reported that the presence of calcium and magnesium in the form of hydroxide was essential in neutralising the soil acidity and increasing soil fertility.

Table 3-5 Elemental composition of PPMS A, PPMS B and PPMS C obtained from EDX analysis

Element (%)	PPMS A	PPMS B	PPMS C
Carbon	24.54	33.78	33.96
Oxygen	28.38	32.61	21.87
Gold	27.64	23.62	25.01
Sulfur	4.18	N.D	N.D
Molybdenum	N.D	4.25	N.D
Calcium	4.31	1.60	19.16
Chlorine	N.D	1.36	N.D
Magnesium	0.92	0.76	N.D
Silicon	2.93	0.86	N.D
Sodium	0.98	0.63	N.D
Bromine	3.92	N.D	N.D
Niobium	2.20	N.D	N.D

3.4.4.2 Ultimate Analysis

The results of the ultimate analysis of PPMS are shown in Table 3-6. All three PPMS samples did not exhibit any similarity in terms of carbon, hydrogen and oxygen content. The carbon content varied between 31.3 and 47.3%. This was slightly above the range reported in the literature (i.e. 28.4 -39.29%) (Rivera et al. 2016). Generally, very little nitrogen was detected. Therefore, in the case of incineration, there is less risk of NO_x emissions. The sulphur content was higher than the values reported in the literature and for conventional heavy fuel oils and bituminous coal, which normally ranges from 2-3% (Kaur et al. 2020). Besides the low calorific values and high

oxygen content, the possibility of SO_x emissions deems all PPMS samples unsuitable as a solid fuel. The presence of carbon in PPMS made it a potential resource for improving soil properties that lack organic matter (Beauchamp et al. 2002). The C:N ratio of PPMS A, B and C were 74.6, 163.1, 142.3, respectively. These values were within the range reported in the literature of 40 to 500 (Chen et al. 2014). The C:N ratios for all PPMS types were lower than reported for virgin Kraft mill sludge of 301.7. The C:N ratio was important in beneficiation pathways such as soil amendment as it was a measure of mineralization, immobilization and nitrification models predicting nitrogen turnover and retention in soils (Chen et al. 2014). The C:N ratio of PPMS A and PPMS C was comparable to the values obtained for primary sludge (75) and secondary sludge (162), respectively (Phillips et al. 1997). A high C:N ratio was undesirable because of the high immobilization of nitrogen, whereas a low C:N is characterized by low nitrogen immobilization and de-amination of carbon sources to produce NH_4^+ (Chen et al. 2014). Furthermore, productive soils have a standard C:N ratio of less than 40. The low nitrogen content deemed all PPMS types studied unsuitable as a growth factor in soils (Wildauer 2006).

Table 3-6 Ultimate analysis of PPMS samples

Sample	Ultimate Analysis (wt.%)				
	Carbon	**Hydrogen**	**Nitrogen**	**Sulphur**	**C: N**
PPMS A	42.5	5.00	0.57	4.31	74.56
PPMSB	47.30	6.34	0.29	5.52	163.10
PPMS C	31.30	4.73	0.22	1.78	142.27

3.4.5 Thermal Analysis

The calorific values of PPMS samples are shown in Table 3-7. All PPMS samples exhibited low calorific values. The highest calorific value was observed for PPMS B at 0.18 MJ kg^{-1}. The lowest calorific value was observed for PPMS C at 0.14 MJ kg^{-1} due to its high ash content (Lou et al. 2012). The caloric values were in range with values reported in the literature for secondary sludge (0-25 MJ kg^{-1}) (Alkasrawi et al. 2016; Kaur et al. 2020). This was attributed to the high ash content and moisture content in PPMS samples (Assis and Chirwa 2021). Research carried out on energy conversion of PPMS indicates that fast pyrolysis or anaerobic digestion on low and high ash containing PPMS types is an economically sustainable option for PPMS valorisation compared with incineration because of the low calorific value of PPMS (Ridout et al. 2015; Faubert et al. 2016). In general, the fixed carbon and volatile matter values of all samples were low. The volatile matter was reported higher for PPMS C (33.16%), followed by PPMS A (28.20%) and PPMS B (24.01%). The volatile solids in PPMC C were slightly higher than those reported for deinking PPMS with 31.8 % but comparable to primary PPMS with a range of 33-40 % (Kaur et al. 2020). The values for fixed carbon were comparable to those reported for primary PPMS (0-2.3%) (Jaria et al. 2017).

Table 3-7 Proximate Analysis of PPMS samples

Sample	Proximate Analysis (wt %)		
	Volatiles Matter	Fixed Carbon	Calorific value ($MJkg^{-1}$)
PPMS A	28.20	1.18	0.15
PPMS B	24.01	2.32	0.18
PPMS C	33.16	0.12	0.14

Further analysis by TGA illustrated the thermal reactivity, and decomposition stages of the samples Figure 3-5 below.

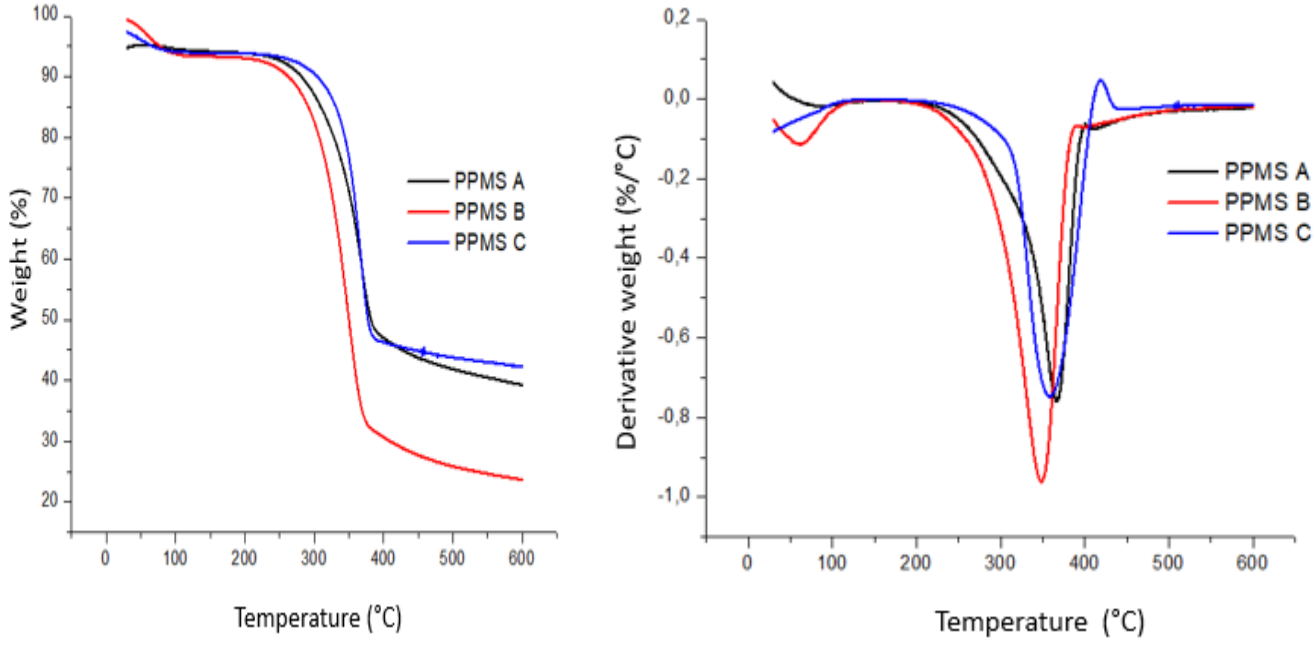

Figure 3-5 (a) TGA and DTG profiles of PPMS A, PPMS B and PPMS C

Figure 3-5 depicts that the decomposition of PPMS samples occurred in stages. The dehydration stage occurred between 30ºC and 100ºC and is illustrated by a peak on the DTG profile at 90ºC, 57ºC and 56.5ºC for PPMS A, B and C. The TGA profile depicts that the main thermal decomposition stage was between 23ºC and 400ºC. The T_{onset} values were 323.3ºC, 304.4ºC and 328.3ºC for PPMS A, PPMS B and PPMS C, respectively. As illustrated in the DTG curves, the maximum decomposition peaks for PPMS A, PPMS B, and PPMS C were at 366.8ºC, 348.5ºC and 358ºC, respectively. Rivera et al. (2016) reported T_{onset} and T_{max} of 270 ºC and 320 ºC respectively for deinking PPMS. Lou et al. (2012) reported a T_{max} of 361ºC for deinking PPMS. Méndez et al. (2009) reported T_{max} values in the range 337-354ºC for 8 different types of PPMS samples. Peaks at temperatures above 400ºC were attributed to the degradation of lignin, volatile inorganic compounds and further oxidation of organic

compounds (Assis and Chirwa 2021). The residue obtained after heating the PPMS fibres to 600°C is shown in Table 3-8. PPMS C had the highest residue of 42.3% due to its high ash content, followed by PPMS A with a residue of 39.3% and lastly, PPMS B with a residue of 23.7 %. The presence of ash resulted in high contents of residues because ash had a low degradation rate (Karimi et al. 2014). The residues highlight the carbonaceous components generated on pyrolysis (Jonoobi et al. 2009; Panyasiri et al. 2018; Narkpiban et al. 2019).

Table 3-8 Degradation characteristics of PPMS A, PPMS B and PPMS C

Sample ID	**T_{onset}**	**Weight loss (%)**	**T_{max}**	**Weight loss (%)**	**Residue at 600°C (%)**
PPMS A	323.3	18.4	366.8	39.7	39.3
PPMS B	304.4	22.7	348.5	56.6	23.7
PPMS C	328.3	14.1	358	29.4	42.3

3.5 Conclusions

In this study, three PPMS samples from different PPMSs were characterized and analysed. The PPMS samples were further screened against possible beneficiation pathways in an effort to assign the most suitable pathway based on characteristics and literature. PPMS B was better suited for ethanol/biofuel production because of its higher glucose content than other PPMS samples. The high cellulose and low ash content of PPMS B were found suitable for the production of nanocellulose. PPMS A and PPMS C were a better fit for composite manufacture based on ash content which would act as a strength enhancer. All the PPMS samples were not suitable for energy harvesting because of the high moisture contents and low calorific values. The low C:N ratios also limited PPMS samples as possible soil amenders.

3.6 Recommendations

In order to achieve full insight into the variations of the PPMS, samples should be collected at different points in the PPMs and on different wastewater treatment stages. For instance, samples should be collected before and after the primary and secondary wastewater treatment process. For improved PPMS analysis, TEM microscopy is recommended, as gold coating required for SEM analysis interfered with both morphological and mineral analysis.

3.7 References

Abdul Rahman NH, Chieng BW, Ibrahim NA, Abdul Rahman N (2017) Extraction and characterisation of cellulose nanocrystals from tea leaf waste fibers. J Polym 9 (11): 588. https://doi.org/10.3390/polym9110588

Abdullah R, Ishak CF, Kadir WR, Bakar RA (2015) Characterisation and feasibility assessment of recycled paper mill sludges for land application in relation to the environment. Int J Environ Res Public Health 12 (8): 9314-9329. https://doi.org/10.3390/ijerph120809314

Adu C, Berglund L, Oksman K, Eichhorn SJ, Jolly M, Zhu C (2018) Properties of cellulose nanofibre networks prepared from never-dried and dried paper mill sludge. J Clean Prod 197: 765-771. https://doi.org/10.1016/j.jclepro.2018.06.263

Ahmad S, Malik MI, Wani MB, Ahmad R (2013) Study of concrete involving use of waste paper sludge ash as partial replacement of cement. J Eng 3 (11): 06-15. http://dx.doi.org/10.9790/3021-031130615

Alkasrawi M, Al-Hamamre Z, Al-Shannag M, Abedin MJ, Singsaas E (2016) Conversion of paper mill residuals to fermentable sugars. BioResources 11 (1): 2287-2296. https://doi.org/10.15376/biores.11.1.2287-2296

Alriksson B, Hörnberg A, Gudnason AE, Knobloch S, Arnason J, Johannsson RJCC, Technology (2014) Fish feed from wood. 48 (9-10): 843-848.

Assis EI, Chirwa EM (2021) Physicochemical Characteristics of Different Pulp and Paper Mill Waste Streams for Hydrothermal Conversion. Chem Eng Trans 86: 607-612.

Beauchamp CJ, Charest M-H, Gosselin A (2002) Examination of environmental quality of raw and composting de-inking paper sludge. Chemosphere 46 (6): 887-895. https://doi.org/10.1016/s0045-6535(01)00134-5

Bekhta P, Sedliačik J, Kačík F, Noshchenko G, Kleinová A (2019) Lignocellulosic waste fibers and their application as a component of urea-formaldehyde adhesive composition in the manufacture of plywood. Eur J Wood Wood Prod 77 (4): 495-508. https://doi.org/10.1007/s00107-019-01409-8

Bester LM (2018) Development and optimisation of a process for cellulose nanoparticle production from waste paper sludge with enzymatic hydrolysis as an integral part. Stellenbosch University.

Bettaieb F, Khiari R, Dufresne A, Mhenni M, Putaux J-L, Boufi S (2015) Nanofibrillar cellulose from Posidonia oceanica: Properties and morphological features. Ind Crops Prod 72: 97-106. https://doi.org/10.1016/j.indcrop.2014.12.060

Boshoff S (2015) Characterisation and fermentation of waste paper sludge for bioethanol production. Stellenbosch University. https://scholar.sun.ac.za/handle/10019.1/98028

Boshoff S, Gottumukkala LD, Van Rensburg E, Görgens J (2016) Paper sludge (PS) to bioethanol: Evaluation of virgin and recycle mill sludge for low enzyme, high-solids fermentation. Bioresour Technol 203: 103-111. https://doi.org/10.1016/j.biortech.2015.12.028

Budhavaram NK, Fan Z (2009) Production of lactic acid from paper sludge using acid-tolerant, thermophilic Bacillus coagulan strains. Bioresour Technol 100 (23): 5966-5972. https://doi.org/10.1016/j.biortech.2009.01.080

Chen H, Han Q, Daniel K, Venditti R, Jameel H (2014) Conversion of industrial paper sludge to ethanol: fractionation of sludge and its impact. Appl Biochem Biotechnol 174 (6): 2096-2113. https://doi.org/10.1007/s12010-014-1083-z

Cherian C, Siddiqua S (2019) Pulp and paper mill fly ash: A review. Sustainability 11 (16): 4394. http://dx.doi.org/10.3390/su11164394

Chimphango A, Amiandamhen SO, Görgens JF, Tyhoda L (2021) Prospects for Paper Sludge in Magnesium Phosphate Cement: Composite Board Properties and Techno-Economic Analysis. Waste Biomass Valori: 1-23. https://doi.org/10.1007/s12649-021-01356-7

Davis E, Shaler SM, Goodell B (2003) The incorporation of paper deinking sludge into fiberboard. For Prod J 53.

de Alda JAO (2008) Feasibility of recycling pulp and paper mill sludge in the paper and board industries. Resour Conserv Recycl 52 (7): 965-972. https://doi.org/10.1016/j.resconrec.2008.02.005

Du H, Parit M, Wu M, Che X, Wang Y, Zhang M, Wang R, Zhang X, Jiang Z, Li B (2020) Sustainable valorization of paper mill sludge into cellulose nanofibrils and cellulose nanopaper. J Hazard Mater 400: 123106. https://doi.org/10.1016/j.jhazmat.2020.123106

Duncan SM, Alkasrawi M, Gurram R, Almomani F, Wiberley-Bradford AE, Singsaas E (2020) Paper mill sludge as a source of sugars for use in the production of bioethanol and isoprene. Energies 13 (18): 4662. https://doi.org/10.3390/en13184662

Elloumi A, Makhlouf M, Elleuchi A, Bradai C (2016) Deinking sludge: A new biofiller for HDPE composites. Polym Plast Technol Eng 55 (10): 1012-1020. https://doi.org/10.1080/03602559.2015.1132432

Eroğlu V, Saatci A (1993) Reuse of sludge from pulp and paper industry pilot and full scale applications. Water Sci Technol 28 (2): 17-26. https://doi.org/10.2166/wst.1993.0069

Faubert P, Barnabé S, Bouchard S, Côté R, Villeneuve C (2016) Pulp and paper mill sludge management practices: What are the challenges to assess the impacts on greenhouse gas emissions? Resour Conserv Recy 108: 107-133.

Gea T, Artola A, Sánchez A (2005) Composting of de-inking sludge from the recycled paper manufacturing industry. Bioresour Technol 96 (10): 1161-1167. https://doi.org/10.1016/j.biortech.2004.09.025

Geng X, Deng J, Zhang SY (2007) Paper mill sludge as a component of wood adhesive formulation. Holzforschung. https://doi.org/10.1515/HF.2007.112

Ghribi M, Meddeb-Mouelhi F, Beauregard M (2016) Microbial diversity in various types of paper mill sludge: identification of enzyme activities with potential industrial applications. SpringerPlus 5 (1): 1-14. https://doi.org/10.1186/s40064-016-3147-8

Gibril ME, Lekha P, Andrew J, Sithole B, Tesfaye T, Ramjugernath D (2018) Beneficiation of pulp and paper mill sludge: production and characterisation of functionalised crystalline nanocellulose. Clean Technol Environ Policy 20 (8): 1835-1845. https://doi.org/10.1007/s10098-018-1578-3

Goel G, Kalamdhad AS (2017) An investigation on use of paper mill sludge in brick manufacturing. Constr Build Mater 148: 334-343. https://doi.org/10.1016/j.conbuildmat.2017.05.087

Hagelqvist A (2013) Sludge from pulp and paper mills for biogas production: Strategies to improve energy performance in wastewater treatment and sludge management. Karlstads universitet. http://urn.kb.se/resolve?urn=urn%3Anbn%3Ase%3Akau%3Adiva-26171

Haile A, Gelebo GG, Tesfaye T, Mengie W, Mebrate MA, Abuhay A, Limeneh DY (2021) Pulp and paper mill wastes: utilizations and prospects for high value-added biomaterials. Bioresour Bioprocess 8 (1): 1-22. https://doi.org/10.1186/s40643-021-00385-3

Ince BK, Cetecioglu Z, Ince O (2011) Pollution prevention in the pulp and paper industries. J Environ Manage: 224-246.

Jaria G, Silva CP, Ferreira CI, Otero M, Calisto V (2017) Sludge from paper mill effluent treatment as raw material to produce carbon adsorbents: an alternative waste management strategy. J Environ Manage 188: 203-211. https://doi.org/10.1016/j.jenvman.2016.12.004

Jonoobi M, Harun J, Mishra M, Oksman K (2009) Chemical composition, crystallinity and thermal degradation of bleached and unbleached kenaf bast (Hibiscus cannabinus) pulp and nanofiber. BioResources 4 (2): 626-639.

Kang L, Wang W, Pallapolu VR, Lee YY (2011) Enhanced ethanol production from de-ashed paper sludge by simultaneous saccharification and fermentation and simultaneous saccharification and co-fermentation. BioResources 6 (4): 3791-3808. http://dx.doi.org/10.15376/biores.6.4.3791-3808

Karimi S, Tahir PM, Karimi A, Dufresne A, Abdulkhani A (2014) Kenaf bast cellulosic fibers hierarchy: a comprehensive approach from micro to nano. Carbohydr Polym 101: 878-885. https://doi.org/10.1016/j.carbpol.2013.09.106

Kaur R, Tyagi RD, Zhang X (2020) Review on pulp and paper activated sludge pretreatment, inhibitory effects and detoxification strategies for biovalorization. Environ Res 182: 109094. https://doi.org/10.1016/j.envres.2019.109094

Khenblouche A, Bechki D, Gouamid M, Charradi K, Segni L, Hadjadj M, Boughali S (2019) Extraction and characterisation of cellulose microfibers from Retama raetam stems. Polímeros 29. https://doi.org/10.1590/0104-1428.05218

Leão AL, Cherian BM, de Souza SF, Sain M, Narine S, Caldeira MS, Toledo MAS (2012) Use of primary sludge from pulp and paper mills for nanocomposites. Mol Cryst 556 (1): 254-263. https://doi.org/10.1080/15421406.2012.635974

Lee S-H, Ohkita T, Kitagawa K (2004) Eco-composite from poly (lactic acid) and bamboo fiber. https://doi.org/10.1515/HF.2004.080

Lekha P, Andrew J, Gibril M, Sithole B (2017) Pulp and Paper mill sludge: a potential resource for producing high-value products. TAPPSA 1: 16-19.

Lou R, Wu S, Lv G, Yang QJAE (2012) Energy and resource utilization of deinking sludge pyrolysis. Appl Energy 90 (1): 46-50. https://doi.org/10.1016/j.apenergy.2010.12.025

Mahmood T, Elliott A (2006) A review of secondary sludge reduction technologies for the pulp and paper industry. Water Res 40 (11): 2093-2112. https://doi.org/10.1016/j.watres.2006.04.001

Manesh ME (2012) Utilization of pulp and paper mill sludge as filler in nylon biocomposite production. University of Toronto Canada

Marques S, Alves L, Roseiro J, Gírio F (2008) Conversion of recycled paper sludge to ethanol by SHF and SSF using Pichia stipitis. Biomass Bioenerg 32 (5): 400-406. https://doi.org/10.1016/j.biombioe.2007.10.011

Méndez A, Fidalgo J, Guerrero F, Gascó G (2009) Characterisation and pyrolysis behaviour of different paper mill waste materials. J Anal Appl Pyrolysis 86 (1): 66-73. http://dx.doi.org/10.1016/j.jaap.2009.04.004

Migneault S, Koubaa A, Nadji H, Riedl B, Zhang ST, Deng J (2010) Medium-density fiberboard produced using pulp and paper sludge from different pulping processes. Wood Fiber Sci 42 (3): 292-303.

Narkpiban K, Sakdaronnarong C, Nimchua T, Pinmanee P, Thongkred P, Poonsawat T (2019) The effect of mechano-enzymatic treatment on the characteristics of cellulose nanofiber obtained from kenaf (Hibiscus cannabinus L.) bark. BioResources 14 (1)**:** 99-119. http://dx.doi.org/10.15376/biores.14.1.99-119

Nikolov T, Bakalova N, Petrova S, Benadova R, Spasov S, Kolev D (2000) An effective method for bioconversion of delignified waste-cellulose fibers from the paper industry with a cellulase complex. Bioresour Technol 71 (1)**:** 1-4. http://dx.doi.org/10.1016/S0960-8524(99)00059-0

Oh SY, Yoo DI, Shin Y, Kim HC, Kim HY, Chung YS, Park WH, Youk JH (2005) Crystalline structure analysis of cellulose treated with sodium hydroxide and carbon dioxide by means of X-ray diffraction and FTIR spectroscopy. Carbohydr Res 340 (15)**:** 2376-2391. https://doi.org/10.1016/j.carres.2005.08.007

Panyasiri P, Yingkamhaeng N, Lam NT, Sukyai P (2018) Extraction of cellulose nanofibrils from amylase-treated cassava bagasse using high-pressure homogenization. Cellulose 25 (3)**:** 1757-1768. https://link.springer.com/article/10.1007/s10570-018-1686-6

Phillips V, Kirkpatrick N, Scotford I, White R, Burton R (1997) The use of paper-mill sludges on agricultural land. Bioresour Technol 60 (1)**:** 73-80. https://doi.org/10.1016/s0960-8524(97)00006-0

Ridout AJ, Carrier M, Görgens J (2015) Fast pyrolysis of low and high ash paper waste sludge: Influence of reactor temperature and pellet size. J Anal Appl Pyrolysis 111**:** 64-75. https://doi.org/10.1016/j.jaap.2014.12.010

Rivera JA, López VP, Casado RR, Hervás J-MS (2016) Thermal degradation of paper industry wastes from a recovered paper mill using TGA. Characterisation and gasification test. J Waste Manag 47**:** 225-235. http://dx.doi.org/10.1016/j.wasman.2015.04.031

Robus CL, Gottumukkala LD, Van Rensburg E, Görgens JF (2016) Feasible process development and techno-economic evaluation of paper sludge to bioethanol conversion: South African paper mills scenario. J Renew Energy 92**:** 333-345. https://doi.org/10.1016/j.renene.2016.02.017

Schroeder BG, Zanoni PRS, Magalhães WLE, Hansel FA, Tavares LBB (2017) Evaluation of biotechnological processes to obtain ethanol from recycled paper sludge. J Mater Cycles Waste Manag 19 (1)**:** 463-472. http://dx.doi.org/10.1007/s10163-015-0445-0

Schwanninger M, Rodrigues J, Pereira H, Hinterstoisser B (2004) Effects of short-time vibratory ball milling on the shape of FT-IR spectra of wood and cellulose. Vib Spectrosc 36 (1)**:** 23-40. https://doi.org/10.1016/j.vibspec.2004.02.003

Segal L, Creely JJ, Martin Jr A, Conrad C (1959) An empirical method for estimating the degree of crystallinity of native cellulose using the X-ray diffractometer. Text Res J 29 (10)**:** 786-794.

Simão L, Hotza D, Raupp-Pereira F, Labrincha JA, Montedo OR (2019) Characterisation of pulp and paper mill waste for the production of waste-based cement. Rev Int de Contam Ambient 35 (1)**:** 237-246. http://dx.doi.org/10.20937/RICA.2019.35.01.17

Singh S, Kulkarni S, Kumar V, Vashistha PJJoCP (2018) Sustainable utilization of deinking paper mill sludge for the manufacture of building bricks. J Clean Prod 204**:** 321-333. https://doi.org/10.1016/j.jclepro.2018.09.028

Široký J, Blackburn RS, Bechtold T, Taylor J, White P (2010) Attenuated total reflectance Fourier-transform Infrared spectroscopy analysis of crystallinity changes in lyocell following continuous treatment with sodium hydroxide. Cellulose 17 (1)**:** 103-115. https://doi.org/10.1007/s10570-009-9378-x

Soucy J, Koubaa A, Migneault S, Riedl B (2016) Chemical composition and surface properties of paper mill sludge and their impact on high density polyethylene (HDPE) composites. Wood Chem Technol 36 (2)**:** 77-93. https://doi.org/10.1080/02773813.2015.1057647

Strezov V, Evans TJ (2009) Thermal processing of paper sludge and characterisation of its pyrolysis products. J Waste Manag 29 (5)**:** 1644-1648. https://doi.org/10.1016/j.wasman.2008.11.024

Tawalbeh M, Rajangam AS, Salameh T, Al-Othman A, Alkasrawi M (2021) Characterisation of paper mill sludge as a renewable feedstock for sustainable hydrogen and biofuels production. Int J of Hydrog Energy 46 (6)**:** 4761-4775. http://dx.doi.org/10.1016/j.ijhydene.2020.02.166

Wang L, Wang J, Littlewood J, Cheng H (2014) Co-production of biorefinery products from kraft paper sludge and agricultural residues: opportunities and challenges. Green Chem 16 (3)**:** 1527-1533. https://doi.org/10.1039/c3gc41984c

Wildauer P (2006) Use of Pulp and Paper Sludge to Improve Performance of Topsoil Layer in a Landfill Capping System. Dissertation, University of Northern British Columbia. https://doi.org/10.24124/2007/bpgub443

Williams A (2017) The production of bioethanol and biogas from paper sludge. Stellenbosch University.

Xing C, Zhang S, Deng J, Riedl B, Cloutier A (2006) Medium-density fiberboard performance as affected by wood fiber acidity, bulk density, and size distribution. Wood Sci Tech 40 (8)**:** 637-646. https://doi.org/10.1007/s00226-006-0076-7

Xing S, Riedl B, Koubaa A, Deng J (2012) Mechanical and physical properties of particleboard made from two pulp and paper mill secondary sludges. World J Eng. https://doi.org/10.1260/1708-5284.9.1.31

Zhang S-Y, Li Y-Y, Wang C-G, Wang X (2017) Thermal insulation boards from bamboo paper sludge. BioResources 12 (1)**:** 56-67. https://doi.org/10.15376/biores.12.1.56-67

Zhu M, Xu W, Li X (2012) Bioconversion of different paper sludge to ethanol by yeast using separate hydrolysis and fermentation. Proceedings of 2012 International Conference on Biobase Material Science and Engineering. IEEE, 141-145. https://doi.org/10.1109/bmse.2012.6466199

4 CHAPTER FOUR: PRODUCTION OF CELLULOSE NANOFIBRILS FROM PULP AND PAPERMILL SLUDGE

Thabisile Brightwell Jele[1], Prabashni Lekha[2], Bruce Sithole[1, 2]

[1]*University of KwaZulu-Natal (Howard Campus), Discipline of Chemical Engineering, College of Agriculture, Engineering and Sciences, Durban,* [2]*Council for Scientific and Industrial Research, Biorefinery Industry Development Facility, Durban, South Africa*

[*]Corresponding Author: thabisilejele94@gmail.com; sitholeb1@ukzn.ac.za

4.1 Abstract

Cellulose nanofibrils (CNFs) were produced from three different types of pulp and paper mill sludge (PPMS) samples viz., virgin (PPMS A), recycle (PPMS B) and deinking (PPMS C). The PPMS samples were treated in stages. The first stage was de-ashing, where PPMS samples were washed through screens. The washed PPMS samples were bleached using $NaClO_2$ under acidic conditions. Finally, the bleached PPMS fibres were reduced to nanoscale by mechanical grinding using the automated Supermasscolloider (SMC). The influence of bleaching and mechanical grinding on the chemical composition of PPMS fibres was investigated. The functional groups, morphology, crystallinity and thermal analysis of PPMS, bleached PPMS and CNFs were studied using the Fourier transform infrared spectroscopy (FTIR), Scanning and Transmission Electron Microscopy, X-ray diffraction (XRD) and Thermogravimetric analysis (TGA), respectively. Chemical composition analysis showed a considerable reduction in ash content, successful cellulose concentration, and removal of lignin due to screen washing and bleaching. The crystallinity index (CrI) was calculated to be 51.1%, 58.1% and 59.4% for CNF A, CNF B and CNF C, respectively. TGA analysis showed a progressive decrease in thermal stability from PPMS to CNFs.The overall yield for the production of CNFs from PPMS A, PPMS B and PPMS C was 27.2%, 32% and 42.8%, respectively.

Keywords: cellulose nanofibrils, pulp, paper, mechanical grinding

4.2 Introduction

Depletion of landfill space, the cost of waste disposal and environmental concerns are pushing biomass processing industries to make changes and improvements in the way waste is handled. The pulp and paper mills (PPMs) are not an exception to this waste management problem. South Africa generates approximately 500 000 tonnes of waste pulp and paper mill sludge (PPMS) per annum (Boshoff et al. 2016; Gibril et al. 2018). Traditionally, in South Africa, the main PPMS management technology is landfilling. Landfilling leads to greenhouse gas emissions, groundwater and surface water pollution caused by leachate generation at the landfill site. In addition to waste management problems, the PPMs experience inefficiencies in the production line. It has been estimated that at least 35% of the woody material used in the PPM becomes waste (Cherian and Siddiqua 2019). Therefore, the PPMS produced is comprised largely of fibrous material such as cellulose, hemicellulose and lignin. Studies have illustrated the valorisation of PPMS for applications such as agriculture (composting and land application), cement production, brick manufacturing, road construction, anaerobic digestion (biogas production), biohydrogen production, incineration (energy harvesting), production of ethanol, pyrolysis (production of bio-oil or char), manufacture of composites and recovery of minerals, nanocellulose production, isolation of enzymes, paper and board industry, production of carbon adsorbents, production of lactic acid and production of animal feed (Gea et al. 2005; Marques et al. 2008; Budhavaram and Fan 2009; Ghribi et al. 2016; Goel and Kalamdhad 2017; Jaria et al. 2017; Tawalbeh et al. 2021). A few studies have focused on the use of PPMS to produce high-value cellulose products such as cellulose nanofibrils (CNFs). CNFs, by standard definition, have an aspect ratio of more than 10 and contain crystalline and amorphous regions. Its dimensions are typically 3-100 nm in width and up to 100 µm in length (ISO/TS 20,477:2017) (Fotie et al. 2020; Jele et al. 2021). Mechanical methods typically used in CNF production are high-pressure homogenisation, microfluidisation, grinding, ball milling, ultrasonication, twin-screw extrusion, cryo crushing, blending and aqueous counter collision (Herrick et al. 1983; Dufresne et al. 2000; Zimmermann et al. 2004; Besbes et al. 2011; Spence et al. 2011). Studies have indicated that the properties of CNFs produced from PPMS were comparable to CNFs produced from other feedstocks (Jonoobi et al. 2012; Leão et al. 2012; Djafari Petroudy et al. 2021). Leão et al. (2012) reported that CNFs produced from PPMS preserved their structure in a polyurethane composite. Adu et al. (2018) reported that the use of dried PPMS in CNF production was advantageous compared to never dried PPMS, although the properties of the CNFs produced were the same. Dried PPMS was easy to handle and was not degraded by microbial activities. However, CNFs were produced from never dried PPMS (8.5 k Wh kg^{-1}) using lower energy compared to dried PPMS (9.3 kW h kg^{-1}). The higher energy consumption for dried PPMS was due to hornification, which occurred during drying of cellulose (Adu et al. 2018; Djafari Petroudy et al. 2021). Jonoobi et al. (2012) reported successful production of high-quality CNFs at low processing costs by use of mechanical grinding without chemical pre-treatments. The mechanical grinding was carried out at a low rotor speed of 1440 rpm, which meant low energy requirements, *viz.,* 1.3 kW h kg^{-1}. Du et al. (2020) reported a yield of 75% for the production of cellulose nanofibrils (CNFs) from PPMS by formic acid (FA) hydrolysis and microfluidisation. Several studies have been carried out for the production of CNFs using the supermasscolloider (SMC). For instance, Lekha et al. (2016) produced CNFs of average diameter 11 nm by passing bleached hardwood and softwood pulp for 200 passes in the SMC. The main advantages of PPMS as a secondary source of CNFs are availability and abundance (Crespo et al. 2012; Dwiarti et al. 2012). Also, PPMS fibres were physically smaller in size than commercial pulp, had a well-dispersed structure and high surface area (Wang et al. 2010). The disadvantage is the high ash content in PPMS, which had

a limiting effect on the cellulose loading capacity as it lowered the cellulose portion of the feedstock and influenced compositional analysis (Kang et al. 2011). Also, the interaction of silica (the main component of ash) and cellulose microfibrils accounted for the difficulty in fibrillation of lignocellulosic material (Biermann 1996). These problems were alleviated by de-ashing the sludge. Therefore, washing of high-ash containing PPMS was necessary for ash removal. In this study, PPMS samples were washed to reduce the ash content and bleached to isolate cellulose from lignin and other impurities and ground using the automated SMC to produce highly fibrillated CNFs. In this study, a higher number of passes were used in order to obtain highly fibrillated and homogeneous CNFs. Variation of time as a function of the number of passes was studied. Furthermore, the surface chemistry of the bleached PPMS samples and the CNFs produced was studied using the Fourier Transform Infrared Spectrophotometry to identify the functional groups. The thermal stability of the bleached PPMS samples and CNFs was also investigated.

4.3 Materials and Methods

4.3.1 Materials

The PPMS samples were obtained from various PPMs in South Africa. The samples were stored prior to analysis at -4°C to minimise any bacterial activity.

4.3.2 Methods

4.3.2.1 De-ashing

The removal of ash from PPMS samples was carried out by washing. PPMS samples that filled a 2L beaker three times using 200 and 10 mesh screens. After washing, excess water was allowed to drain. De-ashed samples were analysed for ash content and thereafter stored at - 4ºC. The de-ashing efficiency (% ash removal) was calculated using Equation 6 (Chen et al. 2014).

$$Ash\ removal\ (\%) = \frac{A_i - A_f}{A_i} \times 100 \quad (6)$$

Where A_i and A_f was the ash content of the initial PPMS sample before and after washing, respectively. The yield of de-ashing was calculated based on the mass of the precursor fibres, *viz.*, untreated PPMS.

4.3.2.2 Bleaching of sludge

De-ashed PPMS A, PPMS B and PPMS C samples were purified by bleaching. The bleaching process was carried out at 80ºC for 1h at a pH of 4.5 using a mixture of 27g NaOH and 75 ml CH_2COOH and 1.7 wt% $NaClO_2$ (Leão et al. 2012). The bleaching was repeated three times. After bleaching, the fibres were rinsed with distilled water until a neutral pH was reached. The bleaching yield was calculated according to Equation 7 below.

$$Bleaching\ yield\ (\%) = \frac{W_1}{W_0} \times 100 \quad (7)$$

Where W_1 is the dry weight of the PPMS sample after bleaching and W_0 is the initial dry weight of the de-ashed PPMS sample.

4.3.2.3 CNF production using the automated SMC

Bleached PPMS samples were investigated as a potential feedstock for the production of CNFs. Sample suspensions of 1% consistency were prepared in 2L beakers using de-ionised water. After 24 h of soaking, the suspensions were dispersed using a laboratory disintegrator (TMI, Ronkonkoma, USA). for 5 minutes. The homogenous suspensions were passed through the automated SMC (Model: MKZA6-2, Disk Model: MKGA6-

Masuko Sangyo Co., Ltd, Japan) for a pre-determined number of passes (200-500 passes). The schematic representation of the production of CNFs from PPMS is shown in Figure 4-1.

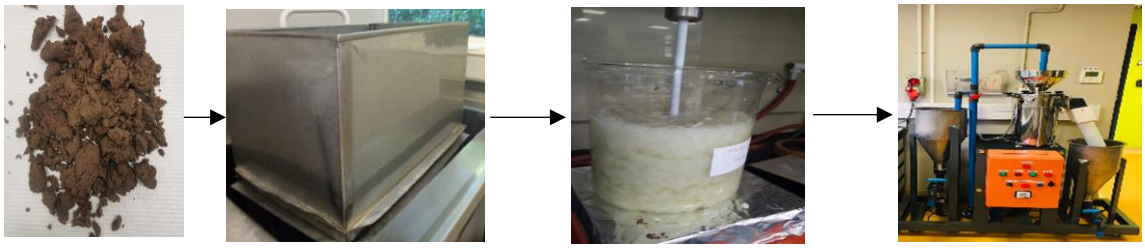

Figure 4-1 Process diagram for the pretreatment and production of CNFs

4.3.2.4 Yield of CNFs

The CNFs produced were centrifuged to remove the bulk amount of water and to increase the concentration of CNFs. The centrifuged samples were freeze dried overnight. The yields of CNFs were calculated by determining the mass of the freeze dried CNFs relative to the initial mass of oven dried feed, as shown by Equation 8 below.

$$Yield = \frac{M_1}{M_0} \quad (8)$$

Where M_o is the initial oven dried feed (*viz.*, bleached PPMS), M_1 is the freeze-dried CNF sample.

4.3.2.5 Fourier-transform infrared spectroscopy (FTIR)

FTIR spectroscopy (PerkinElmer, USA) was utilised to investigate the functional groups of bleached PPMS and CNFs. The scanning conditions were of the spectral range of 4000-400 cm^{-1} and with a resolution of 4 cm^{-1}

4.3.2.6 High-Performance Liquid Chromatography (HPLC)

The polysaccharide content of the PPMS and bleached PPMS samples was measured by HPLC (Thermo Scientific Dionex ICS-5000$^+$, USA) according to TAPPI T249 cm-85. The lignin content was simultaneously determined by drying and weighing the insoluble material remaining after acid hydrolysis and filtration. The obtained lignin content was defined as the Klason lignin, whilst the soluble lignin fraction was determined by analysis of the hydrolysate using the UV/VIS spectroscopy (Varian Cary® 50, USA) at 205 nm

4.3.2.7 Ash content

The ash content of the PPMS before and after washing was measured by combustion in a muffle furnace at 525^{o}C for 4 h in accordance with Tappi T211 om-02.

4.3.2.8 Morfi Analyser

The morphology of the PPMS and bleached PPMS was carried out using a Morfi analyser (Morfi Compact Techpap, France). 0.2g (oven dry) of oven dried samples were suspended in 500 ml of H_2O, disintegrated for 5 mins and analysed while being vigorously mixed to obtain a uniform distribution of fibres. The results were analysed with TechPap MorFi software.

4.3.2.9 Scanning Electron Microscope (SEM)

The SEM (Phenom Pharos Desktop) was used to study the morphology of PPMS and bleached PPMS fibres at a voltage of 10 kV. The dried samples were placed on an aluminium stub using carbon tape. Thereafter, samples were coated with gold using a sputter coater to increase conductivity.

4.3.2.10 TEM

The TEM (JEOL 2100 HRTEM, Japan) was used to measure the diameters of CNFs. At least 90 measurements from each sample were done. The results were reported as the mean values of the data. A droplet of each CNF suspension was deposited on the surface of a carbon-coated copper grid. The CNFs were stained with 1.5% (w/v) uranyl acetate for 2 min and dried at room temperature.

4.3.2.10 Thermogravimetric analysis (TGA)

Bleached PPMS samples and CNFs were thermogravimetrically analysed using the Perkin Elmer Simultaneous Thermal Analyser STA 600, USA. The samples were heated at a rate of 10^{o}C min^{-1} and temperature 30^{o}C to 600^{o}C under a nitrogen atmosphere which was set at a flow rate of 20 ml min^{-1} for 60 min.

4.3.2.11 The X-ray diffraction (XRD) analysis

The XRD analysis (BRUKER AXS, Germany) was used to study the crystallinity of untreated PPMS samples and CNFs. The XRD patterns were produced with scattering radiation at 2θ = 5-90° at a rate of 1 second per step. The crystalline index was calculated according to Equation 9 (Segal et al. 1959).

$$CrI\ (\%) = \frac{I_{200} - I_{am}}{I_{200}} \qquad (9)$$

Where CrI is the crystallinity index (%), I_{200} is the maximum intensity of the most intense peak of the crystalline contribution located at around $2\theta = 22^{o}$, and I_{am} is the minimum intensity of diffraction that represents the amorphous component at around $2\theta = 18^{o}$ (Bettaieb et al. 2015).

4.4 Results and Discussion

4.4.1 De-ashing

Figure 4-2 illustrates that washing of PPMS samples in 200 and 10 mesh screens decreased the ash content. The percentage ash removal for PPMS A, PPMS B and PPMS C was 47.5%, 40% and 83.2%. The main disadvantage of this de-ashing technique was the loss of short fibres, which contributed to the low yields of washed PPMS samples (Gurram et al. 2015; Williams 2017). The yields obtained after deashing were 60.4%, 62.6% and 64.1% for PPMS A, PPMS B and PPMS C, respectively

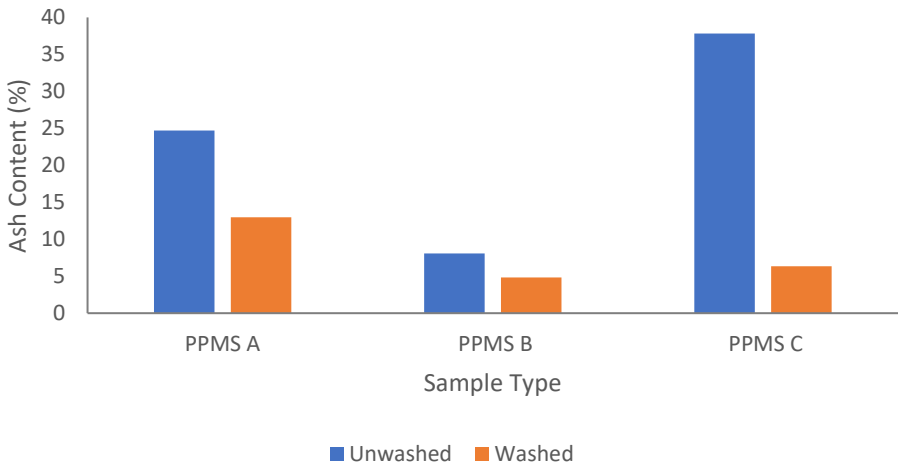

Figure 4-2 Percentage ash content of washed and unwashed PPMS A, PPMS B and PPMS C

4.4.2 Bleaching

In order to determine the effect of bleaching on PPMS samples, the chemical composition, functional groups and morphology was studied using the HPLC, FTIR, and Morfi, respectively. Moreover, photographs and SEM micrographs were used to verify the morphology and chemical composition.

4.4.3 Chemical composition

A comparison of the chemical compositional of PPMS and bleached PPMS is shown in Table 4-1. The results show the successful concentration of glucose/cellulose and the removal of lignin. The removal of lignin was crucial in order to liberate cellulose fibres. However, hemicelluloses remained present in the bleached PPMS samples, as shown in Table 4-1. Bettaieb et al. (2015) reported that bleaching P. oceanica balls using $NaClO_2$ resulted in the complete removal of lignin, but the hemicellulose remained in the bleached fibres. Hemicellulose promoted fibrillation by inhibiting the coalescence of microfibrils (Iwamoto et al. 2008; Bettaieb et al. 2015). In the current study, the yield of bleaching was 48.2%, 60.8% and 71.8% for PPMS A, PPMS B and PPMC respectively.

Table 4-1 The carbohydrate content of bleached PPMS A, PPMS B and PPMS C

Parameter (%)	PPMS A	Bleached PPMS A	PPMS B	Bleached PPMS B	PPMS C	Bleached PPMS C
Arabinose	0.17	0.11	0.43	ND	0.05	ND
Galactose	0.61	0.12	0.99	ND	0.12	ND
Glucose	36.26	69.56	62.83	90.82	52.37	86.77
Xylose	3.11	7.81	3.21	10.94	10.52	20.94
Mannose	0.05	0.50	3.46	ND	ND	ND
Ash	24.69	10.09	8.06	ND	37.81	ND
Insoluble lignin/material	33.5	15.32	19.71	>0.1	7.91	>0.1
Solvent Extractives	1.61	ND	1.31	ND	0.78	ND

4.4.4 Physical appearance

Figure 4-3 and Figure 4-4 shows the difference in the physical appearance of the PPMS samples and bleached PPMS samples in photographs and SEM micrographs, respectively. The PPMS samples displayed non-cellulose materials scattered on the fibres. The bleached PPMS samples in both the photographs and the SEM micrographs appeared cleaner than the untreated samples due to the elimination of non-cellulosic materials and contaminants.

Figure 4-3 Photographs of (a) untreated PPMS A (b) bleached PPMS A (c) untreated PPMS B (d) bleached PPMS B (e) untreated PPMS C (f) bleached PPMS C

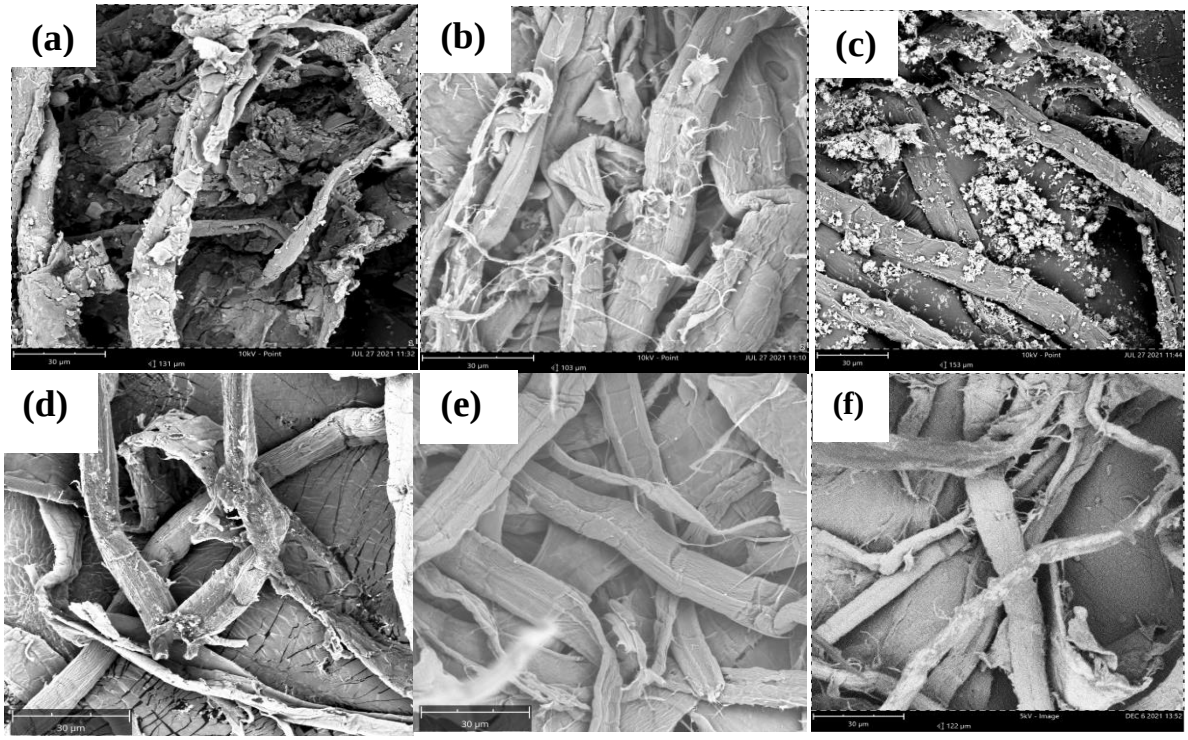

Figure 4- 4 SEM micrographs of (a) untreated PPMS A (b) bleached PPMS A (c) untreated PPMS B (d) bleached PPMS B (e) untreated PPMS C (f) bleached PPMS C

4.4.5 Morphology

The comparison of the morphology of bleached and untreated PPMS samples determined from Morfi analysis is shown in Table 4-2 below. The average width of all PPMS samples was reduced after bleaching. Lignin and hemicelluloses were removed from the inner parts of the fibres by bleaching, thereby causing defibrillation. Hence the diameter of the fibres decreased. Bleaching was an initial step to disintegrate the fibres in order to remove lignin.

Table 4-2 Average width of untreated and bleached PPMS A, PPMS B and PPMS C

Parameter	PPMS A	Bleached PPMS A	PPMS B	Bleached PPMS B	PPMS C	Bleached PPMS C
Average width	25.3	16.6	20.3	17	24.3	14.5

4.4.6 Production of Cellulose Nanofibrils using the automated SMC

4.4.6.1 The gap between the stones and rotation speed

The gap between the grinding stones and the rotational speed directly affected the time and energy required to reach the desired diameter of CNFs. He et al. (2018) dismissed the gap between the grinders as a reliable parameter in the study of CNF production due to the thermal expansion of the stones during operation. The thermal expansion resulted in an increase in the gap size between the grinding stones. Therefore, a constant gap of -160µm was used. A low rotor speed of 1500 rpm was used in order to alleviate direct contact between the grinding stones by

allowing time for the fibres to act as lubrication between the fibres and keep energy requirements at a minimum (Jonoobi et al. 2012).

4.4.6.2 Consistency

It was desired for the automated SMC system to be operated at low consistencies to avoid clogging and promote the free flow of material in the system. Therefore, a constant consistency of 1% was chosen for the current study. In previous studies, the consistencies in the range 0.7-3% have been reported for the production of CNF using the SMC (Abe et al. 2007; Abe and Yano 2009; Uetani and Yano 2011; Jonoobi et al. 2012; Karimi et al. 2014; Lahtinen et al. 2014; Onyianta et al. 2020). Consistency increased during fibrillation in the SMC due to evaporation of water caused by the heat generated by the friction of the grinding stones (Wang et al. 2012; He et al. 2018). Also, high consistencies resulted in high energy requirements (Wang et al. 2012).

4.4.6.3 Time

The graph in Figure 4-5 shows a linear relationship between time and the number of passes. The time taken to produce CNFs from PPMS increased with an increase in the number of passes. The results confirmed that the automated SMC was set to approximately 10 passes per minute. In the current study, the energy consumption was not measured; however, the recorded time was used as a representation of the amount of energy consumed. In previous studies, time was reported to vary linearly with energy consumption (Wang et al. 2012; Nair et al. 2014).

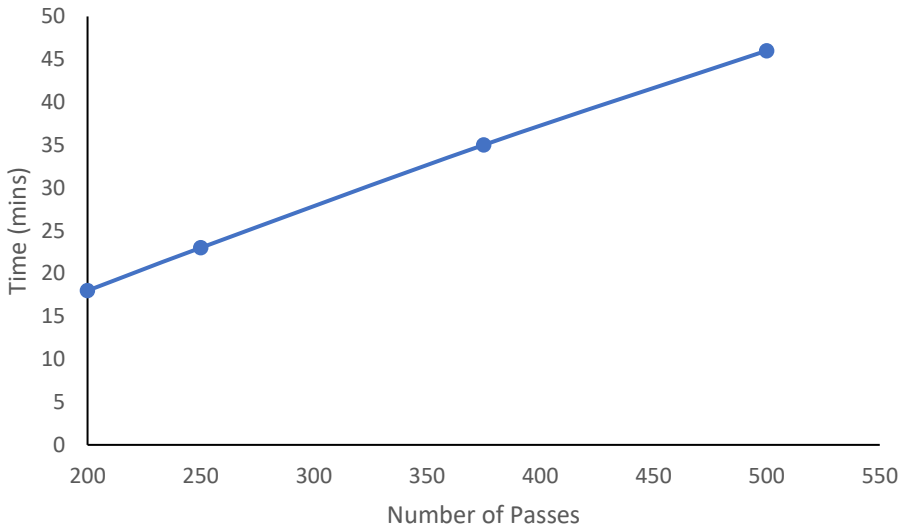

Figure 4-5 Processing time vs number of passes

4.4.6.4 Diameter

The average diameters (nm) of CNFs obtained from bleached PPMS A, PPMS B and PPMS C are shown in Table 4-3 below. The results show that at higher number of passes, highly fibrillated CNFs were produced. In general, the average diameters of CNFs decreased with an increase in the number of passes from 200 to 500 passes.

Table 4-3 Average diameters of CNF A, CNF B and CNF C

Number of Passes	CNF A	CNF B	CNF C
200	6.84 ± 1.28	6.55 ± 1.49	5.61 ± 1.06
250	6.79 ± 1.17	5.42 ± 1.38	5.30 ± 1.57
375	6.20 ± 1.52	4.89 ± 0.86	4.59 ± 0.82
500	4.69 ± 0.94	4.79 ± 1.06	4.45 ± 0.80

Eighteen minutes (200 passes) of grinding CNFs of average diameters 6.84 nm, 6.55 nm and 5.61 nm were obtained from PPMS A, PPMS B and PPMS C, respectively. Forty-five minutes (500 passes) of grinding, CNFs of average diameters 4.69 nm,4.79 nm and 4.45 nm were obtained from PPMS A, PPMS B and PPMS C, respectively. Considering the fact that increasing fibrillation time increases energy requirements, 18 minutes (200 passes) of fibrillation was selected as the optimal condition for the production of highly fibrillated CNFs at a minimum time and energy consumption. Mechanical fibrillation at a higher number of passes did not lead to appreciable improvements in CNF diameter that would justify the added energy consumption. Compared to previous studies, Lekha et al. (2016) reported an average diameter of 11 nm for CNFs produced from both softwood and hardwood fibres after 200 passes in the SMC.

4.4.7 Characterisation of CNFs produced at 200 passes

4.4.7.1 Morphology

The TEM micrographs for CNFs produced from the automated SMC after 200 passes are shown in Figure 4-6. The general morphologies of CNFs revealed long, entangled and web-like CNFs. A minimum of 90 CNF diameter measurements were taken using the TEM. Heterogeneous distributions in the width of CNFs were observed. These observations were similar to those reported for CNFs produced by mechanical methods (Bettaieb et al. 2015). After 200 passes in the automated SMC, the diameter ranged from 4.35 nm to 9.73 nm for CNF B, from 3.77 nm to 10.99 nm for CNF B and from 3.60 to 8.48 nm for CNF C. CNFs with diameters larger than, e.g. 5 nm were aggregations of several CNFs (Bettaieb et al. 2015; Jele et al. 2021).

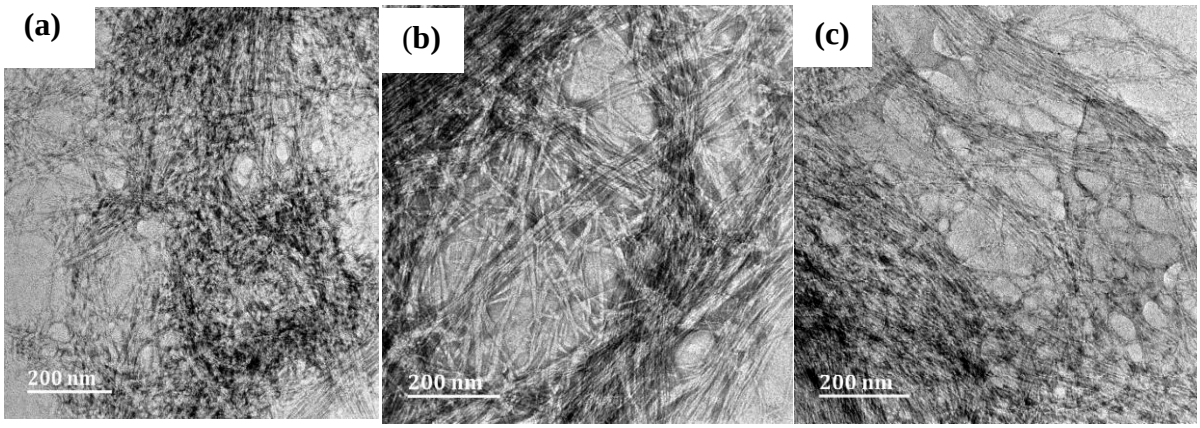

Figure 4-6 TEM images of (a) CNF A (b) CNF B and (c) CNF C after 200 passes in the automated SMC

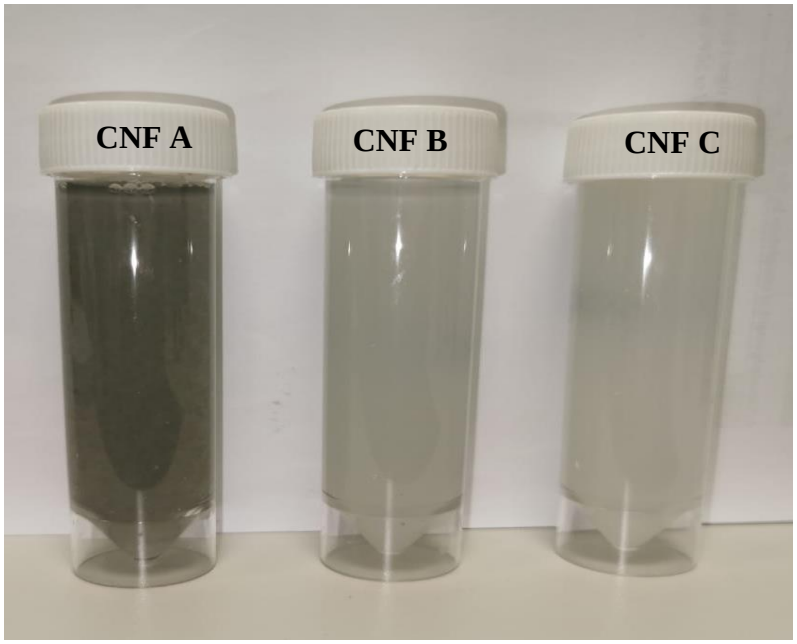

Figure 4-7 Images of CNFs produced after 200 passes using the automated SMC

4.4.7.2 Yield

The yields calculated at each stage of the production of CNFs are shown in Table 4-4 below. The yields of de-ashing were calculated based on the mass of untreated PPMS, the yield of bleaching was calculated based on the mass of de-ashed PPMS, and the yield of CNF was calculated based on the mass of bleached PPMS. The overall yield was 27.2%, 32.04% and 42.8% for CNF production from PPMS A, PPMS B and PPMS C, respectively.

Table 4-4 Yield at each stage of treatment in the production of CNFs

	Unit	PPMS A	PPMS B	PPMS C
Feed Mass Basis	g	100	100	100
Yield of Washing[1]	%	60.4	62.6	64.1
Yield of Bleaching[2]	%	48.2	60.8	71.8
Yield of CNF production[3]	%	93.5	92.9	93.2
Total Yield[4]	%	27.2	32.04	42.8
Mass of CNFs obtained from 100g[5] PPMS	g	27.2	32.04	42.8

Total Yield = [1]*[2]*[3]

4.4.7.3 Structural analysis by FTIR

The FTIR spectra of bleached PPMS and CNFs samples is shown in Figure 4-8 below.

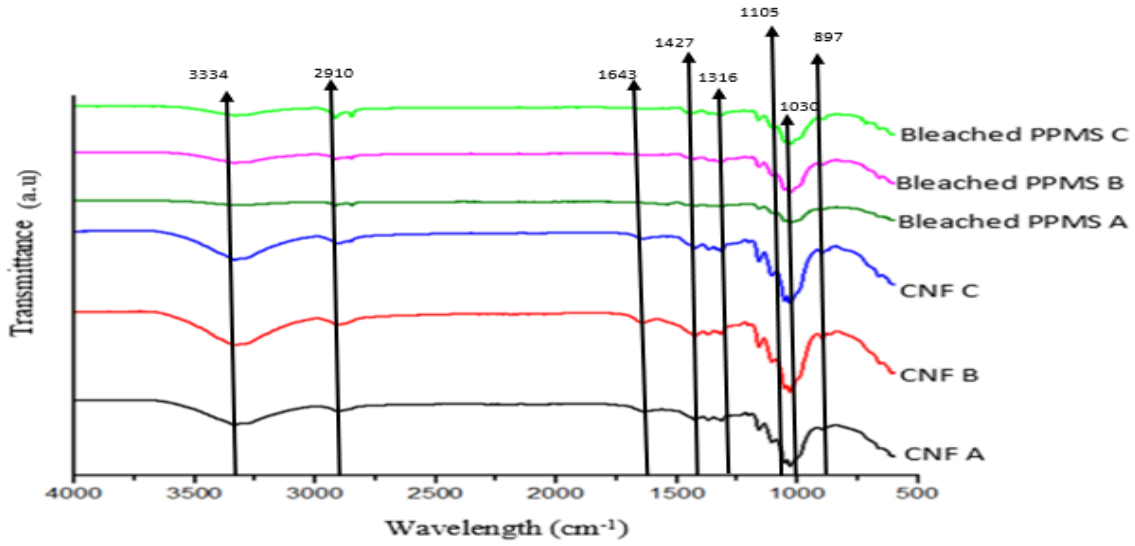

Figure 4-8 Infrared spectra of bleached PPMS and CNF samples

The graphs in Fig. 4-8 illustrate that FTIR spectra of bleached PPMS samples and CNFs was analogous to the spectra of cellulose. The samples showed peaks at 3334-3337 cm^{-1} (O-H stretching vibration), 2910 cm^{-1}-2916 (aliphatic C-H stretching vibration), 1643 cm^{-1} (O-H bending of adsorbed water), 1427 cm^{-1} (–CH_2 scissoring motion in cellulose), 1316cm^{-1} (CH_2 wagging,), 1106 cm^{-1} (C-O-C stretching) and 1031 cm^{-1} (C-O stretching vibration) (Bester 2018). These results show that in the production of cellulose nanofibrils from bleached PPMS, there was no modification of functional groups. The absence of the peak at 1516-1595 cm^{-1} corresponding to aromatic skeletal vibrations confirmed the removal of lignin during bleaching (Chen et al. 2011; Du et al. 2016).

4.4.7.4 XRD

The XRD patterns and crystalline indices of PPMS A, PPMS B, PPMS C, CNF A, CNF B and CNF C are shown in Figure 4-9 and Table 4-5, respectively.

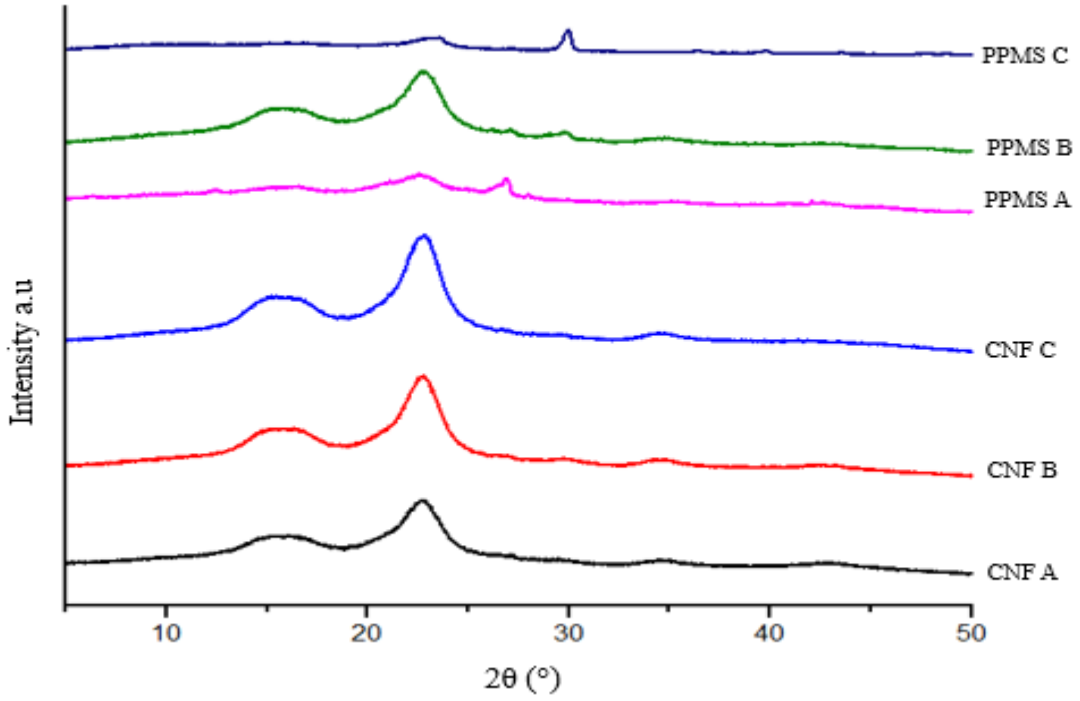

Figure 4-9 XRD patterns of PPMS A, PPMS B, PPMS C, CNF A, CNF B and CNF C

The graphs in Figure 4-9 illustrate that CNFs samples exhibited characteristics of cellulose at peaks 2θ = 16 and 2θ = 22. Therefore, bleaching and mechanical grinding did not alter the cellulose crystal structure. The Crl was calculated to be 51.1%, 58.1% and 59.4% for CNF A, CNF B and CNF C, respectively. The Crl was calculated to be 33.9%, 53.8% and 39.8% for PPMS A, PPMS B and PPMS C, respectively. Du et al. (2020) reported a CRI of 58.5% and 62.4% for PPMS and CNFs, respectively. The crystalline index of CNFs produced from wood Kraft pulp, flax, and rutabaga were 54%, 59% and 64%, respectively (Bhatnagar and Sain 2005). Adu et al. (2018) reported CrIs of 69% and 67% for CNFs produced from never dried and dried PPMS, respectively. CrIs of 35.1% and 49.4% were reported for the virgin pulp PPMS and printed recycle PPMS, respectively (Bester 2018). Malgas et al. (2020) reported a CrI of 91.5% for PPMS with a high glucan content (89.7%). It was concluded that the Crl was high for PPMS with high cellulose content than for PPMS with low cellulose content (Thygesen et al. 2005; Malgas et al. 2020). The CrI increased from PPMS to CNFs due to the partial removal of lignin and hemicelluloses during bleaching and mechanical grinding (Bettaieb et al. 2015; Nuruddin et al. 2016; Podder et al. 2016; Narkpiban et al. 2019). Also, bleaching resulted in the cleavage of the amorphous region (Karimi et al. 2014; Panyasiri et al. 2018). As displayed in Figure 4-9, the increase in the magnitude of the peaks from PPMS to CNFs confirmed the increase in CrI.

Table 4-5 CrI values for PPMS and CNF samples

Sample ID	PPMS A	PPMS B	PPMS C	CNF A	CNF B	CNF C
CrI (%)	33.9	53.8	39.8	51.1	58.1	59.4

4.4.7.5 Thermographic analysis

The thermal stability of the bleached PPMS samples and the CNFs obtained were evaluated and compared. Figure 4-10 shows the thermogravimetric analysis and differential thermograms (DTG) curves for bleached PPMS samples and CNFs.

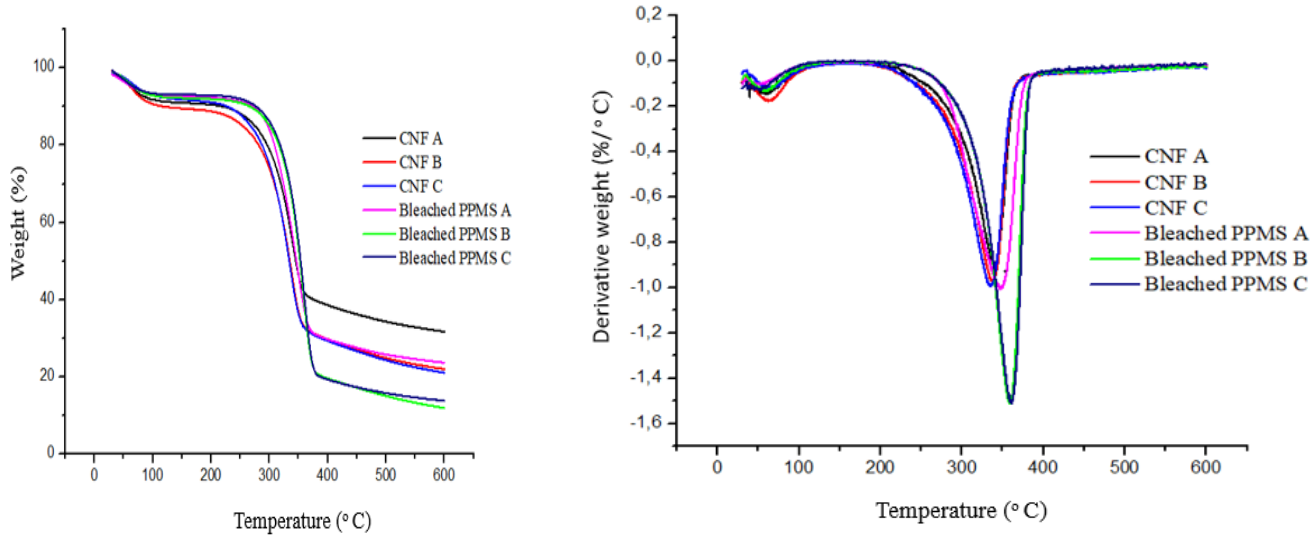

Figure 4-10 TGA curves and their respective derivative curve for bleached pulp and CNFs

The thermal degradation occurred in three main steps *viz.*, (1) moisture loss/water evaporation (<100°C), (2) decomposition of hemicellulose, lignin and non-cellulosic components (200-300°) (3) decomposition of cellulose (300-400°C). The temperature at the start of decomposition is referred to as the onset temperature (T_{onset}), and the temperature at the maximum rate of degradation is represented as the temperature of maximum thermal decomposition (T_{max}). The results in Table 4-6 show that T_{onset} values of PPMS samples were higher than their respective CNFs. For instance, the T_{onset} of PPMS A, and CNF A were 323.3 °C and 275.9 °C, respectively. The same trend was observed where the PPMS samples had higher T_{max} values compared to their respective bleached PPMS and CNFs. The degradation temperature of PPMS B, bleached PPMS B and CNF B were 366.8 °C, 358.2 °C and 337.9°C, respectively. The presence of waste mineral materials was responsible for the higher T_{max} for PPMS fibres (Yang et al. 2006; Méndez et al. 2009). In the case of bleached PPMS, the thermal stability was lower than that of PPMS. This was assumed to be caused by the change in the molecular structure of cellulose due to the removal of lignin. The molecular structure became looser, causing an increase in the contact area and a decrease in thermal stability (Saelee et al. 2016; Narkpiban et al. 2019). Based on the results, the thermal stability of CNFs was lower than that of their respective bleached PPMS and PPMS. This was due to the degradation of cellulose during grinding in the automated SMC and the high surface area of CNFs, resulting in low heat resistance

and ease of degradation (Qing et al. 2013; Yousefi et al. 2013; Mtibe et al. 2015; Lekha et al. 2016; Karimi et al. 2014). The high surface area of CNFs resulted in faster heat transfer (Kalita et al. 2015). The T_{max} for the CNFs produced from PPMS was comparable to CNFs produced from wood (332.9 °C), bamboo (331.7 °C), wheat straw (332.2 °C) and flax (347.4 °C) (Chen et al. 2011). Kalita et al. (2015) reported an T_{onset} and T_{max} of 257 °C and 315 °C, respectively, for CNFs produced from rice husk. The residue obtained after heating the PPMS fibres to 600°C is shown in Table 4-6. PPMS C had the highest residue of 42.3%, followed by PPMS A with a residue of 39.3% and lastly, PPMS B with a residue of 23.68 %. The residue in PPMS was higher than that of bleached fibres due to the presence of ash which had a low degradation rate (Karimi et al. 2014). The residues highlighted volatile carbonaceous components generated on pyrolysis (Panyasiri et al. 2018). After mechanical grinding, the amount of residue increased. The percentage residues for PPMS B, bleached PPMS B and CNF B were 23.7%, 12% and 22%, respectively. This may have been due to the better heat transfer capacity of CNFs, resulting in degradation of surrounding fibres when one fibre is exposed to heat. The better heat transfer capacity was attributed to the higher crystallinity and larger specific surface area compared to bleached PMMS fibres (Du et al. 2016; Radakisnin et al. 2020). Also, the CNFs degraded at low temperatures, which increased the residual rate (Radakisnin et al. 2020).

Table 4-6 Thermal characteristics of PPMS, bleached PPMS and CNFs determined from the TGA and DTGA graphs

Sample ID	**T_{onset} (°C)**	**Weight loss (%)**	**T_{max} (°C)**	**Weight loss (%)**	**Residue at 600°C**
PPMS A	323.3	18.4	366.8	39.7	39.3
PPMS B	304.4	22.7	348.5	56.6	23.7
PPMS C	328.3	14.1	358	29.4	42.3
Bleached PPMS A	290.5	13.1	346.7	50.32	23.7
Bleached PPMS B	310.9	18.03	358.2	58.44	12
Bleached PPMS C	306.6	15.6	360.8	60.3	13.9
CNF A	275.9	15.1	340.7	46.15	31.7
CNF B	277.3	18.9	337.9	52.63	22
CNF C	280.4	17.9	335.9	51.78	21.1

4.5 Conclusions

CNFs were produced from three types of PPMS *viz.*, virgin, recycle and deinking. The PPMS samples were treated in stages. The first stage was de-ashing, where PPMS samples were washed through screens. The de-ashed PPMS samples were bleached using $NaClO_2$ under acidic conditions. Bleaching was an important step in order to remove impurities and whiten fibres. The colour of the fibres is important as it influences consumer acceptance in various applications (Saelee et al. 2016). Finally, the bleached PPMS fibres were reduced to nanoscale by

mechanical grinding using the automated SMC. Microscopy, HPLC, and FTIR spectra analysis showed that de-ashing, bleaching and mechanical grinding successfully concentrated cellulose by removal of contaminates, lignin and isolation of cellulose nanofibers from three different types of PPMS samples, respectively. PPMS A, PPMS B and PPMS C yielded 27.2%, 32.04% and 42.8% of CNFs, respectively. XRD results indicated an increase in crystallinity of CNFs compared to PPMS samples. This was believed to be due to the degradation of cellulose during grinding and the partial removal of lignin and hemicelluloses during bleaching.

4.6 Recommendations

In order to counter the low yields of de-ashing and bleaching, impurities should be recovered and utilised for other applications. For instance, alkaline pretreatment of the PPMS could produce lignin pellets as a by-product (Wang et al. 2014). The $CaCO_3$ could be recovered and reused in the mill or used for soil amendment. The ash could also be used in cement manufacture (Ahmad et al. 2013). In scaling up the production of CNFs from PPMS, the variability in the characteristics of PPMS from different mills and within the same mill should be considered (Djafari Petroudy et al. 2021).

4.7 References

Abe K, Iwamoto S, Yano H (2007) Obtaining cellulose nanofibers with a uniform width of 15 nm from wood. Biomacromolecules 8 (10)**:** 3276-3278. https://doi.org/10.1021/bm700624p

Abe K, Yano H (2009) Comparison of the characteristics of cellulose microfibril aggregates of wood, rice straw and potato tuber. Cellulose 16 (6)**:** 1017-1023. http://dx.doi.org/10.1007/s10570-009-9334-9

Adu C, Berglund L, Oksman K, Eichhorn SJ, Jolly M, Zhu C (2018) Properties of cellulose nanofibre networks prepared from never-dried and dried paper mill sludge. Journal of Cleaner Production 197**:** 765-771. https://doi.org/10.1016/j.jclepro.2018.06.263

Ahmad S, Malik MI, Wani MB, Ahmad R (2013) Study of concrete involving use of waste paper sludge ash as partial replacement of cement. J Eng 3 (11)**:** 06-15. http://dx.doi.org/10.9790/3021-031130615

Besbes I, Alila S, Boufi S (2011) Nanofibrillated cellulose from TEMPO-oxidized eucalyptus fibres: effect of the carboxyl content. Carbohydr Polym 84 (3)**:** 975-983. https://doi.org/10.1016/j.carbpol.2010.12.052

Bester LM (2018) Development and optimisation of a process for cellulose nanoparticle production from waste paper sludge with enzymatic hydrolysis as an integral part. Stellenbosch University.

Bettaieb F, Khiari R, Dufresne A, Mhenni M, Putaux J-L, Boufi S (2015) Nanofibrillar cellulose from Posidonia oceanica: Properties and morphological features. Ind Crops Prod 72**:** 97-106. https://doi.org/10.1016/j.indcrop.2014.12.060

Bhatnagar A, Sain M (2005) Processing of cellulose nanofiber-reinforced composites. J Reinf Plast Compos 24 (12)**:** 1259-1268. http://dx.doi.org/10.1177/0731684405049864

Biermann CJ (1996) Handbook of pulping and papermaking. Elsevier,

Boshoff S, Gottumukkala LD, Van Rensburg E, Görgens J (2016) Paper sludge (PS) to bioethanol: Evaluation of virgin and recycle mill sludge for low enzyme, high-solids fermentation. Bioresour Technol 203**:** 103-111.

Budhavaram NK, Fan Z (2009) Production of lactic acid from paper sludge using acid-tolerant, thermophilic Bacillus coagulan strains. Bioresour Technol 100 (23)**:** 5966-5972. https://doi.org/10.1016/j.biortech.2009.01.080

Chen H, Han Q, Daniel K, Venditti R, Jameel H (2014) Conversion of industrial paper sludge to ethanol: fractionation of sludge and its impact. Appl Biochem Biotechnol 174 (6)**:** 2096-2113. https://doi.org/10.1007/s12010-014-1083-z

Chen W, Yu H, Liu Y, Hai Y, Zhang M, Chen P (2011) Isolation and characterisation of cellulose nanofibers from four plant cellulose fibers using a chemical-ultrasonic process. Cellulose 18 (2)**:** 433-442.

Cherian C, Siddiqua S (2019) Pulp and paper mill fly ash: A review. Sustainability 11 (16)**:** 4394. http://dx.doi.org/10.3390/su11164394

Crespo CF, Badshah M, Alvarez MT, Mattiasson B (2012) Ethanol production by continuous fermentation of d-(+)-cellobiose, d-(+)-xylose and sugarcane bagasse hydrolysate using the thermoanaerobe Caloramator boliviensis. Bioresour Technol 103 (1)**:** 186-191. https://doi.org/10.1016/j.biortech.2011.10.020

Djafari Petroudy SR, Chabot B, Loranger E, Naebe M, Shojaeiarani J, Gharehkhani S, Ahvazi B, Hu J, Thomas S (2021) Recent Advances in Cellulose Nanofibers Preparation through Energy-Efficient Approaches: A Review. Energies 14 (20)**:** 6792. https://doi.org/10.3390/en14206792

Du C, Li H, Li B, Liu M, Zhan H (2016) Characteristics and properties of cellulose nanofibers prepared by TEMPO oxidation of corn husk. BioResources 11 (2)**:** 5276-5284. https://doi.org/10.15376/biores.11.2.5276-5284

Du H, Parit M, Wu M, Che X, Wang Y, Zhang M, Wang R, Zhang X, Jiang Z, Li B (2020) Sustainable valorization of paper mill sludge into cellulose nanofibrils and cellulose nanopaper. J Hazard Mater 400**:** 123106. https://doi.org/10.1016/j.jhazmat.2020.123106

Dufresne A, Dupeyre D, Vignon MR (2000) Cellulose microfibrils from potato tuber cells: processing and characterisation of starch–cellulose microfibril composites. J Appl Polym Sci 76 (14)**:** 2080-2092. https://doi.org/10.1002/(sici)1097-4628(20000628)76:14%3C2080::aid-app12%3E3.0.co;2-u

Dwiarti L, Boonchird C, Harashima S, Park EY (2012) Simultaneous saccharification and fermentation of paper sludge without pretreatment using cellulase from Acremonium cellulolyticus and thermotolerant Saccharomyces cerevisiae. Biomass Bioenerg 42**:** 114-122. https://doi.org/10.1016/j.biombioe.2012.02.019

Fotie G, Limbo S, Piergiovanni L (2020) Manufacturing of Food Packaging Based on Nanocellulose: Current Advances and Challenges. Nanomaterials 10 (9)**:** 1726. https://doi.org/10.3390/nano10091726

Gea T, Artola A, Sánchez A (2005) Composting of de-inking sludge from the recycled paper manufacturing industry. Bioresour Technol 96 (10)**:** 1161-1167. https://doi.org/10.1016/j.biortech.2004.09.025

Ghribi M, Meddeb-Mouelhi F, Beauregard M (2016) Microbial diversity in various types of paper mill sludge: identification of enzyme activities with potential industrial applications. SpringerPlus 5 (1)**:** 1-14. https://doi.org/10.1186/s40064-016-3147-8

Gibril ME, Lekha P, Andrew J, Sithole B, Tesfaye T, Ramjugernath D (2018) Beneficiation of pulp and paper mill sludge: production and characterisation of functionalised crystalline nanocellulose. Clean Technol Environ Policy 20 (8)**:** 1835-1845. https://doi.org/10.1007/s10098-018-1578-3

Goel G, Kalamdhad AS (2017) An investigation on use of paper mill sludge in brick manufacturing. Constr Build Mater 148**:** 334-343. https://doi.org/10.1016/j.conbuildmat.2017.05.087

Gurram RN, Al-Shannag M, Lecher NJ, Duncan SM, Singsaas EL, Alkasrawi M (2015) Bioconversion of paper mill sludge to bioethanol in the presence of accelerants or hydrogen peroxide pretreatment. Bioresour Technol 192**:** 529-539. https://doi.org/10.1016/j.biortech.2015.06.010

He M, Yang G, Chen J, Ji X, Wang Q (2018) Production and characterisation of cellulose nanofibrils from different chemical and mechanical pulps. J Wood Chem Technol 38 (2)**:** 149-158. https://doi.org/10.1080/02773813.2017.1411368

Herrick FW, Casebier RL, Hamilton JK, Sandberg KR (1983) Microfibrillated cellulose: morphology and accessibility. J. Appl. Polym. Sci.: Appl. Polym. Symp.;(United States). ITT Rayonier Inc., Shelton, WA.

Iwamoto S, Abe K, Yano H (2008) The effect of hemicelluloses on wood pulp nanofibrillation and nanofiber network characteristics. Biomacromolecules 9 (3)**:** 1022-1026. https://doi.org/10.1021/bm701157n

Jaria G, Silva CP, Ferreira CI, Otero M, Calisto V (2017) Sludge from paper mill effluent treatment as raw material to produce carbon adsorbents: an alternative waste management strategy. J Environ Manage 188**:** 203-211. https://doi.org/10.1016/j.jenvman.2016.12.004

Jele TB, Lekha P, Sithole B (2021) Role of cellulose nanofibrils in improving the strength properties of paper: a review. Cellulose**:** 1-27. https://doi.org/10.1007/s10570-021-04294-8

Jonoobi M, Mathew AP, Oksman K (2012) Producing low-cost cellulose nanofiber from sludge as new source of raw materials. Ind Crops Prod 40**:** 232-238. https://doi.org/10.1016/j.indcrop.2012.03.018

Kalita E, Nath B, Deb P, Agan F, Islam MR, Saikia K (2015) High quality fluorescent cellulose nanofibers from endemic rice husk: Isolation and characterisation. Carbohydr Polym 122**:** 308-313. https://doi.org/10.1016/j.carbpol.2014.12.075

Kang L, Wang W, Pallapolu VR, Lee YY (2011) Enhanced ethanol production from de-ashed paper sludge by simultaneous saccharification and fermentation and simultaneous saccharification and co-fermentation. 6 (4)**:** 3791-3808. http://dx.doi.org/10.15376/biores.6.4.3791-3808

Karimi S, Tahir PM, Karimi A, Dufresne A, Abdulkhani A (2014) Kenaf bast cellulosic fibers hierarchy: a comprehensive approach from micro to nano. Carbohydr Polym 101**:** 878-885. https://doi.org/10.1016/j.carbpol.2013.09.106

Lahtinen P, Liukkonen S, Pere J, Sneck A, Kangas H (2014) A comparative study of fibrillated fibers from different mechanical and chemical pulps. BioResources 9 (2)**:** 2115-2127. https://doi.org/10.15376/biores.9.2.2115-2127

Leão AL, Cherian BM, de Souza SF, Sain M, Narine S, Caldeira MS, Toledo MAS (2012) Use of primary sludge from pulp and paper mills for nanocomposites. Mol Cryst Liq Cryst 556 (1)**:** 254-263. https://doi.org/10.1080/15421406.2012.635974

Lekha P, Mtibe A, Motaung T, Andrew JE, Sitholè BB, Gibril M (2016) Effect of mechanical treatment on properties of cellulose nanofibrils produced from bleached hardwood and softwood pulps. Maderas Cienc Tecnol 18 (3)**:** 457-466. https://doi.org/10.4067/S0718-221X2016005000041

Malgas S, Rose SH, van Zyl WH, Pletschke BI (2020) Enzymatic hydrolysis of softwood derived paper sludge by an in vitro recombinant cellulase cocktail for the production of fermentable sugars. Catalysts 10 (7)**:** 775. https://doi.org/10.3390/catal10070775

Marques S, Alves L, Roseiro J, Gírio F (2008) Conversion of recycled paper sludge to ethanol by SHF and SSF using Pichia stipitis. Biomass Bioenerg 32 (5)**:** 400-406. https://doi.org/10.1016/j.biombioe.2007.10.011

Méndez A, Fidalgo J, Guerrero F, Gascó G (2009) Characterisation and pyrolysis behaviour of different paper mill waste materials. J Anal Appl Pyrolysis 86 (1)**:** 66-73. http://dx.doi.org/10.1016/j.jaap.2009.04.004

Mtibe A, Linganiso LZ, Mathew AP, Oksman K, John MJ, Anandjiwala RD (2015) A comparative study on properties of micro and nanopapers produced from cellulose and cellulose nanofibres. Carbohydr Polym 118**:** 1-8. https://doi.org/10.1016/j.carbpol.2014.10.007

Nair SS, Zhu J, Deng Y, Ragauskas AJ (2014) Characterisation of cellulose nanofibrillation by micro grinding. J Nanopart Res 16 (4)**:** 1-10. https://doi.org/10.1007/s11051-014-2349-7

Narkpiban K, Sakdaronnarong C, Nimchua T, Pinmanee P, Thongkred P, Poonsawat T (2019) The effect of mechano-enzymatic treatment on the characteristics of cellulose nanofiber obtained from kenaf (Hibiscus cannabinus L.) bark. BioResources 14 (1)**:** 99-119. http://dx.doi.org/10.15376/biores.14.1.99-119

Nuruddin M, Hosur M, Uddin MJ, Baah D, Jeelani S (2016) A novel approach for extracting cellulose nanofibers from lignocellulosic biomass by ball milling combined with chemical treatment. J Appl Polym Sci 133 (9). https://doi.org/10.1002/app.42990

Onyianta AJ, O'Rourke D, Sun D, Popescu C-M, Dorris M (2020) High aspect ratio cellulose nanofibrils from macroalgae Laminaria hyperborea cellulose extract via a zero-waste low energy process. Cellulose 27 (14)**:** 7997-8010.

Panyasiri P, Yingkamhaeng N, Lam NT, Sukyai P (2018) Extraction of cellulose nanofibrils from amylase-treated cassava bagasse using high-pressure homogenization. Cellulose 25 (3)**:** 1757-1768. https://link.springer.com/article/10.1007/s10570-018-1686-6

Podder PK, Gupta A, Jamari SSB, Rashid SS, Sharma S, Subramaniam M, Thraisingam J (2016) Isolation of nano cellulose from rubber wood fibre and fibrillation effects on nano cellulose reinforced poly (Ethylene Oxide). The National Conference for Postgraduate Research. 704-711.

Qing Y, Sabo R, Zhu J, Agarwal U, Cai Z, Wu Y (2013) A comparative study of cellulose nanofibrils disintegrated via multiple processing approaches. Carbohydr Polym 97 (1)**:** 226-234. https://doi.org/10.1016/j.carbpol.2013.04.086

Radakisnin R, Abdul Majid MS, Jamir MRM, Jawaid M, Sultan MTH, Mat Tahir MF (2020) Structural, Morphological and Thermal Properties of Cellulose Nanofibers from Napier fiber (Pennisetum purpureum). Materials 13 (18)**:** 4125. https://doi.org/10.3390/ma13184125

Saelee K, Yingkamhaeng N, Nimchua T, Sukyai P (2016) An environmentally friendly xylanase-assisted pretreatment for cellulose nanofibrils isolation from sugarcane bagasse by high-pressure homogenization. Ind Crop Prod 82**:** 149-160. https://doi.org/10.1016/j.indcrop.2015.11.064

Segal L, Creely JJ, Martin Jr A, Conrad C (1959) An empirical method for estimating the degree of crystallinity of native cellulose using the X-ray diffractometer. Textile research journal 29 (10)**:** 786-794.

Spence KL, Venditti RA, Rojas OJ, Habibi Y, Pawlak JJ (2011) A comparative study of energy consumption and physical properties of microfibrillated cellulose produced by different processing methods. Cellulose 18 (4)**:** 1097-1111. https://doi.org/10.1007/s10570-011-9533-z

Tawalbeh M, Rajangam AS, Salameh T, Al-Othman A, Alkasrawi M (2021) Characterisation of paper mill sludge as a renewable feedstock for sustainable hydrogen and biofuels production. Int J Hydrog 46 (6)**:** 4761-4775. http://dx.doi.org/10.1016/j.ijhydene.2020.02.166

Thygesen A, Oddershede J, Lilholt H, Thomsen AB, Ståhl K (2005) On the determination of crystallinity and cellulose content in plant fibres. Cellulose 12 (6)**:** 563-576. https://doi.org/10.1007/s10570-005-9001-8

Uetani K, Yano H (2011) Nanofibrillation of wood pulp using a high-speed blender. Biomacromolecules 12 (2)**:** 348-353.

Wang L, Wang J, Littlewood J, Cheng H (2014) Co-production of biorefinery products from kraft paper sludge and agricultural residues: opportunities and challenges. Green Chem 16 (3)**:** 1527-1533. https://doi.org/10.1039/c3gc41984c

Wang Q, Zhu J, Gleisner R, Kuster T, Baxa U, McNeil S (2012) Morphological development of cellulose fibrils of a bleached eucalyptus pulp by mechanical fibrillation. Cellulose 19 (5)**:** 1631-1643. https://doi.org/10.1007/s10570-012-9745-x

Wang W, Kang L, Lee YY (2010) Production of cellulase from kraft paper mill sludge by Trichoderma reesei rut C-30. Appl Biochem Biotechnol 161 (1)**:** 382-394. https://doi.org/10.1007/s12010-009-8863-x

Williams A (2017) The production of bioethanol and biogas from paper sludge. Stellenbosch University.

Yang H, Yan R, Chen H, Zheng C, Lee DH, Liang DT (2006) Influence of mineral matter on pyrolysis of palm oil wastes. Combust Flame 146 (4)**:** 605-611. https://doi.org/10.1016/j.combustflame.2006.07.006

Yousefi H, Faezipour M, Hedjazi S, Mousavi MM, Azusa Y, Heidari AH (2013) Comparative study of paper and nanopaper properties prepared from bacterial cellulose nanofibers and fibers/ground cellulose nanofibers of canola straw. Ind Crop Prod 43**:** 732-737. https://doi.org/10.1016/j.indcrop.2012.08.030

Zimmermann T, Pöhler E, Geiger T (2004) Cellulose fibrils for polymer reinforcement. Adv Eng Mater 6 (9)**:** 754-761. https://doi.org/10.1002/adem.200400097

5 CHAPTER 5: A TRANSITION FROM MANUAL GRINDING TO AUTOMATION IN CNF PRODUCTION

Thabisile Brightwell Jele[1], Prabashni Lekha[2], Bruce Sithole[1, 2]

[1]*University of KwaZulu-Natal (Howard Campus), Discipline of Chemical Engineering, College of Agriculture, Engineering and Sciences, Durban,* [2]*Council for Scientific and Industrial Research, Biorefinery Industry Development Facility, Durban, South Africa*

[*]Corresponding Author: thabisilejele94@gmail.com

5.1 Abstract

This paper describes the transition from manual grinding using the supermasscolloider (SMC) to an automated operation. The automated system was designed to pump the feedstock suspension through the SMC via sample holding tanks for a predetermined number of passes. The automated operation alleviated challenges associated with the manual operation, which included high labour demands, loss of material due to spillages, thus affecting yield and posing a safety risk in the working environment, inconsistent product due to human error in counting the number of cycles, low productivity due to long working hours. The introduction of the automated SMC system was a worthwhile investment justifiable by improving efficiency and operator safety.

Keywords: supermasscolloider, automated, suspension, grinding

5.2 Introduction

The SMC MKCA6-2 (Masuko Sangio, Kawaguchi, Japan) is one of the many series of grinders developed in 1965, patented in 12 countries, and ISO 9001 certified (http://www.masuko.com). The SMC is a friction grinder that finds application in plants, food, pharmaceuticals (medicine and cosmetics), fuel and chemicals due to its ease to assemble and disassemble (Jonoobi et al. 2012; Osong 2014; Kakimov et al. 2016; Wang et al. 2016; Adu et al. 2018; Nagano et al. 2020; Mousavi et al. 2021). The SMC consists of one pair of non-porous grinding stones working on the rotor-stator principle. The rotor stone turns at high speeds (1500-20 000 rpm) while the stator stone remains still (Troy 2005). The suspension is introduced into the hopper and passed through the grinding area consisting of grinding stones that have bursts and grooves that contact the feedstock to disintegrate it by repeated cyclic stresses leading to defibrillation, structure breakdown or particle size reduction (Abe et al. 2007; Uetani and Yano 2011; Jonoobi et al. 2012; Wang et al. 2012; Nair et al. 2014; Berglund et al. 2016; Lekha et al. 2016; He et al. 2018). The quality and size of the product are controlled by adjusting the clearance between the two ceramic non-porous grinding stones.

5.3 Old Method

The old process entailed manually loading the feedstock into the hopper of the SMC using a bucket (Fig. 5-1). This constituted a “pass”. The product was collected through the product chute and re-introduced back into the hopper for further grinding. The process was continued until the desired number of passes/product quality was achieved. The problems encountered with the use of a manually operated SMC were as follows:

- Labour intensive.
- Loss of material due to spillages, thus affecting yield and posing a safety risk in the working environment.

- Inconsistent product due to human error in counting the number of cycles.
- Low productivity due to long working hours.

Due to the above-mentioned problems, automation of the equipment was suggested and implemented. The automated SMC was anticipated to improve production rates, quality, safety, decrease labour demand, and reduce working times.

Figure 5-1 The photographic diagram of (a) the manually operated supermasscolloider MKCA6-2 (Masuko Sangio, Kawaguchi, Japan) (b) manually operated supermasscolloider during operation

5.4 The new process

The process flow diagram diagram of the automated system is shown in Fig. 5-2. The suspension is introduced into tank 1, where it is pumped to tank 2 to promote agitation and homogeneity of the suspension

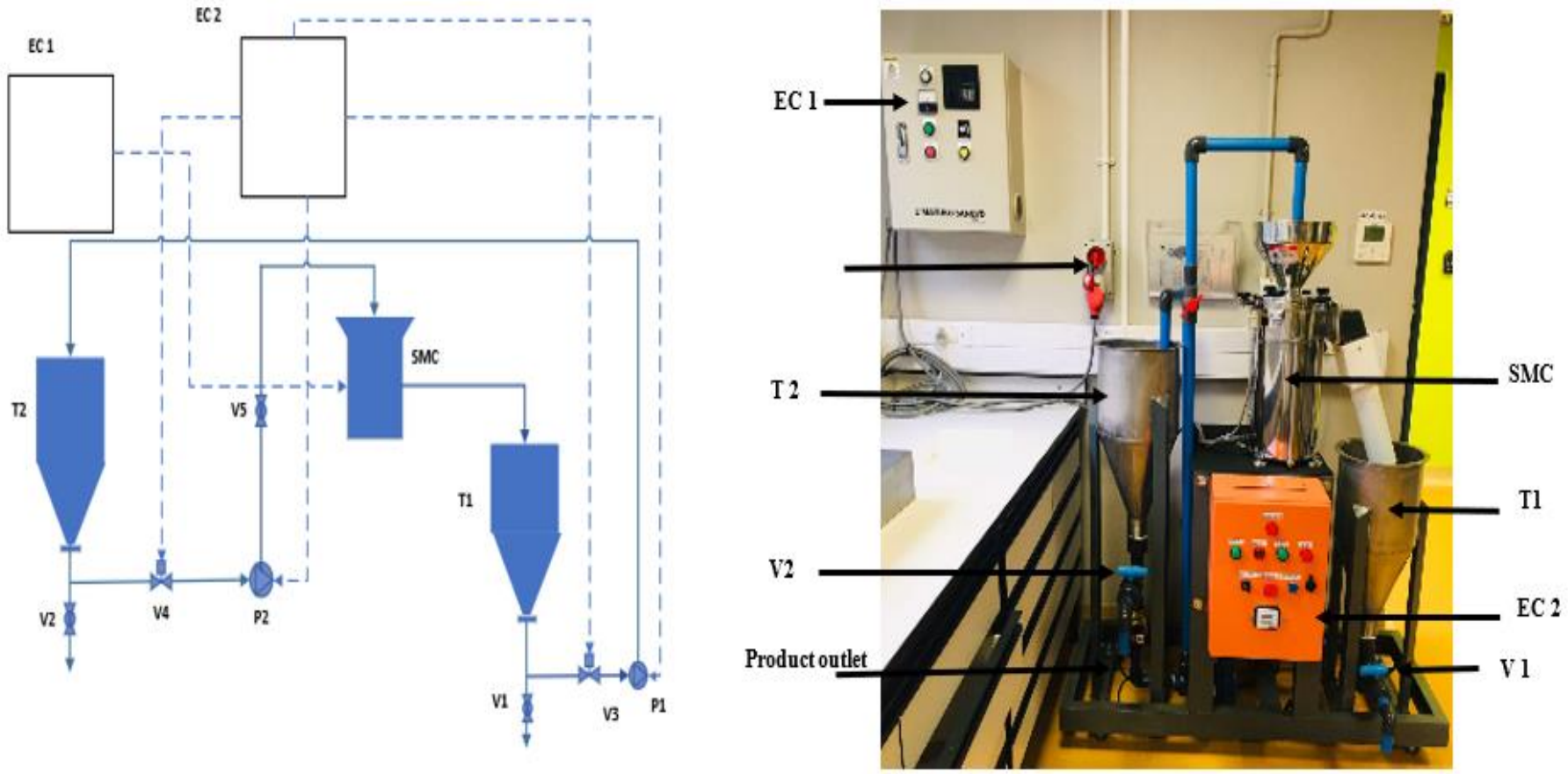

Figure 5-2 (a) Process flow diagram of the automated SMC (b) Photographic diagram of the automated SMC

Table 5-1 Description of symbols in Figure 5-2

Abbreviation	Description	Specification
T1	Feed Tank to Tank 2	Steel tank-1000L
T2	Feed tank to SMC	Steel tank-1000L
V1	Product valve	Ball valve Plimex
V2	Product valve	Ball valve Plimex
V3	Flow control valve to tank 2	Solenoid valve (ZW-25N), Air/water, Temp 5-130ºC, Pressure 0-8bar
V4	Flow control valve to tank 1	Solenoid valve (ZW-25N), Air/water, Temp 5-130ºC, Pressure 0-8bar
P1	Feed Pump to T2	Pedrollo centrifugal water PKm 60, Motor 0.37W
P2	Feed Pump to SMC	Pedrollo centrifugal PKm 60, Motor 0.37W
EC1	Electric Control for SMC	Electrical powered control panel
EC 2	Electric control for V3 and V4 and pumps	Electrical powered control panel

5.4.1 Working Principle

The working principle of the automated SMC tank system with reference to Figure 5-2 is as follows:

Electric power is used for driving the process and running the control systems. Before operation, the grinding plates of the SMC are set at point 0 (zero) by turning the handle on the side of the SMC. The speed of the grinding stones is adjusted by the knob on the SMC control box mounted on the wall (maximum recommended – 1500 rpm). The required number of cycles for the experiment are predetermined and set using the set, up, and down arrow buttons on the automated tank system control box. The sample in suspension form is introduced into tank 1, and the grinding process is started by clicking on the "START" button (green button) on the SMC control box and turning the selector switch on the automated tank system control box into the "ON" position. The distance between grinding stones is set. After completing the set number of passes/cycles, the system automatically stops, and the SMC is immediately stopped by clicking the "STOP" button (red button) on the SMC control box on the wall to avoid dry grinding and damage to the grinding stones. The product is received at the collection points by opening the valve on tank 1 and then on tank 2.

5.4.2 Advantages of the automated SMC system

The advantages of the automated Supermasscolloider system are as follows:

- Improved accuracy and repeatability
- Reduced labour input
- Increased yield and production rates

5.4.3 Conclusions

This paper described the transition from manual grinding to an automated grinding operation. The automated process proved to be worthwhile and beneficial in the following ways:

- Guaranteed consistency of product
- Increased ease of operation
- Reduced labour demand
- Improved operator's safety and cleaner working environment
- Improved yield

5.5 References

Abe K, Iwamoto S, Yano H (2007) Obtaining cellulose nanofibers with a uniform width of 15 nm from wood. Biomacromolecules 8 (10)**:** 3276-3278. https://doi.org/10.1021/bm700624p

Adu C, Berglund L, Oksman K, Eichhorn SJ, Jolly M, Zhu C (2018) Properties of cellulose nanofibre networks prepared from never-dried and dried paper mill sludge. J Clean Prod 197**:** 765-771. https://doi.org/10.1016/j.jclepro.2018.06.263

Berglund L, Noël M, Aitomäki Y, Öman T, Oksman K (2016) Production potential of cellulose nanofibers from industrial residues: Efficiency and nanofiber characteristics. Ind Crops Prod 92**:** 84-92. https://doi.org/10.1016/j.indcrop.2016.08.003

He M, Yang G, Chen J, Ji X, Wang Q (2018) Production and characterisation of cellulose nanofibrils from different chemical and mechanical pulps. J Wood Chem Technol 38 (2)**:** 149-158. https://doi.org/10.1080/02773813.2017.1411368

Jonoobi M, Mathew AP, Oksman K (2012) Producing low-cost cellulose nanofiber from sludge as new source of raw materials. Ind Crops Prod 40**:** 232-238. https://doi.org/10.1016/j.indcrop.2012.03.018

Kakimov A, Yessimbekov Z, Kabulov B, Bepeyeva A, Kuderinova N, Ibragimov N (2016) Studying chemical composition and yield stress of micronized grinded cattle bone paste. Res J Pharm Biol Chem 7 (2)**:** 805-812.

Lekha P, Mtibe A, Motaung T, Andrew JE, Sitholè BB, Gibril M (2016) Effect of mechanical treatment on properties of cellulose nanofibrils produced from bleached hardwood and softwood pulps. Maderas-Cienc Tecnol 18 (3)**:** 457-466. https://doi.org/10.4067/s0718-221x2016005000041

Mousavi SN, Nazarnezhad N, Asadpour G, Ramamoorthy SK, Zamani A (2021) Ultrafine Friction Grinding of Lignin for Development of Starch Biocomposite Films. Polymers 13 (12)**:** 2024. https://doi.org/10.3390/polym13122024

Nagano T, Arai Y, Yano H, Aoki T, Kurihara S, Hirano R, Nishinari K (2020) Improved physicochemical and functional properties of okara, a soybean residue, by nanocellulose technologies for food development–A review. Food Hydrocoll 109**:** 105964. https://doi.org/10.1016/j.foodhyd.2020.105964

Nair SS, Zhu J, Deng Y, Ragauskas A (2014) Characterisation of cellulose nanofibrillation by micro grinding. J Nanopart Res 16 (4)**:** 1-10. https://doi.org/10.1007/s11051-014-2349-7

Osong SH (2014) Mechanical pulp based nano-ligno-cellulose: production, characterisation and their effect on paper properties. Mid Sweden University.

Troy DB (2005) Remington: The science and practice of pharmacy. Lippincott Williams & Wilkins,

Uetani K, Yano H (2011) Nanofibrillation of wood pulp using a high-speed blender. Biomacromolecules 12**:** 348–353. https://doi.org/10.1021/bm101103p

Wang Q, Zhu J, Gleisner R, Kuster T, Baxa U, McNeil S (2012) Morphological development of cellulose fibrils of a bleached eucalyptus pulp by mechanical fibrillation. Cellulose 19 (5)**:** 1631-1643. https://doi.org/10.1007/s10570-012-9745-x

Wang W, Mozuch MD, Sabo RC, Kersten P, Zhu J, Jin Y (2016) Endoglucanase post-milling treatment for producing cellulose nanofibers from bleached eucalyptus fibers by a supermasscolloider. Cellulose 23 (3)**:** 1859-1870. https://doi.org/10.1007/s10570-016-0946-6

6 CHAPTER 6: GENERAL CONCLUSIONS, RECOMMENDATIONS AND FUTURE WORK

In this study, three types of PPMS samples ((viz., virgin, recycle and deinking) were compared. Firstly, extensive characterisation for PPMS was conducted to determine the best beneficiation pathway in line with characterisation results. Secondly, CNFs were produced by mechanical grinding using the automated SMC. Finally, a description of the automated SMC was done.

6.1 Conclusions

The main conclusions drawn from this study are as follows:

i) Characterisation of three types of PPMS

Significant differences in PPMS characteristics were observed due to the differences in the mill operations, raw materials and wastewater treatment processes. PPMS A and PPMS C were a better fit for composite manufacture based on ash content which would act as a strength enhancer. All the PPMS samples were not suitable for energy harvesting because of the high moisture content and low calorific values. The high C:N ratios also limited PPMS samples as possible soil amenders. PPMS B was better suited for ethanol/biofuel production because of its higher glucose content than other PPMS samples. The high cellulose and low ash content of PPMS B were found suitable for nanocellulose production.

ii) Production of cellulose nanofibrils from PPMS

Highly fibrillated CNFs were produced from three types of PPMS using the automated SMC. The average diameters of CNFs obtained after 200 passes were 6.84 nm, 6.55 nm and 5.61 nm for CNF A, CNF B and CNF C, respectively. PPMS A, PPMS B and PPMS C yielded 27.2%, 32.04% and 42.8% of CNFs, respectively.

iii) The automated SMC

The use of the automated SMC was beneficial in reducing the amount of production time. The automated SMC operated at approximately 10 passes per minute. Given that production time is directly proportional to energy consumption, the production of CNFs using the automated SMC was energy efficient.

6.2 Recommendations

Although a lot of research has been done on the application of CNFs in papermaking, no research has focused particularly on paper straws. There is a need to improve the mechanical strength properties of paper straws in order to eliminate plastic straws, which are an environmental hazard.

6.3 Future works

This research work could be continued as follows:

- Preforming an economic evaluation for the production of CNFs from PPMS
- Application of CNFs in papermaking in order to improve the strength properties of paper used for paper straw manufacture.

Appendices

Appendix A: Original measured data, mean and standard deviation calculation

Table 7.1 Original measured data for chemical compostion of PPMS samples

Sample ID	Arabinose	Galactose	Glucose	Xylose	Mannose	Lignin
PPMS A R1	0.13	0.59	37.06	3.15	0.11	33.25
PPMS A R2	0.19	0.58	36.61	3.26	0.06	33.89
PPMS A R3	0.18	0.66	35.12	2.91	0.00	
Mean	0.17	0.61	36.26	3.11	0.05	33.5
Standard deviation	0.04	0.05	1.01	0.18	0.05	0.45
PPMS B R1	0.50	0.91	63.05	3.63	3.48	22.99
PPMS B R2	0.39	0.98	62.67	2.92	3.45	16.57
PPMS B R3	0.40	1.07	62.76	3.06	3.44	
Mean	0.43	0.99	62.83	3.21	3.46	19.7
Standard deviation	0.06	0.08	0.20	0.37	0.02	4.6
PPMS C R1	0.06	0.11	52.23	10.46	ND	13.55
PPMS C R2	0.05	0.13	52.50	10.58	ND	10.58
Mean	0.055	0.12	52.37	10.52	ND	5.25
Standard deviation	0.01	0.01	0.19	0.09	ND	7.9 ± 3.8

The mean standard deviation was calculated using conducted in the software program, Excel (Microsoft Office, 2016). For instance, the calculations were conducted according to the following equations

$$Mean = \frac{Sum\ of\ all\ data\ values}{Number\ of\ data\ values} \quad (10)$$

$$Standard\ deviation = \sqrt{\frac{\sum_{i=n}^{n}(X_i - \bar{X})^2}{n-1}} \quad (11)$$

where n is the total number of sample elements, X_i represents each of the values of the data and $\bar{X}$ is the sample mean

Appendix B: FTIR software captured images

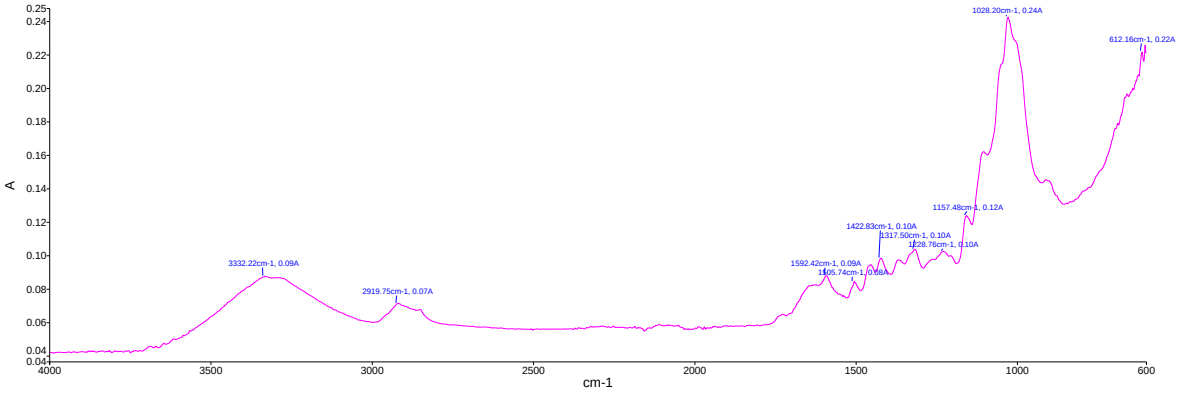

Figure 7- 1 Infrared spectra of PPMS A

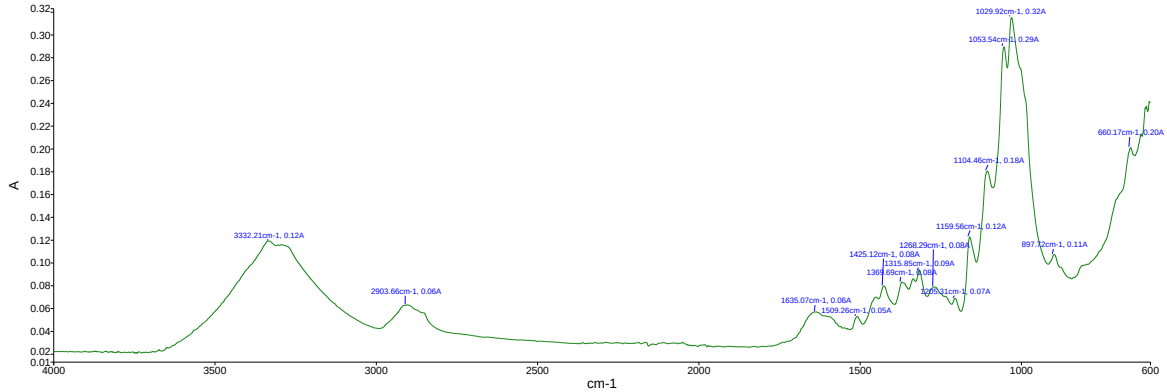

Figure 7- 2 Infrared spectra of PPMS B

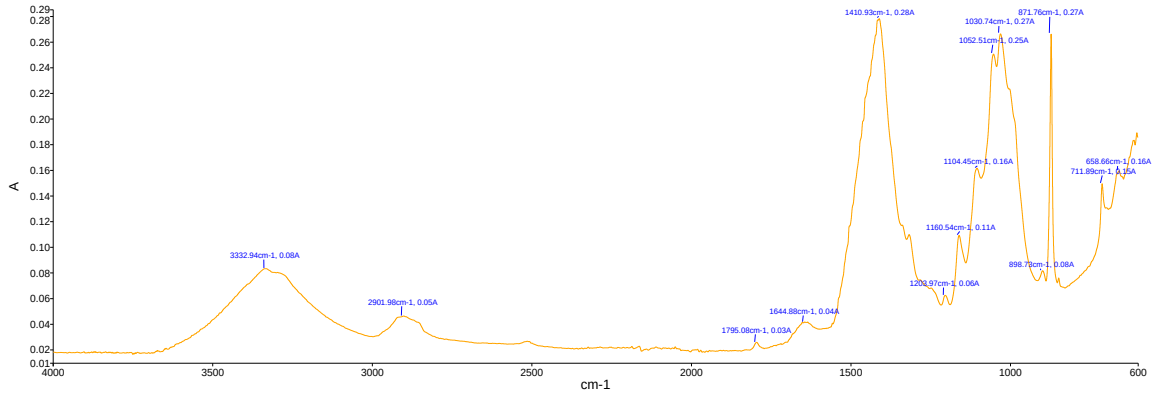

Figure 7- 3 Infrared spectra of PPMS C

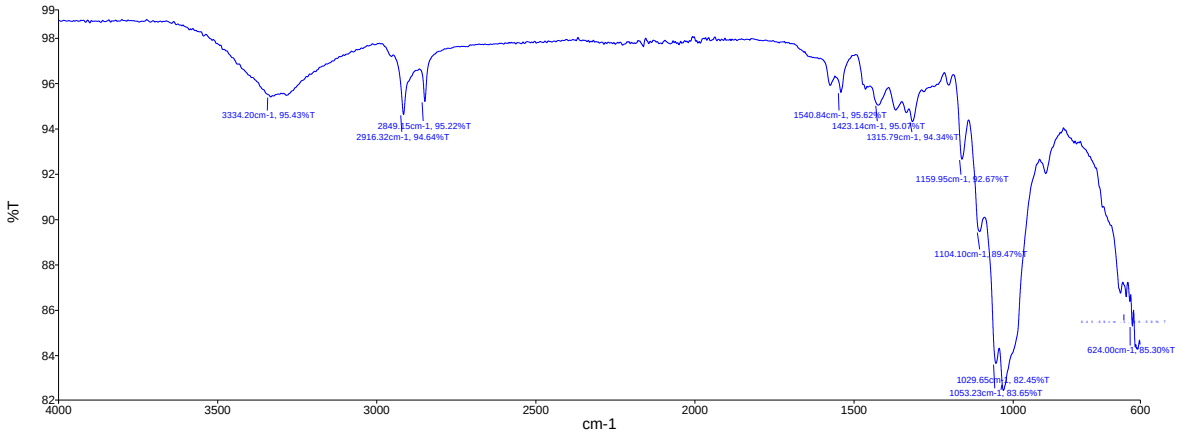

Figure 7- 4 Infared spectra of bleached PPMS A

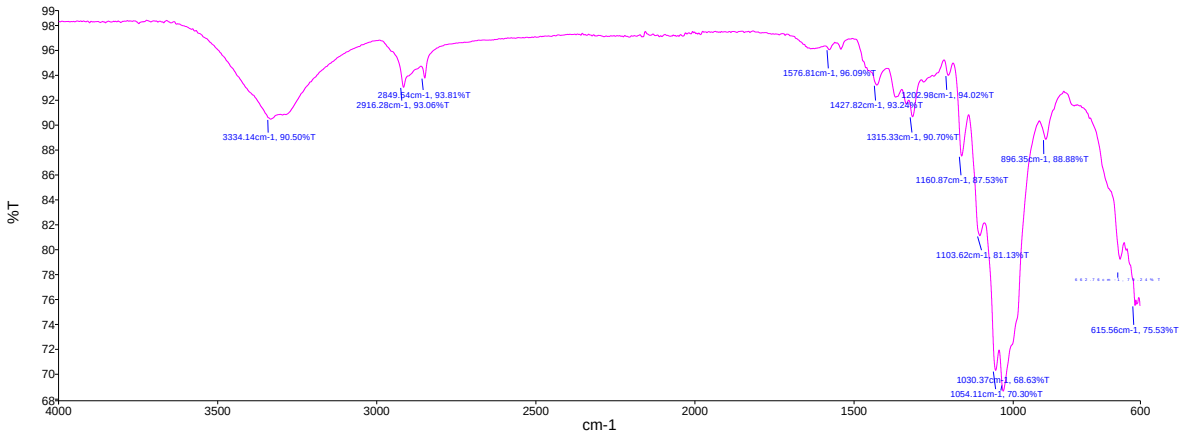

Figure 7- 5 Infared spetra of bleached PPMS B

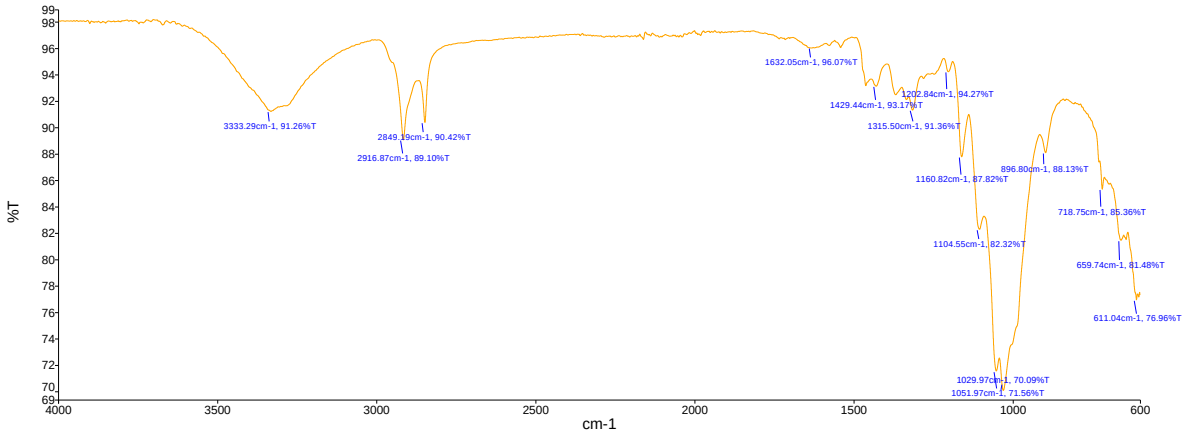

Figure 7- 6 Infarred spectra of bleached PPMS C

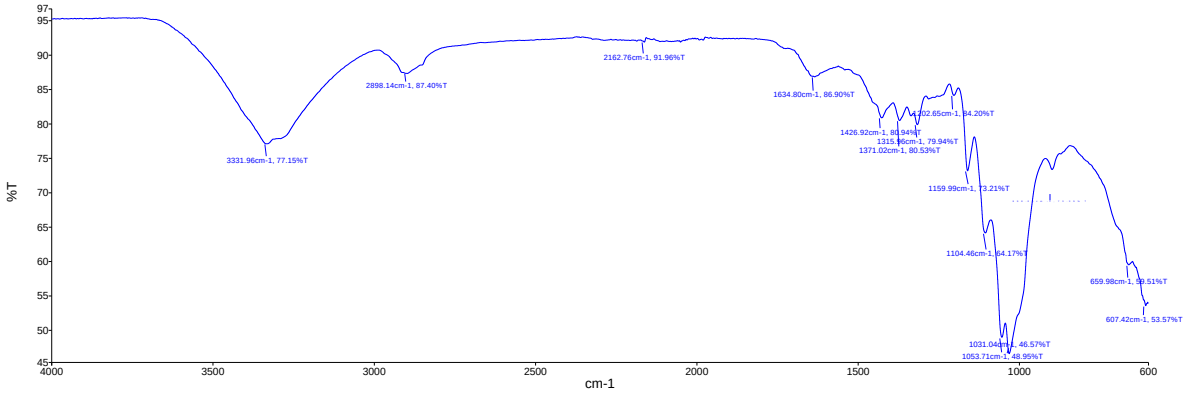

Figure 7- 7 Infrared spectra of CNF A

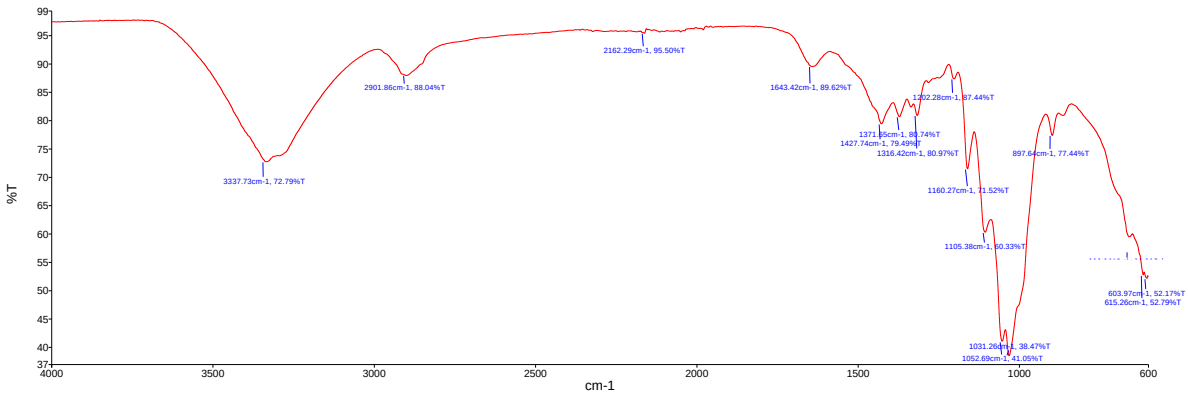

Figure 7- 8 Infared spectra of CNF B

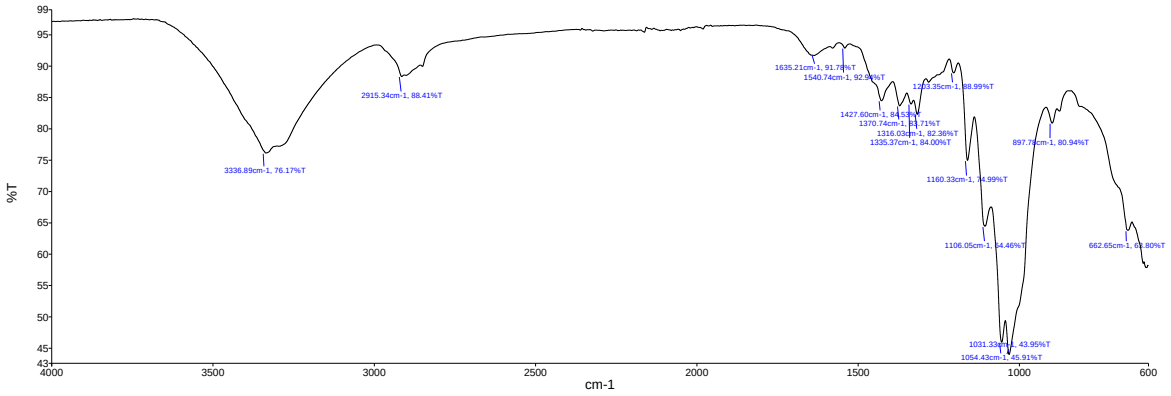

Figure 7- 9 Infared spectra of CNF B

Appendix C: TGA software captured images

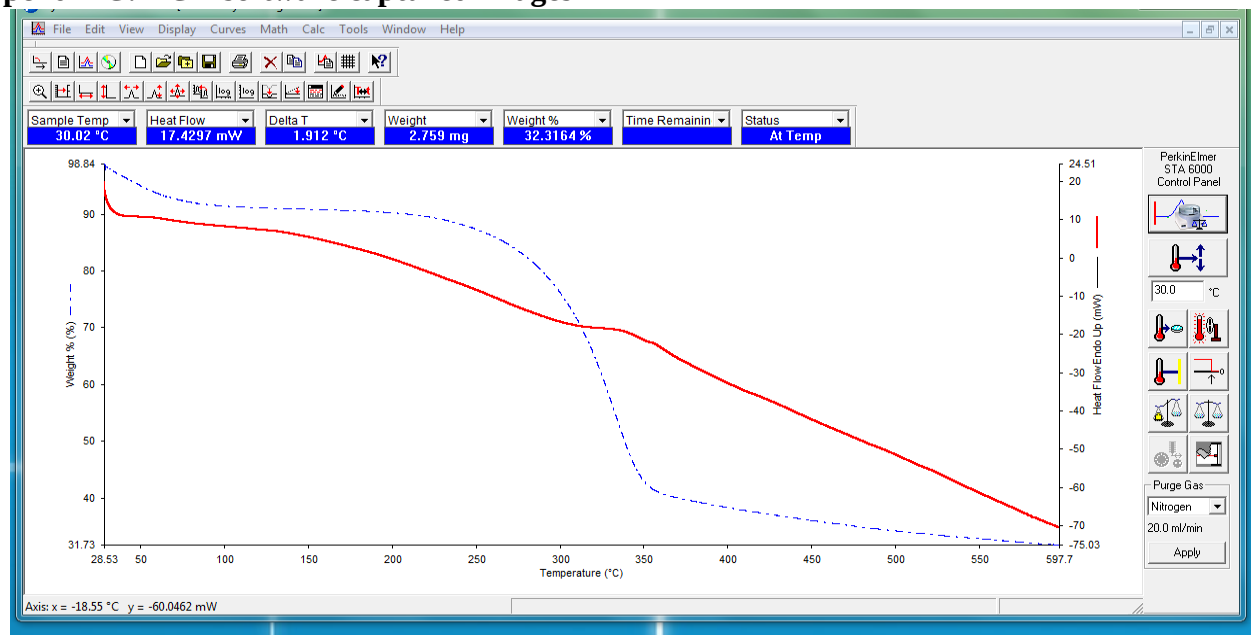

Figure 7- 10 TGA curve for CNF A

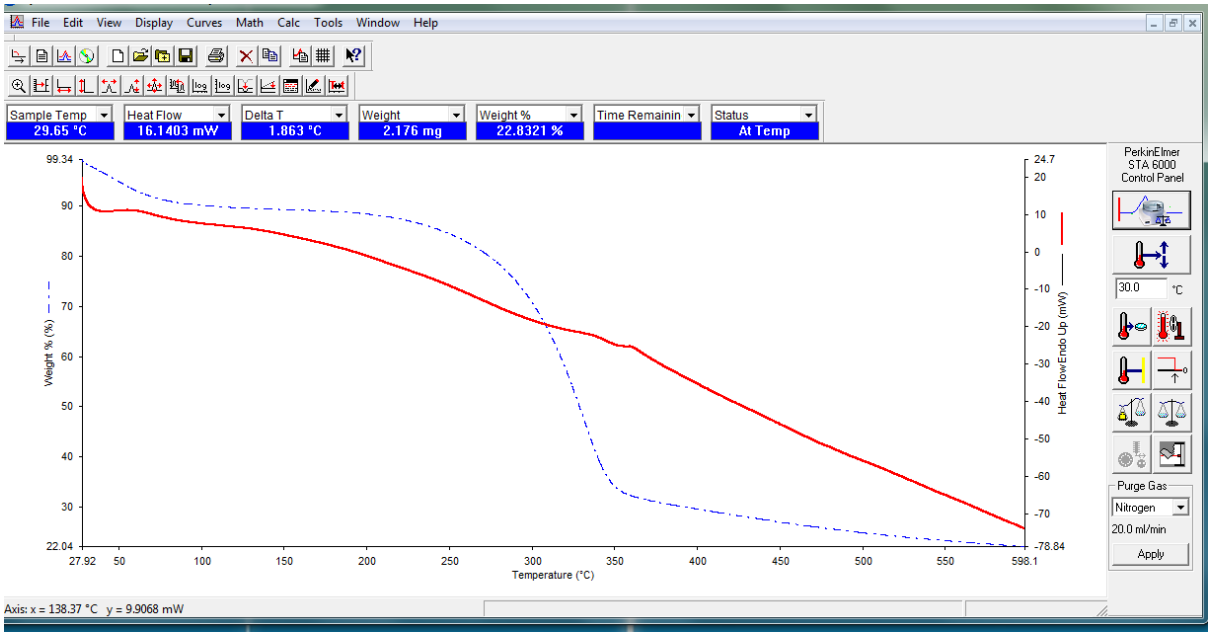

Figure 7- 11 TGA for CNF B

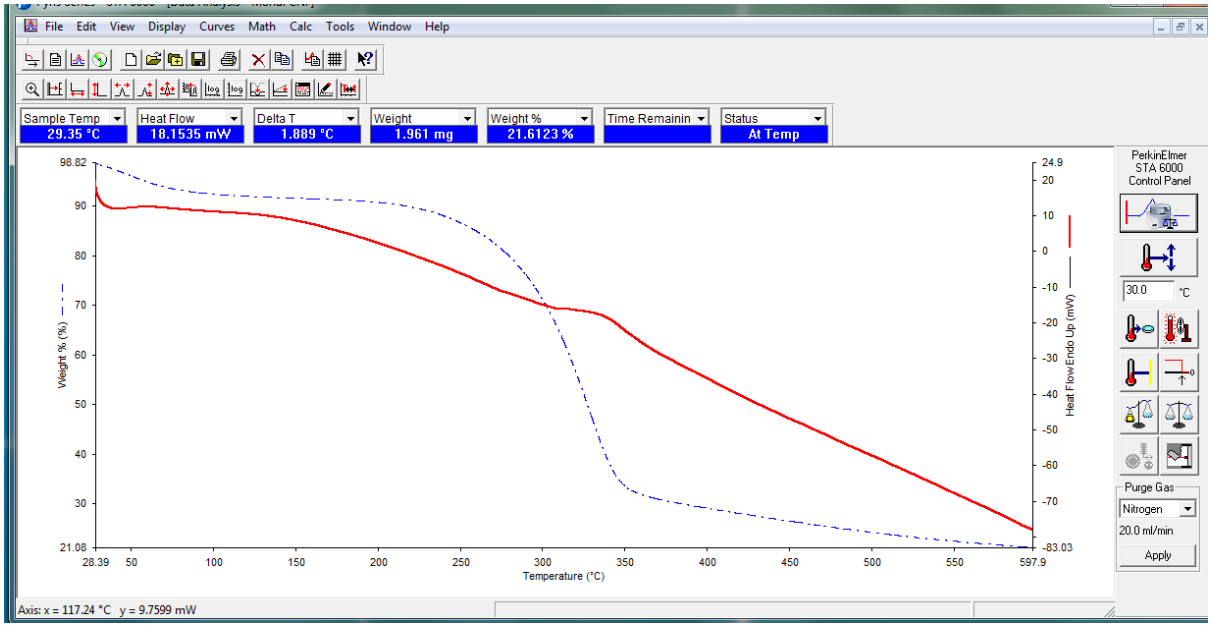

Figure 7- 12 TGA for CNF C

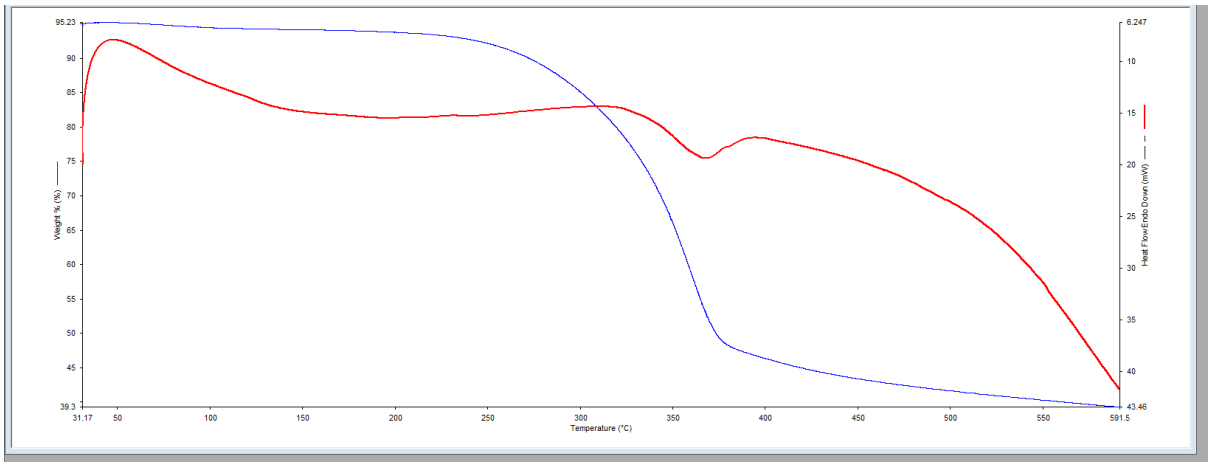

Figure 7- 13 TGA for PPMS A

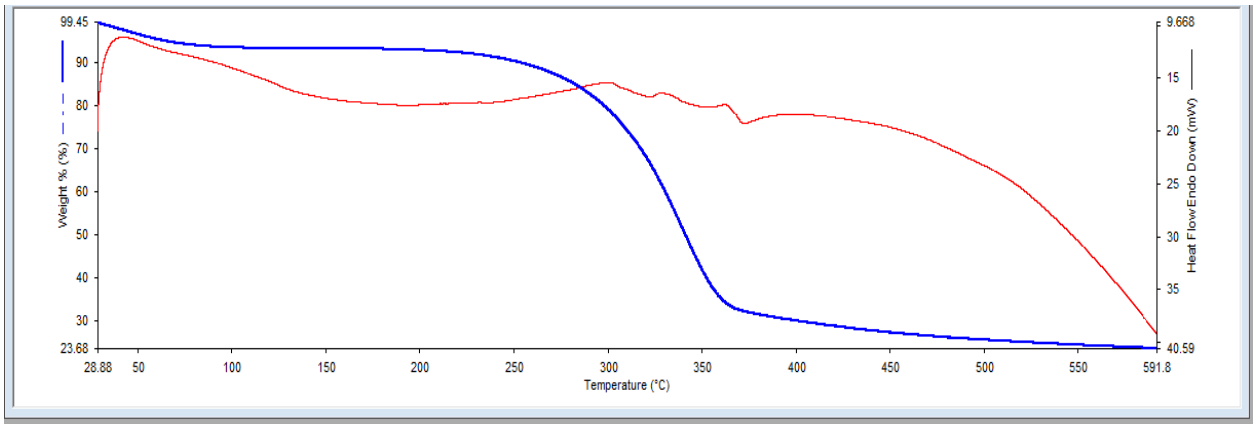

Figure 7- 14 TGA for PPMS B

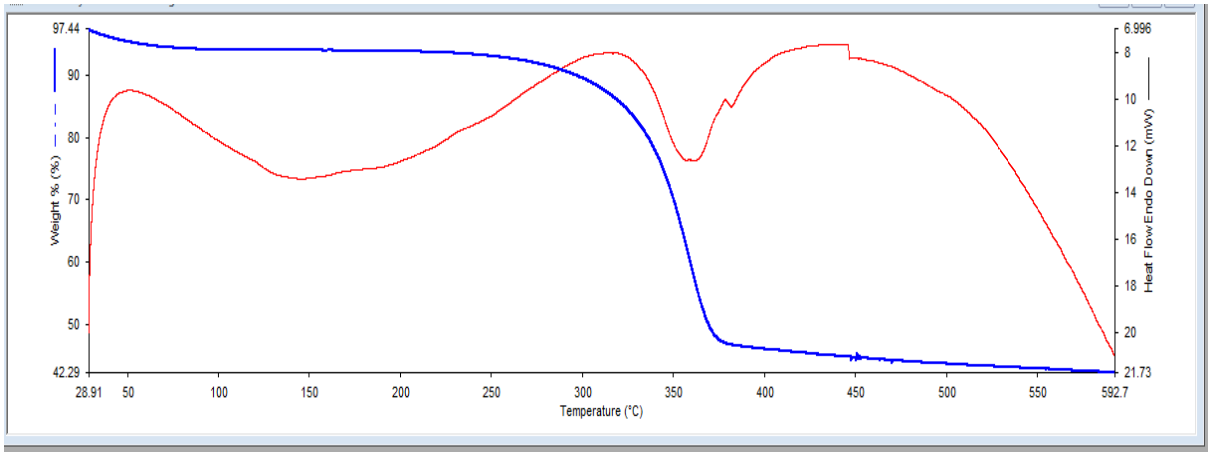

Figure 7- 15 TGA for PPMS C

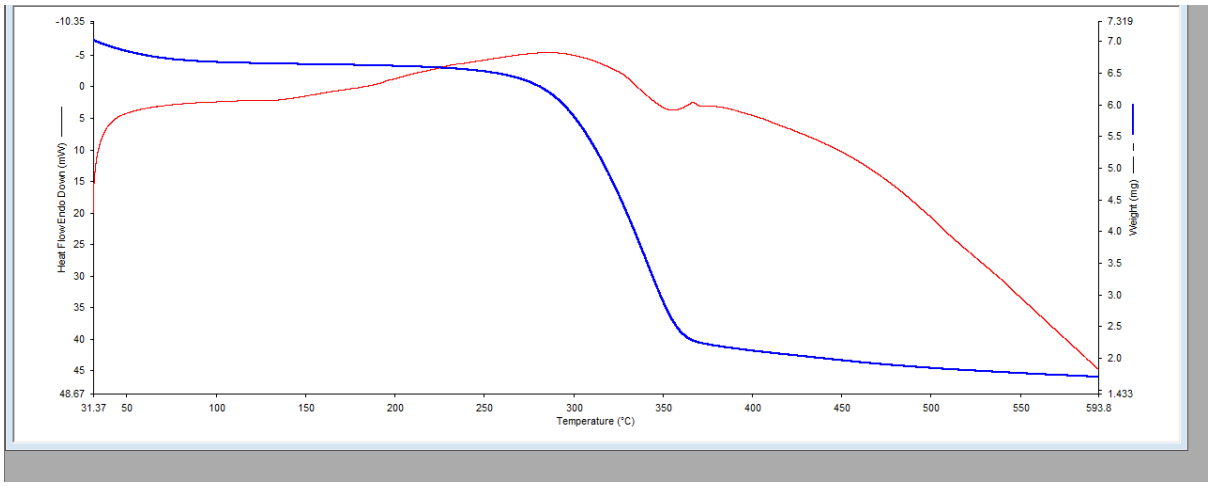

Figure 7- 16 TGA curve for bleached PPMS A

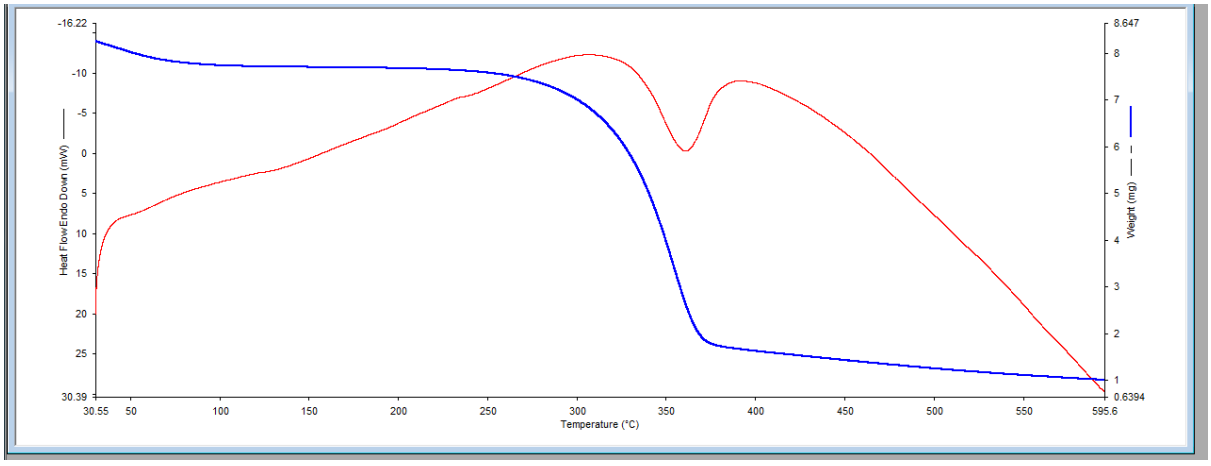

Figure 7- 17 TGA curve for bleached PPMS B

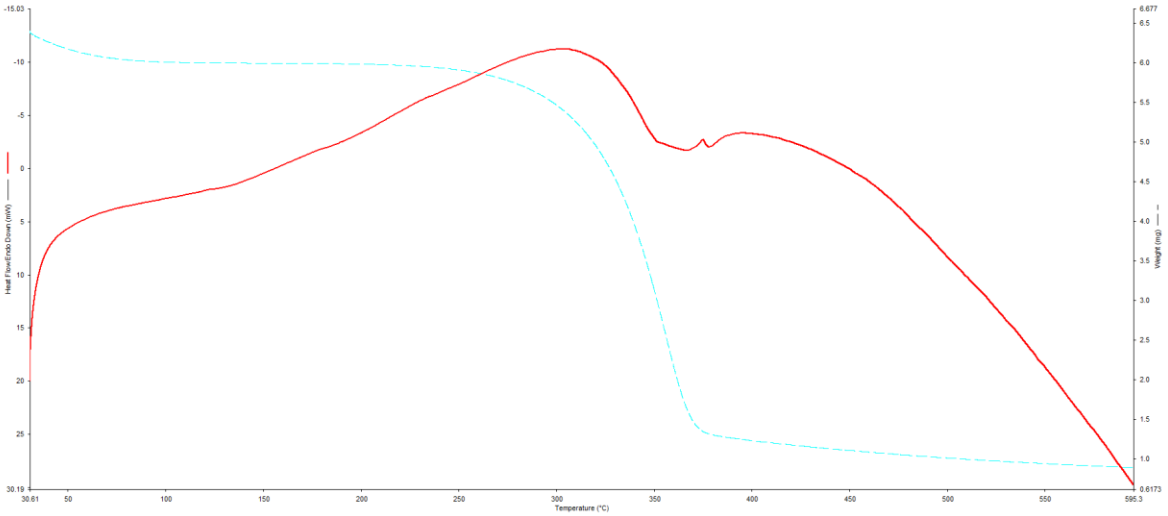

Figure 7- 18 TGA curve for bleached PPMS C